



universität  
wien

# DISSERTATION

Titel der Dissertation

Modulation of oncogenic transformation by Raf proteins

angestrebter akademischer Grad

Doktor der Naturwissenschaften (Dr. rer.nat.)

Verfasser:	Mag. rer. nat. Florian Karreth
Matrikel-Nummer:	9800192
Dissertationsgebiet (lt. Studienblatt):	Genetik
Betreuer:	Univ.-Prof. Dr. Erwin Wagner, Prof. David Tuveson

Wien, im Oktober 2009



## **Index**

1. <u>Acknowledgements</u> .....	3
2. <u>Abstract</u> .....	4
3. <u>Introduction</u> .....	7
3.1 The Ras/Raf/MEK/ERK pathway.....	7
3.2 Ras proteins.....	8
3.3 Raf proteins.....	12
3.4 Regulation of the MAPK pathway.....	18
3.5 Ras and cancer.....	19
3.6 Raf and cancer.....	20
3.7 Modelling oncogenic Ras/Raf signalling in the mouse (published review article).....	22
4. <u>Material and Methods</u> .....	31
4.1 DNA Manipulation.....	31
4.2 Polymerase Chain Reaction (PCR) .....	32
4.3 Colony lift.....	32
4.4 Plasmids.....	33
4.5 Cell lines and transfections.....	34
4.6 Embryonic stem cell culture and targeting.....	35
4.7 Mouse embryonic fibroblasts.....	36
4.8 Proliferation, focus formation, soft agar and apoptosis assay.....	37
4.9 Alkaline phosphatase staining.....	38
4.10 Immunoprecipitation.....	38
4.11 Western blotting.....	39
4.12 Quantification of amount of Raf molecules per cell.....	40
4.13 RNA isolation, cDNA synthesis, and PCR analysis.....	41
4.14 DNA isolation and Southern blotting.....	41
4.15 Mouse strains, genotyping and intranasal Ad-Cre instillation.....	43
4.16 Histology and immunohistochemistry and quantification of lung tumor burden.....	44

4.17	Statistical analysis.....	44
5.	<u>Results and Discussion</u> .....	45
5.1	C-Raf inhibits MAPK activation and transformation by B-Raf <sup>V600E</sup> (Molecular Cell, in press).....	46
5.1.1	Additional data not included in the manuscript.....	98
5.2	Generation of a conditional and reversible oncogenic B-Raf mutant mouse model (unpublished data) .....	101
5.2.1	The rationale and strategy for generating a LSL-B-Raf <sup>V619E</sup> mouse.....	102
5.2.2	Design of the LSL-B-Raf <sup>V619E</sup> allele and targeting strategy.....	105
5.2.3	Design, cloning and targeting of the LSL-FRT targeting vector.....	107
5.2.4	Design, cloning and targeting of the V619E-Neo-TK targeting vector.....	110
5.2.5	LSL-B-Raf <sup>V619E</sup> MEFs and mice.....	113
5.2.6	Generation of R26-LSL-FlpERT2 mice.....	116
5.3	The role of B-Raf and C-Raf in K-Ras <sup>G12D</sup> -induced lung tumorigenesis (unpublished data).....	121
5.3.1	Rationale.....	122
5.3.2	Lung tumor development.....	122
5.3.3	Survival of B-Raf <sup>fl/fl</sup> , K-Ras <sup>G12D</sup> and C-Raf <sup>fl/fl</sup> , K-Ras <sup>G12D</sup> mice.....	125
5.3.4	MAPK activation and proliferation <i>in vivo</i> .....	126
5.3.5	B-Raf <sup>fl/fl</sup> ; K-Ras <sup>G12D</sup> and C-Raf <sup>fl/fl</sup> ; K-Ras <sup>G12D</sup> MEFs.....	127
5.3.6	Future directions.....	132
6.	<u>Conclusions</u> .....	134
7.	<u>References</u> .....	140
8.	<u>List of Figures</u> .....	149
9.	<u>Curriculum vitae</u> .....	151

## **1. Acknowledgements**

I am indebted to Dave Tuveson for giving me the opportunity to do research in his lab as a PhD student, even though I was not enrolled at the University of Pennsylvania. Dave mentored when mentoring was required, but his laissez-faire approach to science was what really formed me as an individual scientist. I am grateful for the professional and inspiring work environment Dave provided and for pointing out the difference between 'interesting' and 'important'.

I want to thank the members of my PhD thesis committee, Professors Manuela Baccarini, Erwin Heberle-Bors and Erwin Wagner for their advice and encouragement. Also, carrying out my PhD work externally would not have been possible without their support.

I am thankful to Professor Richard Marais for providing numerous reagents and for serving as the external reviewer and examiner.

I want to thank all Tuveson lab members, past and present, for creating a hardworking, helpful and fun lab atmosphere. We shared many moments of scientific and social joy, drama, and hilarity that will truly be missed in the future.

I acknowledge receipt of a PhD fellowship from the Boehringer Ingelheim Fonds, which made living in the US a real bargain.

Last but not least, I am grateful to my family, friends and Gina for their continuous support and encouragement.

## **2. Abstract**

Aberrant activation of the MAP kinase pathway is of fundamental importance for the transformation of numerous cell types. This can be achieved by oncogenic Ras and B-Raf missense mutations, which are common genetic lesions found in human cancers. Although a causal role of MAP kinase pathway hyperactivation in cancer development has been established, modulation of the pathway by the complex interplay of Ras and Raf proteins remains poorly understood. Here, I show that proto-oncogenic C-Raf antagonizes the oncogenic activity of the most frequent cancer-associated B-Raf mutant, B-Raf<sup>V600E</sup>, through the formation of B-Raf<sup>V600E</sup>-C-Raf complexes with low kinase activity. B-Raf-C-Raf association is promoted by oncogenic Ras, providing a potential explanation for the exclusivity of oncogenic Ras mutations and B-Raf<sup>V600E</sup> in human cancer. To study the suppressive function of C-Raf on B-Raf<sup>V600E</sup> *in vivo*, a mouse model of B-Raf<sup>V600E</sup> was developed. Activated murine B-Raf<sup>V619E</sup>, analogous to human B-Raf<sup>V600E</sup>, transforms MEFs and, when expressed in melanocytes, induces hyper-pigmentation in mice. As B-Raf<sup>V619E</sup> expression results in a transformed phenotype *in vitro* and *in vivo*, this mouse model will be useful to further evaluate the relationship between C-Raf and B-Raf<sup>V600E</sup>. As C-Raf has adverse effects on B-Raf<sup>V600E</sup>-induced transformation, its role in mediating transformation by oncogenic K-Ras<sup>G12D</sup> was examined. Homozygous loss of C-Raf impairs K-Ras<sup>G12D</sup>-mediated lung tumor initiation and cell survival in MEFs. In contrast, B-Raf is required for the proliferative advantage conferred by K-Ras<sup>G12D</sup> *in vitro* and *in vivo*. Together, I demonstrate that Raf proteins can have cancer promoting as well as preventing roles depending on the oncogenic context.

Die abnormale Aktivierung des MAP Kinasen Signalweges ist von grundlegender Bedeutung für die Transformation zahlreicher Zelltypen. Dies kann durch häufig in menschlichen Tumoren vorkommenden Ras und B-Raf Punktmutationen erreicht werden. Obwohl die kausale Rolle des hyperaktiven MAPK Signalweges in der Krebsentstehung etabliert ist, ist die Regulierung des Signalweges durch das komplexe Zusammenspiel von Ras und Raf Proteinen nur teilweise bekannt. In dieser Arbeit zeige ich, daß das Proto-onkogen C-Raf der onkogenen Aktivität der am häufigsten im Krebs vorkommenden B-Raf Mutante (B-Raf<sup>V600E</sup>) entgegenwirkt, indem es einen B-Raf<sup>V600E</sup>-C-Raf Komplex mit verminderter Kinaseaktivität bildet. Interessanterweise werden B-Raf<sup>V600E</sup>-C-Raf Komplexe von onkogenem Ras stabilisiert, was das Fehlen von gemeinsam auftretenden Ras und B-Raf Mutationen in humanem Krebs erklären könnte. Um den hemmenden Einfluß von C-Raf auf B-Raf<sup>V600E</sup> *in vivo* untersuchen zu können, wurde ein B-Raf<sup>V619E</sup> Mausmodell entwickelt (murines B-Raf<sup>V619E</sup> entspricht dem humanen B-Raf<sup>V600E</sup>). B-Raf<sup>V619E</sup> transformiert von diesen Mäusen gewonnene MEFs und induziert Überpigmentierung wenn B-Raf<sup>V619E</sup> in den Melanozyten dieser Mäuse aktiviert wird. Da die Expression von B-Raf<sup>V619E</sup> zur Zelltransformation *in vitro* und *in vivo* führt, kann dieses Mausmodell zur weiteren Aufklärung der B-Raf<sup>V600E</sup>-C-Raf Beziehung herangezogen werden. Da C-Raf einen negative Effekt auf B-Raf<sup>V600E</sup> ausübt, wurde untersucht, ob C-Raf in der K-Ras<sup>G12D</sup>-induzierten Zelltransformation eine Rolle spielt. Der homozygote Knock-out von C-Raf unterdrückt K-Ras<sup>G12D</sup>-induzierte Lungenkrebsentstehung und die anti-apoptotische Funktion von K-Ras<sup>G12D</sup> in MEFs. Im Gegensatz dazu reguliert K-Ras<sup>G12D</sup> die Zellteilung von Lungenkrebszellen *in vivo* und MEFs *in*

*vitro* durch B-Raf. Zusammenfassend habe ich gezeigt, daß Raf Proteine sowohl den Krebs begünstigende als auch unterdrückende Rollen spielen können und daß dies von dem onkogenen Kontext abhängig ist.



### **3. Introduction**

#### **3.1 The Ras/Raf/MEK/ERK pathway**

Normal cellular behavior is controlled by complex signaling networks that ensure that the proper response to intra- and extracellular cues is executed. Signaling through the Ras/Raf/MEK/ERK pathway (or mitogen-activated protein kinase (MAPK) pathway) is triggered by extracellular stimuli and regulates a variety of biological processes, such as proliferation, differentiation and cell death. Binding of mitogenic ligands to receptor tyrosine kinases (RTKs), such as the epidermal-growth-factor-receptor (EGFR), induces activation of RTKs through autophosphorylation. Phosphorylated receptors recruit the adaptor protein growth-factor-receptor-bound protein 2 (GRB2) by binding to its SH2 domain. SH2 (Src homology 2) domains are protein domains capable of binding to phosphorylated tyrosine residues. GRB2 binds the guanine exchange factor (GEF) son-of-sevenless (SOS) through its SH3 domain (a domain capable of binding Proline-rich motifs), thereby locating SOS to the plasma membrane. Ras proteins are also localized to the plasma membrane as a result of post-translational modifications. The close proximity of SOS and Ras results in activation of the latter by promoting nucleotide exchange on Ras. Active Ras recruits Raf proteins to the plasma membrane where it binds them and promotes their activation. Subsequently, Raf phosphorylates MAPK and extracellular signal-regulated kinase (ERK) kinase 1 and 2 (MEK1 and MEK2), which in turn activate ERK1 and ERK2 by phosphorylation. Activated ERK has both cytoplasmic and nuclear effectors and most attention has been focused on its ability to phosphorylate transcription factors. Among the transcription factors

that are activated by ERK are the ETS family of transcription factors and AP1. As a consequence of engaging these transcription factors, key regulatory proteins of the cell cycle, such as the Cyclin D family, are expressed to promote cell cycle progression. This model of the pathway is widely accepted (for review see Downward, 2003), however, it certainly is an oversimplification. There are additional mediators of the receptor-GRB2 interaction. Furthermore, tyrosine phosphorylated non-receptor proteins can recruit GRB2 to the plasma membrane and additional enzymes can regulate the nucleotide exchange on Ras. Moreover, several proteins such as 14-3-3, kinase suppressor of Ras (KSR), and connector enhancer of KSR (CNK) are important regulators of the activation of the Raf/MEK/ERK cascade. Finally, negative regulators, some of which are regulated by the pathway itself, assure that the pathway is tightly controlled. Deregulation of the MAPK pathway is frequently observed in disease. Indeed, mutation of key components, such as Ras and B-Raf, results in hyperactivation of the pathway and commonly occurs in cancer.

### 3.2 Ras proteins

Ras research began in the 1960s when it was discovered that murine leukemia viruses prepared from a leukemic rat could induce sarcomas in newborn mice (Harvey, 1964). Several other retroviruses with similar tumor inducing potential were subsequently identified (Kirsten and Mayer, 1967; Peters et al., 1974; Rasheed et al., 1978). It was later established that these recombinant viruses had incorporated rat genes into their genomes (H-Ras in the Ha-MSV strain, K-Ras in the Ki-MSV strain) (Ellis et al., 1981). H-Ras and

K-Ras were discovered to be human oncogenes when genomic DNA isolated from human tumor cell lines was shown to transform NIH3T3 fibroblasts (Shih and Weinberg, 1982) and that these transformed cells contained genes homologous to the *v-ras* oncogenes (Der et al., 1982; Parada et al., 1982; Santos et al., 1982). Later, a third Ras gene, N-Ras, was discovered in human neuroblastoma and sarcoma cell lines (Hall et al., 1983; Reddy et al., 1982).

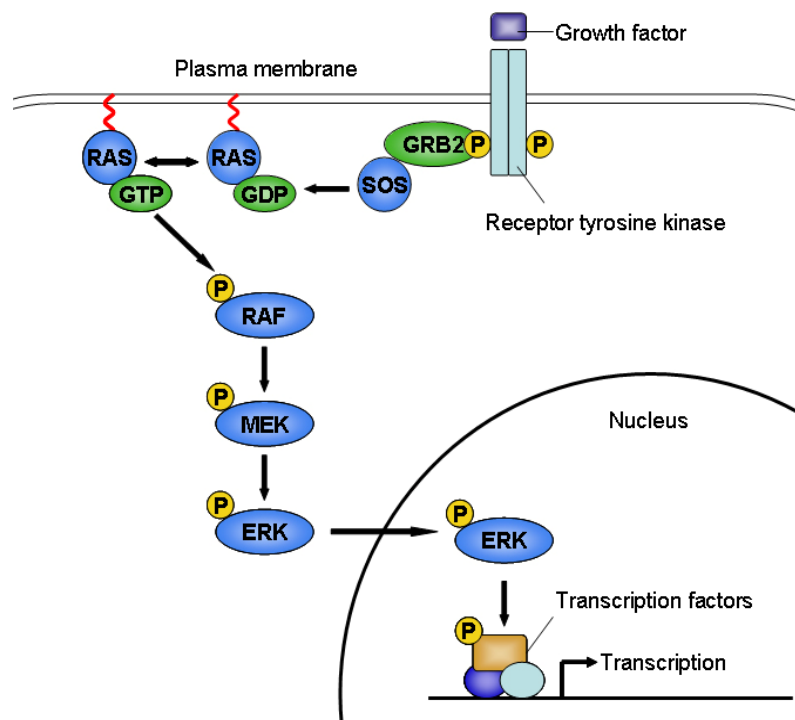


Figure 3.1: The Ras/Raf/MEK/ERK signaling pathway. See text for detailed description.

The Ras genes code for small GTPases and are ubiquitously expressed (Chesa et al., 1987; Furth et al., 1987; Leon et al., 1987). Interestingly, two alternative splice variants of K-Ras exist, K-Ras4A and K-Ras4B, which differ in their composition of the C-terminus. Ras proteins share a high degree of sequence homology (85%) and have comparable transforming and ERK-

activating abilities, which led to the belief that Ras proteins are functionally redundant. However, gene targeting experiments revealed that Ras proteins have unique functions. H-Ras knock-out mice display no obvious phenotype (Esteban et al., 2001), indicating that H-Ras is dispensable for mouse development. A role for H-Ras in tumorigenesis has been established as H-Ras deficiency impairs carcinogen-induced skin tumor formation (Ise et al., 2000). Similar to H-Ras, N-Ras is not required for mouse development as N-Ras null mice are viable (Esteban et al., 2001; Umanoff et al., 1995). N-Ras knock-out mice show a defective immune response and T-cell function (Perez de Castro et al., 2003). In contrast, K-Ras deficiency is embryonic lethal due to fetal liver defects and anemia (Johnson et al., 1997; Koera et al., 1997). However, this phenotype appears to be due to the lack of K-Ras4B expression, as K-Ras4A is dispensable for mouse development (Plowman et al., 2003). These results indicate that Ras proteins have non-overlapping functions and that K-Ras deficiency can not be compensated for by H-Ras and N-Ras. Furthermore, many human tumor types are associated with predominant mutations in one of the Ras genes, indicating that Ras proteins possess distinct oncogenic properties in different cell types.

Ras proteins need to be localized to the plasma membrane in order to be activated (reviewed in Downward, 2003; Konstantinopoulos et al., 2007). Membrane anchoring is promoted by post-translational modification of the carboxy-terminal CAAX motif. Newly synthesized Ras is cytosolic and becomes isoprenylated on the Cysteine residue of its CAAX motif by Farnesyltransferase (FTase). This results in association of Ras with

intracellular membranes. Next, Ras converting enzyme 1 (RCE1) catalyzes the release of the three amino acids downstream of the isoprenylcysteine by endoproteolytic digest. Finally, the isoprenylcysteine is methylated by isoprenylcysteine carboxyl methyltransferase (ICMT) and translocated to the plasma membrane. Palmitoyltransferase adds one (N-Ras, K-Ras4A) or two (H-Ras) palmitoyl long-chain fatty acids to Cysteine residues just upstream of the farnesylated carboxy-terminal Cysteine, which stabilizes the interaction with the plasma membrane. K-Ras4B is not palmitoylated; instead, a lysine-rich peptide in the C-terminus interacts with the negatively charged lipid head groups thereby enhancing the interaction with the plasma membrane. In the absence of FTase activity, K-Ras and N-Ras can be isoprenylated by geranylgeranyltransferase type I (GGTase-I), potentially explaining the disappointing performance of FTase inhibitors in an attempt to therapeutically target oncogenic Ras in cancer patients.

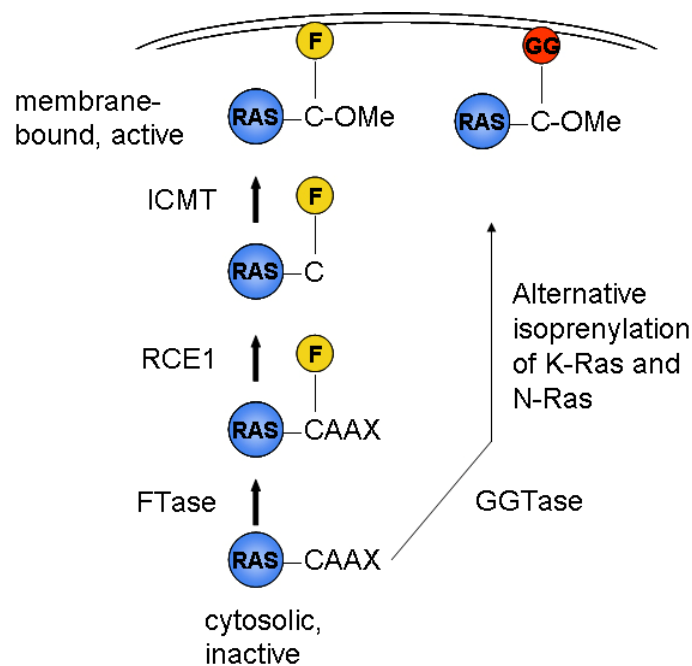


Figure 3.2: Post-translational modification of Ras. See text for detailed description. F, 15-C farnesyl isoprenoid; GG, 20-C geranylgeranyl isoprenoid.

Once Ras is localized to the plasma membrane, it can be activated. Inactive Ras is bound to GDP and fails to interact with downstream effectors. However, guanine nucleotide exchange factors (GEFs), such as SOS catalyze the replacement of GDP with GTP, the most abundant guanine nucleotide in the cytoplasm. GTP-bound, active Ras can bind several effector substrates thereby activating about a dozen signaling pathways including the PI3K-AKT and Raf/MEK/ERK pathways. Ras has low intrinsic GTPase activity and slowly converts bound GTP to GDP. Importantly, GTP hydrolysis is greatly catalyzed by GTPase activating proteins (GAPs), resulting in inactivation of Ras. It is the balance of GEFs and GAPs that regulates the activation of wildtype Ras and its downstream signaling pathways.

### 3.3 Raf proteins

Like Ras oncogenes, C-Raf was discovered as an acquired oncogene in tumor-inducing retroviruses. The mouse type C virus 3611-MSV induced rapidly growing fibrosarcomas in mice and the oncogene that was cloned from it was termed v-raf while its cellular homologue was named C-Raf (Rapp et al., 1983). Shortly thereafter, the avian acute leukemia retrovirus MH2 was found to carry another potential oncogene in addition to v-myc (Jansen et al., 1983a; Jansen et al., 1983b). Hybridization and sequencing analysis of the two viruses confirmed that they had in fact incorporated orthologic gene sequences of C-Raf (Jansen et al., 1984; Sutrave et al., 1984). Subsequently, two additional members of the Raf family were identified and termed A-Raf and B-Raf (Beck et al., 1987; Huebner et al., 1986; Huleihel et al., 1986; Ikawa et al., 1988; Sithanandam et al., 1990).

Raf proteins are Serine/Threonine kinases that share very high amino acid sequence homology in three conserved regions (CR1-3). CR1 contains the Ras-binding domain (RBD) and a Cysteine-rich domain (CRD), CR2 is thought to be the 'hinge-region' of the protein and contains regulatory Serine and Threonine residues, and CR3 spans the highly conserved kinase domain. Raf proteins are broadly expressed but vary in their expression levels. C-Raf is expressed at high levels in all tissues, whereas A-Raf and B-Raf are expressed highest in urogenital and neuronal tissues, respectively (Mercer and Pritchard, 2003 and references therein). Interestingly, B-Raf is subjected to alternative splicing which results in proteins that harbor a truncated N-terminus or contain alternative exon 8b or 10a. Indeed, some B-Raf antibodies detect proteins between 60 and 96 kDa in size. Exons 8b and 10a localize to the hinge-region and are believed to change the conformation, thereby impacting on the kinase activity (Barnier et al., 1995; Papin et al., 1998).

All three Raf proteins possess kinase activity towards MEK but MAPK-independent functions have only been described for C-Raf. In a kinase-independent fashion, C-Raf antagonizes the pro-apoptotic proteins MST2 (O'Neill et al., 2004), ASK1 (Chen et al., 2001) and BAD (Wang et al., 1996). Furthermore, C-Raf inhibits ROK $\alpha$  by direct interaction, thereby regulating cell death and migration (Ehrenreiter et al., 2005; Piazzolla et al., 2005). Whether A-Raf or B-Raf phosphorylate substrates other than MEK1/2, and have kinase-independent functions remains to be determined.

Upon Ras activation, Raf proteins are recruited to the plasma membrane. Ras binds to the RBD and with lower affinity to the Cysteine-rich domain located in CR1 (reviewed in Mercer and Pritchard, 2003). All Ras isoforms are able to bind to C-Raf but with varying intensities. K-Ras binds more efficiently than N-Ras, which binds better than H-Ras (Voice et al., 1999). Less is known about the interaction of B-Raf or A-Raf with Ras, but B-Raf appears to bind H-Ras *in vitro* as efficiently as C-Raf (Okada et al., 1999; Shinkai et al., 1996). Ras-binding itself is not sufficient to activate Raf but rather serves to translocate Raf to the plasma membrane where it is activated by phosphorylation and dephosphorylation events. A model for C-Raf activation has been proposed recently (Dhillon et al., 2002; Wellbrock et al., 2004a). Cytoplasmic inactive C-Raf is phosphorylated at Serines 43, 259 and 621 by the cAMP-dependent kinase protein kinase A (PKA). S43 phosphorylation prevents the interaction of Ras with Raf through sterical hindrance, while phosphorylation of S259 and S621 promotes binding of 14-3-3 proteins and maintains C-Raf in an inactive conformation. S259 can also be phosphorylated by AKT. Ras-GTP displaces 14-3-3 from C-Raf and, at the plasma membrane, S259 is dephosphorylated by phosphatases such as PP2A. Next, Serine 338 and Tyrosine 341 are phosphorylated by activating kinases, thereby negatively charging the N-region, which is essential for full C-Raf activation. Src phosphorylates Y341 (Mason et al., 1999; Wellbrock et al., 2004a); and the identity of the S338 kinase may be PAK Serine/Threonine kinases (Wellbrock et al., 2004a). Finally, phosphorylation of T491 and S494 in the activation segment is required for C-Raf activation but the activating kinases remain elusive. The activation process of B-Raf is fundamentally different from that of C-Raf. In



contrast to C-Raf, B-Raf has two Aspartic Acid residues at the equivalent positions to Tyr340 and Tyr341 (Asp448 and Asp449). The negative charge of the Aspartic Acid residues is likely to mimic phosphorylation of these sites. Furthermore, Ser446 (equivalent to S338 in C-Raf) is constitutively phosphorylated. The presence of D448, D449 and pS446 allows inactive B-Raf to adopt a fairly open conformation compared to C-Raf. Upon ligand binding B-Raf is recruited to the plasma membrane by Ras-GTP, where it is dephosphorylated at S365 (S259 in C-Raf), thereby releasing 14-3-3. Unknown kinase(s) then phosphorylate(s) B-Raf at Thr599 and Ser602, resulting in full activation of the kinase. The different mechanisms of activation may result in the frequent occurrence of activating mutations in B-Raf but not in C-Raf. Even though a model for A-Raf activation has not been proposed, A-Raf activation is likely very similar to that of C-Raf based on their sequence similarities. This is supported by the notion that, similar to C-Raf, single amino acid substitution is not sufficient to activate A-Raf. Thus, all Raf proteins rely on phosphorylation of the activation segment within the kinase domain but differ in that A-Raf and C-Raf require additional phosphorylation within the N region of the kinase domain for full activity (Chong et al., 2001; Mason et al., 1999; Zhang and Guan, 2000).

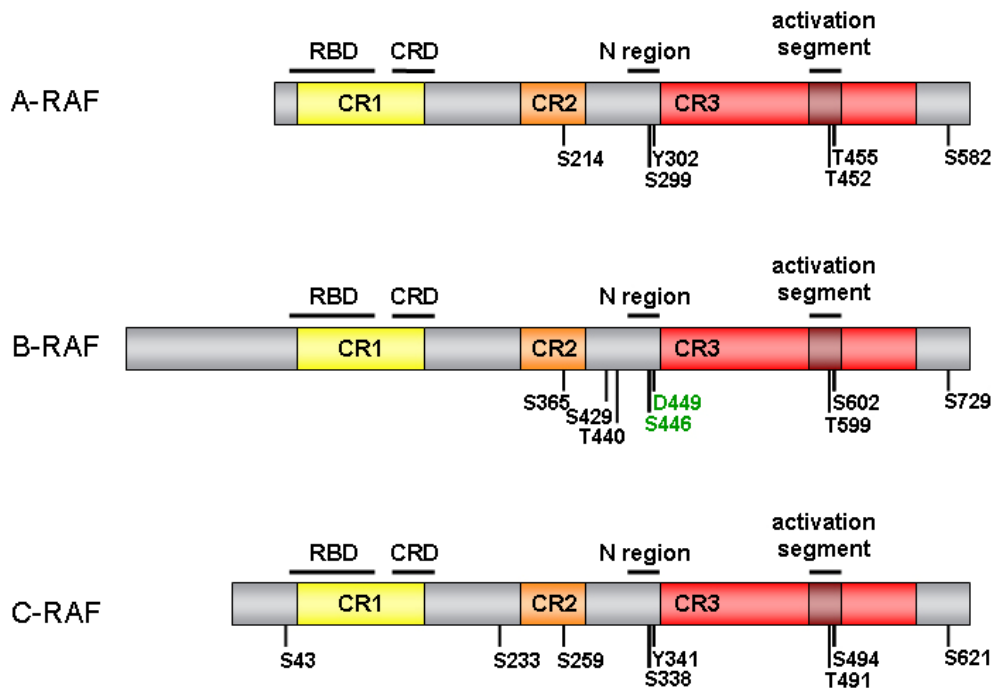


Figure 3.3: Schematic outline of Raf proteins. Conserved regions (CR) 1, 2, and 3 are depicted in yellow, orange, and red, respectively. The phosphorylation sites required for activation are highlighted. Note that S446 in B-Raf is constitutively phosphorylated (see text for detailed description). RBD, Ras binding domain; CRD, Cysteine-rich domain.

Knock-out mouse models have provided further insight into the functions of Raf proteins. A-Raf knock-out mice survive embryonic development but die around weaning age due to postnatal neurological and gastrointestinal defects (Pritchard et al., 1996). Mice deficient for C-Raf die during embryonic development due to fetal liver apoptosis (Huser et al., 2001; Mikula et al., 2001). Interestingly, neither A-Raf null nor C-Raf null cells exhibit defective MEK activation, suggesting that either B-Raf is the major activator of the MAPK pathway or that deficiency of one Raf protein is compensated for by

the other two (Huser et al., 2001; Mercer et al., 2002; Mikula et al., 2001; Zhong et al., 2007). Conditional deletion of C-Raf in cardiomyocytes leads to apoptosis and cardiac dysfunction, which is rescued by ASK1 ablation (Yamaguchi et al., 2004). Furthermore, C-Raf is required for erythroid differentiation (Kolbus et al., 2002; Rubiolo et al., 2006). B-Raf knock-out mice die during midgestation due to apoptosis of terminally differentiated endothelial cells and systemic vascular collapse (Wojnowski et al., 1997). A recent report showed that conditional deletion of B-Raf impaired placental vascularization, leading to embryonic lethality, whereas B-Raf expression in the embryo proper is dispensable for development (Galabova-Kovacs et al., 2006). This discrepancy between the germline and conditional knock-out mice could potentially be due to expression of a truncated B-Raf protein in the germline knock-out mice. Conditional B-Raf knock-out mice further revealed that B-Raf is critical for the development of the central nervous system (Chen et al., 2006; Galabova-Kovacs et al., 2008; Zhong et al., 2007) as well as for tumor angiogenesis and progression in the RIP-Tag model of insulinomas (Sobczak et al., 2008). Importantly, cells derived from conditional B-Raf knock-out mice exhibit decreased activation of the MAPK pathway (Galabova-Kovacs et al., 2008; Galabova-Kovacs et al., 2006; Sobczak et al., 2008; Zhong et al., 2007). Thus, Raf proteins have distinct functions during embryonic development and B-Raf seems to be the major activator of the MAPK pathway in several cell types and contexts.

### 3.4 Regulation of the MAPK pathway

As the MAPK pathway controls a multitude of biological processes, the transduction of extracellular stimuli has to be tightly regulated and is often ligand, context- and cell type-dependent. The first level of regulation of the MAPK pathway is represented by Ras-mediated Raf activation. The four Ras proteins vary in their affinity for the Ras binding domains of the individual Raf proteins (Weber et al., 2000). Furthermore, Ras proteins localize to distinct microdomains in the plasma membrane, thereby exposing Raf proteins to different environments (Hancock, 2003). In addition, Raf proteins may be activated by several activating kinases in Ras-dependent and -independent manners. Moreover, RHEB has been suggested to reduce Raf activity and dimerization potential by antagonizing phosphorylation of the N-region (Karbowniczek et al., 2004; Karbowniczek et al., 2006). Another layer of regulation is added by scaffolding and adaptor proteins. Binding to 14-3-3 proteins maintains Raf in an inactive conformation, and displacement of 14-3-3 is mediated by dephosphorylation of 14-3-3 binding residues on Raf. Moreover, kinase suppressor of Ras (KSR) mediates complex formation of Raf, MEK, and ERK, thereby promoting MAPK activation (Kolch, 2005). Another adaptor protein, connector enhancer of KSR (CNK), associates with Raf and co-operates with Ras to stimulate Raf activation (Kolch, 2005). Finally, Raf kinase inhibitor protein (RKIP) binds both Raf and MEK to prevent their physical interaction, thereby inhibiting MEK activation (Kolch, 2005). The biological outcomes also depend on signal intensity. Raf proteins form both homo- and heterodimers (Farrar et al., 1996; Luo et al., 1996; Weber et al., 2001), and these complexes exhibit distinct activities towards MEK (Garnett et

al., 2005; Rushworth et al., 2006, Karreth et al., in press). Inactivation of the MAPK pathway is regulated by several mechanisms. First, SOS is phosphorylated by active ERK and p90 RSK-2, a MAPK target, leading to dissociation of GRB2 and down-regulation of the MAPK pathway (Dong et al., 1996; Douville and Downward, 1997; Waters et al., 1995). Furthermore, ERK directly phosphorylates C-Raf to disrupt the interaction with Ras, thereby desensitizing C-Raf for additional stimuli (Dougherty et al., 2005). Second, MAPK signaling transcriptionally up-regulates the negative regulators Sprouty and Sprouty-related proteins with an EVH1 domain (SPRED). These proteins can bind and sequester both GRB2 and Raf, thereby antagonizing activation of the MAPK pathway (Kim and Bar-Sagi, 2004). Finally, the MAPK pathway is subjected to regulation by phosphates, such as dual-specificity phosphatases (DUSP) on several levels (Dhillon et al., 2007).

### 3.5 Ras and cancer

Ras is one of the most commonly mutated oncogenes in cancer. In fact, approximately 30% of cancer cases harbor a Ras mutation (Bos, 1989). Three hotspot residues have been identified – G12, G13, Q61 – but other, less common cancer-associated mutations with transforming ability have been found (for example Scholl et al., 2009). Mechanistically, the hotspot mutations impair the intrinsic GTPase activity of Ras and prevent the association with extrinsic GAPs, thereby locking it in the GTP-bound state. Thus, all Ras effector pathways are constitutively and growth-factor-independently activated. K-Ras is mutated in about 85% of cancers with Ras mutations and the K-Ras4A splice form has been shown to have higher oncogenic potential

than K-Ras4B (To et al., 2008; Voice et al., 1999). N-Ras and H-Ras mutations are relatively rare and found in 15% and <1% of cases. Interestingly, each Ras family member is mutated in a specific subset of human malignancies: K-Ras is commonly mutated in epithelial cancers of the pancreas, lung and colon; N-Ras mutations occur frequently in melanoma, liver and myeloid malignancies; and H-Ras mutations have been observed in bladder cancer. Intriguingly, the occurrence of Ras mutations in certain cell types appears to be dependent on the genomic locus rather than the gene itself (To et al., 2008). Furthermore, the wildtype K-Ras allele can act as a tumor suppressor in lung tumorigenesis driven by carcinogen-induced K-Ras mutations (Zhang et al., 2001), suggesting that Ras-mediated carcinogenesis is subject to multiple forms of modulation.

### 3.6 Raf and cancer

Despite being first identified as a viral oncogene, C-Raf is very rarely mutated in human cancer. In fact, only two germ-line C-Raf polymorphisms have been found in patients with therapy-related AML. Both of these mutations possess transforming properties but only one showed increased kinase activity (Zebisch et al., 2006). Furthermore, sequencing of 545 tumor cell lines identified four C-Raf mutations, three of which displayed no appreciable increase in kinase and transforming activity (Emuss et al., 2005). The remaining mutation showed increased kinase activity but failed to transform NIH3T3 fibroblasts (Emuss et al., 2005). These data suggest that C-Raf is not a target of somatic mutation in cancer, as single amino acid substitutions fail to hyperactivate C-Raf. This is likely due to the complex activation of C-Raf,

which cannot be mimicked by a single mutation. Similar to C-Raf, cancer-associated mutations in A-Raf are extremely infrequent. One study found a single A-Raf mutation in 60 cell lines and 323 primary tissue samples but did not report on its transforming ability (Lee et al., 2005). B-Raf is the member of the Raf family that is frequently mutated in cancer. 8% of human tumors harbor a B-Raf mutation and cancers commonly associated with B-Raf mutations are melanoma, thyroid, ovarian and intestinal cancers. Cell types commonly harboring B-Raf and Ras mutations partially overlap, suggesting that these cell types are particularly susceptible to MAPK hyperactivation. Over 30 B-Raf mutations have been observed, all of which are in the kinase domain. There are two hotspots for B-Raf mutations, the DFG motif and the P loop, which interact to maintain B-Raf in the inactive conformation (Wan et al., 2004). Mutations located in these motifs disrupt their interaction and promote the active conformation of B-Raf. Two distinct classes of B-Raf mutations have been identified. The more prominent class of mutations constitutively activates B-Raf, leading to increased activity towards MEK. The Glutamic Acid to Valine amino acid substitution at position 600 is the predominant B-Raf mutation and is found in over 85% of B-Raf mutant tumors. Val600 is flanked by activating phospho-residues Thr599 and Ser602 and replacing Val600 with a Glutamic Acid places a negative charge between Thr599 and Ser602, thereby mimicking phosphorylation of the two sites. The second class of mutations impairs the catalytic activity of B-Raf. These mutations localize to the Glycine residues of the GXGXXG motif in the P loop of the kinase domain. Even though these mutants adopt an open conformation, they have very limited activity towards MEK because they cannot optimally catalyze ATP.

However, impaired activity mutants are able to associate and co-operate with C-Raf to hyperactive the MAPK pathway (Garnett et al., 2005; Wan et al., 2004). Interestingly, impaired activity mutations and increased activity mutations predominate in distinct cancer types, indicating that their transforming potential is cell type dependent and that additional factors are important for their full oncogenic activity.

### 3.7 Modelling oncogenic Ras/Raf signalling in the mouse

Karreth FA and Tuveson DA, Curr Opin Genet Dev. 2009;19(1):4-11



# Modelling oncogenic Ras/Raf signalling in the mouse

Florian A Karreth<sup>1,2</sup> and David A Tuveson<sup>1</sup>

The Ras/Raf/MEK/ERK (or MAPK) signalling pathway relays extracellular stimuli to the nucleus, thereby regulating diverse cellular responses such as proliferation, growth, differentiation and apoptosis. Perturbation of these processes by aberrant MAPK signalling often leads to malignant transformation as indicated by the frequent occurrence in human cancers of genetic alterations affecting this pathway. In recent years, genetically modified mouse models have proven instrumental in unravelling how deregulated MAPK signalling leads to disease. Indeed, conditional activation of oncogenic K-Ras or B-Raf in mice resulted in neoplasms that closely resemble the human disease. Such tractable mouse models will enable the pursuit of basic biological mechanisms and translational applications regarding the MAPK pathway.

## Addresses

<sup>1</sup> Li Ka Shing Centre, Cambridge Research Institute, Cancer Research UK, Robinson Way, Cambridge CB2 0RE, United Kingdom

<sup>2</sup> University of Vienna, Dr. Bohrgasse, 1030 Vienna, Austria

Corresponding author: Tuveson, David A ([david.tuveson@cancer.org.uk](mailto:david.tuveson@cancer.org.uk))

Current Opinion in Genetics & Development 2009, 19:4–11

This review comes from a themed issue on  
Genetic and cellular mechanisms of oncogenesis  
Edited by Julian Downward and William Hahn

Available online 7th February 2009

0959-437X/\$ – see front matter

© 2009 Elsevier Ltd. All rights reserved.

DOI 10.1016/j.gde.2008.12.006

## Introduction: the MAPK pathway

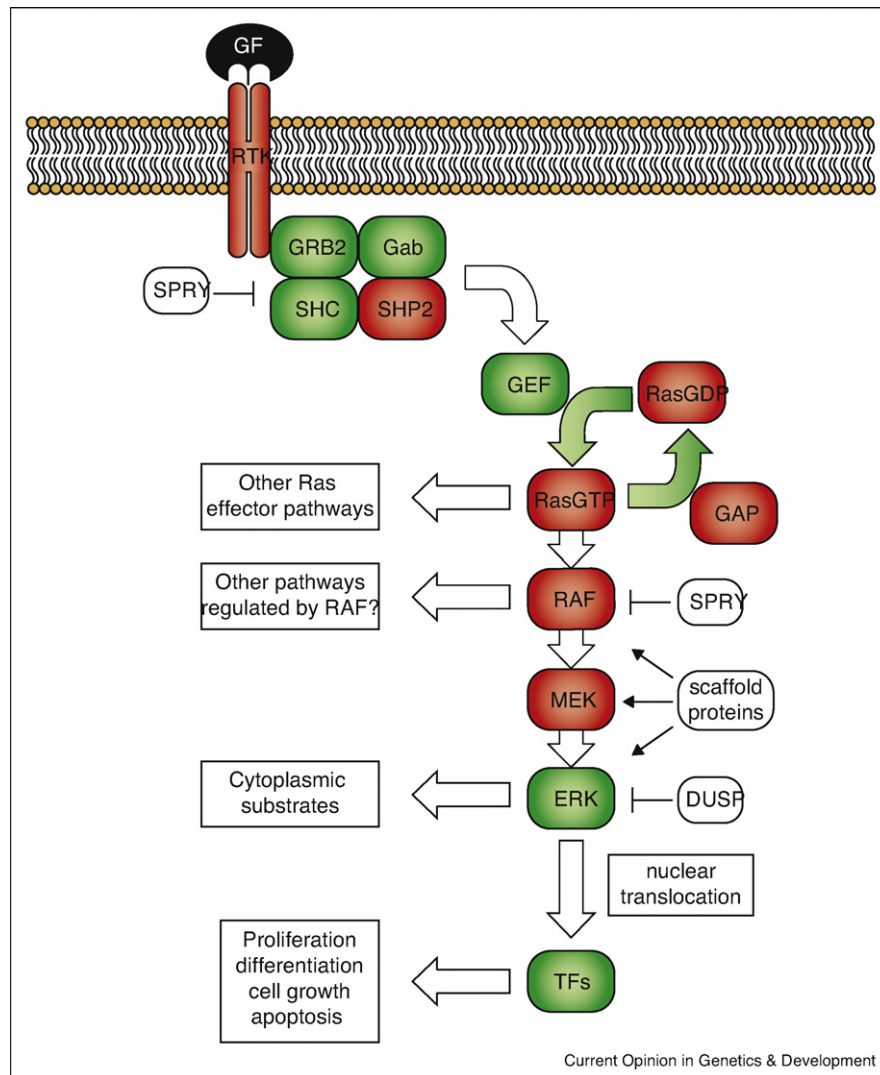
The MAPK pathway is essential for organismal development and has been elucidated through genetic and biochemical approaches over the past several decades. The pathway is proximally activated by growth factor binding to receptor tyrosine kinases (RTK), resulting in RTK phosphorylation and activation. Consequently, adaptor molecules localize to RTKs followed by recruitment and activation of guanine nucleotide-exchange factors (GEFs). GEFs catalyse the transition from GDP-bound, inactive Ras to GTP-bound, active Ras. Ras-GTP interacts with more than a dozen effector molecules to regulate a variety of biological processes [1]. GTPase-activating proteins (GAPs) allosterically stimulate the intrinsic GTPase activity of Ras, leading to GTP hydrolysis and Ras inactivation. To activate the MAPK signalling cascade, Ras recruits Raf to the cell membrane, where Raf is activated and subsequently forms complexes with MEK, ERK and scaffolding proteins. Raf then phosphor-

ylates MEK, which in turn phosphorylates ERK. ERK both activates cytosolic substrates and translocates to the nucleus to stimulate diverse gene expression programs through transcription factors such as JUN and ELK1 (Figure 1). The recent recognition of inhibitory feedback loops through phosphatases and binding proteins with no obvious catalytic activity has added a new dimension to our understanding of the MAPK pathway. Therefore, the MAPK ‘pathway’ is rather a complex network that is still being elucidated.

The importance of the MAPK pathway in neoplasms is evident through the discovery of mutant alleles that hyperactivate the pathway in a variety of human cancers. First, oncogenic mutations in RTKs abnormally activate Ras and its downstream substrates [2]. Second, activating Ras mutations have been detected in approximately 30% of human cancers [3]. These mutations occur in codons 12, 13, and 61 and markedly diminish GTPase activity, thereby rendering Ras locked in the GTP-bound, active state. In mammals, the *Ras* family consists of three genes: *K-Ras*, *N-Ras* and *H-Ras*. While *K-Ras* is the predominantly mutated family member (in ~85% of cancers harboring *Ras* mutations), *N-Ras* and *H-Ras* mutations are relatively uncommon (~15% and <1%, respectively) [4]. Interestingly, each *Ras* family member is mutated in a specific subset of human malignancies: *K-Ras* is commonly mutated in epithelial cancers of the pancreas, lung and colon; *N-Ras* mutations occur frequently in melanoma, liver and myeloid malignancies; and *H-Ras* mutations have been observed in bladder cancer (Table 1). Third, activating mutations in *B-Raf*, a member of the *Raf* family, have been discovered with high frequency in melanoma (in a non-overlapping pattern with mutations in *N-Ras*) and, to a lesser extent, in thyroid, ovarian and colon cancer [5–7]. Importantly, activating missense mutations do not occur in the other members of the *Raf* family, *A-Raf* and *Raf-1*, which may be due to their more complex mode of activation [8]. Single amino acid substitutions are sufficient to promote the active conformation of B-Raf, thereby constitutively activating the MAPK pathway. Finally, loss of negative regulators, such as members of the Sprouty family and GAPs such as NF1, can indirectly hyperactivate the MAPK signalling cascade. It is estimated that most tumors exhibit deregulation of the MAPK pathway, making it an attractive target for therapeutic intervention.

In recent years, several mouse models have been generated to establish a causal relationship between MAPK mutations found in human cancer and tumor development. These mouse models have furthered our understanding of

Figure 1



The Ras/Raf/MEK/ERK pathway. Binding of growth factors (GF) to receptor tyrosine kinases (RTK) leads to recruitment of adaptor proteins and guanine exchange factors (GEF). GEFs promote the active form of Ras (RasGTP). Ras signals to different pathways, one being the Raf/MEK/ERK pathway. Ras activates Raf, which may have several downstream effectors. Raf phosphorylates MEK followed by ERK phosphorylated by MEK. ERK has cytoplasmic substrates and also translocates to the nucleus to activate a variety of transcriptional programmes through several transcription factors (TFs). The signalling cascade is negatively regulated by Sprouty proteins (SPRY) and dual-specificity phosphatases (DUSP). Proteins in red have been found genetically altered in human cancers resulting in hyperactivation of the MAPK pathway.

cellular transformation by aberrant MAPK signalling and offer a powerful tool for preclinical testing of novel therapeutics. In this review, we will discuss the most recent advances of mouse cancer models that involve deregulated MAPK pathway activation.

### Oncogenic Ras mouse models

Mouse models of cancer are most valuable when they recapitulate the cardinal pathophysiological and molecular aspects of the corresponding human malignancy [9]. For example, accurate mouse models of neoplasias that utilize the conditional endogenous expression of onco-

genic K-Ras have been described [10–12]. These models incorporated a loxP-flanked transcriptional stop cassette (lox-stop-lox or LSL) to conditionally permit spatiotemporal regulation of oncogenic K-Ras expression by Cre-mediated excision of the LSL. This approach allows oncogenic K-Ras expression at physiological levels; however, a potential weakness is the expression of only one copy of wildtype K-Ras in cells lacking Cre. Even though the models by Guerra *et al.* [10] and Jacks and colleagues [11–13] differed in their neoplastic phenotypes, in each model expression of oncogenic K-Ras was sufficient to induce hyperplasia. While the Jacks laboratory described

**Table 1****Occurrence of Ras and B-Raf in human cancers.**

Tissue	K-Ras (%)	N-Ras (%)	H-Ras (%)	BRAF (%)
Biliary tract	32	1	0	14
Bone	1	0	2	0
Breast	5	1	1	2
CNS	1	2	0	3
Cervix	8	1	9	1
Endometrium	14	0	1	1
GI tract (site indeterminate)	19	0	0	0
Haematopoietic and Lymphoid tissue	5	12	0	2
Kidney	1	0	0	0
Large intestine	32	3	0	13
Liver	7	4	0	3
Lung	17	1	0	2
Melanoma	1	17	1	64
Oesophagus	4	0	0	2
Ovary	15	4	0	13
Pancreas	60	2	0	2
Prostate	8	1	6	6
Salivary gland	4	0	16	0
Skin <sup>a</sup>	2	19	5	41
Small intestine	20	25	0	5
Soft tissue	12	6	7	3
Stomach	6	2	4	1
Testis	5	4	0	0
Thyroid	3	7	4	37
Urinary tract	4	3	12	0

Data derived from COSMIC database; <http://www.sanger.ac.uk/genetics/CGP/cosmic>.

<sup>a</sup> Skin cancers including melanoma.

pulmonary [12], pancreatic [13] and colonic [11] hyperplasia and neoplasms, Guerra *et al.* reported lung adenomas, histiocytic sarcomas and sarcomas [10]. Further phenotypes have been characterized in both models and will be discussed in more detail below. The phenotypic differences may be attributed to the genetic backgrounds of the mouse strains used, the amino acid substitution modelled (G12V vs. G12D in ref. [10] vs. refs. [11–13], respectively), or the use of a bicistronic K-Ras<sup>G12V</sup>-IRES-βgeo mRNA that could influence transcription and/or translation [10]. Using an inducible transgenic approach, it has been shown *in vivo* that variations in mutant Ras levels manifested different biological outcomes [14<sup>••</sup>]. Indeed, high levels of mutant H-Ras<sup>G12V</sup> induced a growth arrest in mammary epithelial cells in a p16<sup>INK4A</sup>/p19<sup>ARF</sup>- and p53-dependent manner, whereas expression levels similar to endogenously expressed K-Ras<sup>G12D</sup> resulted in mammary epithelial hyperplasia but were insufficient to induce frank malignancy [14<sup>••</sup>]. Although Ras mutations are uncommon in human breast cancer, these findings further substantiate the notion that initial expression of mutant Ras genes at physiological levels is required to accurately study Ras-induced human cancers in mice. Because mutations in *K-Ras* are common in many human tumor types, the development of mice expressing physiological levels of oncogenic K-Ras thus provided the opportunity to study a variety of human cancers in mice.

To this end, K-Ras mutant mice have been crossed to several tissue-specific Cre transgenic mouse strains. These mouse models displayed hyperplastic and neoplastic phenotypes in epithelial, mesenchymal and haematopoietic cells. When crossed to pancreas-specific Cre strains, LSL-K-Ras<sup>G12D</sup> mice developed a preinvasive neoplasm of pancreatic ductal adenocarcinoma (PDA), termed pancreatic intraepithelial neoplasia (PanIN), which spontaneously progressed to metastatic PDA at a low frequency [13]. Furthermore, oncogenic K-Ras cooperated with p16<sup>INK4A</sup>/p19<sup>ARF</sup> deficiency [15], p53 mutation [16], perturbed TGFβ signalling [17–19], TGFα activation [20] and chronic pancreatitis [21] to accelerate the formation of PanIN and metastatic cancer. Interestingly, LSL-K-Ras<sup>G12D</sup> mice deficient in TGFβ signalling also developed intraductal papillary mucinous neoplasms (IPMN) [17] and mucinous cystic neoplasms (MCN) [19], which are additional preinvasive precursor lesions of PDA, suggesting that more than one route to pancreatic ductal adenocarcinoma may exist. It is currently unclear which pancreas cell type initiates PanIN in response to oncogenic K-Ras. Some reports point to the exocrine compartment [21–23]; however, it remains incompletely understood whether progenitor cells or terminally differentiated ductal or acinar cells give rise to PanIN and PDA. These pancreatic cancer models closely recapitulate the initiation and progression of the human disease and will allow further characterization of pancreatic cancer development.

In addition to pancreatic cancer, lung cancer can also be modelled with oncogenic K-Ras mice. Intranasal adenoviral Cre (Ad-Cre) instillation in LSL-K-Ras<sup>G12D</sup> mice led to atypical adenomatous hyperplasia, epithelial hyperplasia and adenomas that spontaneously progressed to pulmonary adenocarcinoma [12]. Bronchioalveolar stem cells (BASCs) have been identified in the bronchioalveolar duct junction of mouse lungs [24]. Importantly, BASCs expanded in response to oncogenic K-Ras expression in early lung tumors [24], suggesting that transformed lung stem cells may possess cancer-initiating properties. Furthermore, cooperation of K-Ras<sup>G12D</sup> with both loss and mutation of p53 as well as with PTEN deficiency was demonstrated [25,26]. Interestingly, MAPK activation was not seen in precursor lesions but could be detected in later stage lesions in K-Ras<sup>G12D</sup> mice lacking functional p53 [12,26]. These studies suggest that oncogenic K-Ras-induced MAPK pathway activation remains low, possibly through negative feedback loops. However, in precursor lesions loss of p53 function permits the acquisition of additional mutations that attenuate those feedback loops, leading to elevated MAPK pathway signalling and overt malignancy. This model will prove useful for determining the role of oncogenic K-Ras in lung cancer as well as effector pathways relevant for therapeutic treatment.

In contrast to the lung and pancreas, K-Ras mutations are not an initiating event in colon cancer [27]. Expression of K-Ras<sup>G12V-IRE5-βgeo</sup> alone was not sufficient to induce colonic hyperplasia; however, cooperation with loss of Apc was observed [28]. In other studies, activation of K-Ras<sup>G12D</sup> in colonic epithelium promoted hyperproliferation [11,29,30], which could be rescued by pharmacological MEK inhibition, thus demonstrating dependence of hyperplasias on the MAPK pathway [30]. Furthermore, K-Ras<sup>G12D</sup> expression accelerated colon cancer progression induced by Apc deficiency [30]. The discrepancies in the induction of hyperplasia observed in the two models may be attributed to the reasons discussed above. Nevertheless, both models demonstrated promotion of colonic tumor progression by oncogenic K-Ras.

As opposed to pancreas, lung and colon cancer, K-Ras mutations occur infrequently in the endometrium and soft tissue. Interestingly, injection of Ad-Cre in the bursal cavity of LSL-K-Ras<sup>G12D</sup> mice induced endometriotic-like lesions and peritoneal endometriosis [31]. In addition, concomitant loss of PTEN led to endometrioid ovarian adenocarcinoma, suggesting that K-Ras<sup>G12D</sup>-induced endometriosis may represent a precursor lesion to ovarian adenocarcinoma [31]. K-Ras<sup>G12D</sup> was also reported to be oncogenic in mesenchymal cells, as intramuscular Ad-Cre injection in K-Ras<sup>G12D</sup> mice lacking either functional p53 or p16<sup>INK4A/p19ARF</sup> promoted the formation of soft tissue sarcoma [32]. Thus, LSL-K-Ras<sup>G12D</sup> mice appear to recapitulate the full spectrum of human malignancies carrying K-Ras mutations.

In contrast to solid tumors, K-Ras is not the predominant Ras oncogene in haematopoietic malignancies. Nevertheless, expression of K-Ras<sup>G12D</sup> in haematopoietic cells caused a fatal myeloproliferative disease similar to human juvenile myelomonocytic leukaemia and chronic myelomonocytic leukaemia [33,34] that never progressed to acute myeloid leukaemia. By contrast, mice concomitantly expressing oncogenic K-Ras and a PML-RAR $\alpha$  translocation transgene succumbed to a rapid onset, highly penetrant acute promyelocytic leukaemia-like disease [35], suggesting cooperation of K-Ras<sup>G12D</sup> and secondary mutations in leukaemogenesis. These K-Ras mouse models provided experimental support to a model in which mutation of K-Ras is the neoplasia-initiating event and progression to malignant cancer requires additional genetic changes such as inactivation of tumor suppressor genes.

Compared to oncogenic K-Ras, studies on mutant N-Ras and H-Ras function have largely remained limited in their use of transgenic approaches. For instance, retroviral infection of bone marrow cells with mutant N-Ras [36] as well as H-Ras and K-Ras [37] alleles, followed by transplantation into lethally irradiated hosts, revealed

the leukemogenic potential of all Ras isoforms. In another study, melanocyte-specific expression of H-Ras<sup>G12V</sup> promoted melanomagenesis, which was accelerated by p16<sup>INK4A/p19ARF</sup> deficiency [38]. In addition, mice expressing an H-Ras<sup>G12V</sup> transgene in livers deficient for  $\beta$ -catenin developed hepatocellular carcinomas [39]. Although these transgenic mouse models have contributed to the understanding of Ras-mediated tumorigenesis, they are limited by non-physiological expression levels and the fact that H-RAS mutations are not found in human leukaemia, melanoma or hepatocellular carcinoma.

The successful development of conditional K-Ras mouse models prompted the generation of mouse models carrying cancer-associated mutations in the other Ras family members. Mice conditionally expressing endogenous mutant N-Ras were generated in a fashion similar to LSL-K-Ras<sup>G12D</sup> mice and crossed to colonic epithelium-specific Cre mice. In contrast to K-Ras<sup>G12D</sup> mice, colonic expression of N-Ras<sup>G12D</sup> neither induced hyperplasia nor cooperated with loss of Apc to promote tumor progression [30], providing a rationale for the absence of mutations in colon cancer. The phenotypic differences could reflect that the G12D mutation confers a weaker oncogenic potential on N-Ras than on K-Ras or could reflect different expression levels of the two oncogenes. Accordingly, N-Ras Q61 mutations are more frequently found in human cancers than G12 mutations (COSMIC database; <http://www.sanger.ac.uk/genetics/CGP/cosmic>). Given the lack of a neoplastic phenotype in the mouse colon it will be of future interest to evaluate the oncogenic potential of N-Ras in cell types that show frequent N-RAS mutations in humans such as melanocytes and haematopoietic cells.

H-RAS mutations are uncommon in spontaneous human cancer. However, germline expression of mutant H-RAS is associated with Costello syndrome (CS) and CS patients display a certain predisposition to neuroblastomas, rhabdomyosarcomas, and bladder carcinomas [1]. Mice expressing germline H-Ras<sup>G12V</sup> phenocopied certain features of CS; however tumors were extremely rare [40]. This phenotype suggests that H-Ras is a poor initiating oncogene and may be mutationally activated in spontaneous cancers only at later stages during tumor development when cooperating genetic lesions have already occurred. Alternatively, H-Ras could be a less potent oncogene in mice compared to humans.

### Oncogenic Raf mouse models

Following the identification of BRAF mutations in human malignancies, novel mouse strains modelling those mutations have been developed. Pritchard and colleagues created a B-Raf<sup>V600E</sup> mouse by employing a strategy in which mice are heterozygous mutant for B-Raf in cells expressing Cre and homozygous wildtype for



B-Raf in all other cells, thus closely resembling B-Raf status in human neoplasms as well as in surrounding normal tissues [41\*\*]. B-Raf<sup>V600E</sup> activation in a variety of somatic tissues by Mx1-Cre caused death in all animals within a month due to the development of nonlymphoid leukaemia of the histiocytic type [41\*\*]. Interestingly, human leukaemia has not been associated with BRAF mutations thus far. This discrepancy may represent distinct susceptibility of haematopoietic cells to oncogenic stimuli in humans and mice. A second study using a similar mouse model reported lung adenoma formation in B-Raf<sup>V600E</sup> mice after intranasal Ad-Cre instillation [42\*\*]. Even though adenomas developed with complete penetrance, they rarely progressed to adenocarcinoma, and rather demonstrated a senescence-like growth arrest following hyperplasia [42\*\*]. Interestingly, no growth arrest was observed in Kras<sup>G12D</sup>-induced lung adenomas, which eventually progressed to malignancy [12], suggesting that activation of other Ras effector pathways may be required for tumor progression (or example see ref. [57\*\*]). B-Raf<sup>V600E</sup> could, however, cooperate with loss of p53 or p16<sup>INK4A</sup>/p19<sup>Arf</sup>, known mediators of senescence, to induce adenocarcinomas [42\*\*]. These studies provided experimental evidence for murine tumor initiation by mutation of *B-Raf*. It is expected that oncogenic B-Raf mice will prove valuable for investigating B-Raf-mediated transformation in a variety of other cancers such as melanoma, thyroid and colon cancer.

Further evidence for the oncogenic properties of B-Raf was provided by a forward genetic screen employing transposon-mediated mutagenesis. In a p19<sup>Arf</sup>-deficient background, B-Raf was the most frequently disrupted gene, leading to acceleration of sarcoma formation [43]. In the majority of cases, the T2/Onc transposon integrated in intron 9, in the orientation that directed expression of the C-terminal B-Raf kinase domain [43]. Similarly, transgenic expression of the kinase domain of Raf-1 sufficed to induce lung adenomas [44], and additional deletion of E-cadherin led to metastatic progression [45]. Furthermore, Raf-1 lacking the N-terminal negative regulatory domain cooperated with Akt activation and p19<sup>Arf</sup> loss to promote the formation of gliomas [46]. However, expression of truncated forms of B-Raf or Raf-1 has not been associated with sporadic human malignancies and activating mutations in CRAF have not been found in cancer thus far. Even though the preclinical potential of these models may be limited for the above reasons, they have confirmed the importance of MAPK pathway activation in tumor development.

### Mouse models of regulators of the MAPK pathway

The MAPK pathway is subjected to extensive regulation by posttranslational processing enzymes, phosphatases and negative feedback loops. Disruption of this regulation leads to pathway hyperactivation that mimics acti-

vating Ras mutations as has been demonstrated in mouse models lacking the Ras GAP neurofibromin (NF1) (reviewed in [47,48]). In addition to GAPs for Ras, other proteins function to attenuate the MAPK pathway such as the dual-specificity phosphatases (DUSPs) and Sprouty (Spry) proteins. Spry proteins inhibit the MAPK pathway by binding to Raf as well as to Grb2, an adaptor protein important for the recruitment of Ras GEFs [49]. Expression of Spry-1, Spry-2, and Spry-4 was increased upon K-Ras<sup>G12D</sup> expression in the lung [50], indicating that negative feedback loops are upregulated in response to oncogenic K-Ras to compensate for augmented MAPK signalling. Furthermore, Spry-2-deficiency increased the size of K-Ras<sup>G12D</sup>-induced lung tumors [50], suggesting that negative feedback regulation has tumor suppressive activity in the context of oncogenic K-Ras. Besides Spry proteins, MAPK phosphatases represent another way of negatively regulating the MAPK pathway through dephosphorylation of ERK1 and ERK2. Tyrosine, serine/threonine as well as dual-specificity phosphatases that act on ERK proteins have been identified and knockout mice have been generated to several of these (reviewed in [51]). However, the effect of phosphatase depletion on oncogenic Ras and Raf signalling has not yet been determined.

In addition to regulation of its downstream signalling effectors, Ras itself is regulated through post-translational modification. To increase membrane affinity and promote protein interaction, Ras is modified at the carboxy-terminal CAAX motif. First, the cysteine residue is isoprenylated by farnesyltransferase (FTase), followed by endoproteolytic release by Ras converting enzyme 1 (RCE1) of the three amino acids downstream of the isoprenylcysteine. Finally, the isoprenylcysteine residue is carboxyl methylated by isoprenylcysteine carboxyl methyltransferase (ICMT). However, in the absence of FTase activity, K-Ras and N-Ras can be isoprenylated by geranylgeranyltransferase type 1 (GGTase-I), a phenomenon providing an explanation for the disappointing performance of FTase inhibitors in clinical trials. Accordingly, genetic ablation of *FNTB*, the gene encoding FTase, in K-Ras<sup>G12V</sup>-expressing cells did not prevent lung tumorigenesis [52\*\*]. Surprisingly, the K-Ras<sup>G12D</sup>-induced myeloproliferative disease was accelerated upon genetic deletion of RCE1 [53\*\*], suggesting that RCE1 may have a poorly understood tumor suppressor role in cells and that RCE1 is not required for Ras oncogenesis. By contrast, the lack of either GGTase-I or ICMT ameliorated the lung tumor and myeloproliferative disease-like phenotypes in K-Ras<sup>G12D</sup> mutant mice [54\*\*,55\*\*]. As K-Ras is still farnesylated in the setting of GGTase-I ablation, other CAAX proteins that undergo geranylgeranylation must also be required for K-Ras<sup>G12D</sup>-mediated transformation. These findings imply that GGTase-I or ICMT may represent more suitable targets than RCE1 for therapeutic intervention in Ras associated malignancies, either alone or in combination

with FTase inhibitors. However, the suitability of Ras-modifying enzymes as therapeutic targets needs further investigation.

### Conclusions and future outlook

The development of preclinical mouse models has confirmed a causal role of oncogenic K-Ras expression in a variety of tumor types. Oncogenic K-Ras expression can initiate multiple malignancies, consistent with the demonstration of K-Ras mutations in different types of human preneoplasms. The cancer-initiating cell type described by Kim *et al.* for pulmonary adenocarcinoma [24] should now be pursued for other K-Ras-driven cancers.

The finding that N-Ras and H-Ras have weak oncogenic abilities in mice was somewhat surprising and may not reflect observations made in human malignancies. Alternatively and in contrast to K-Ras, N-Ras and H-Ras may not be initiating oncogenes and may be mutated only at later stages during tumor progression. Therefore, to distinguish between these two possibilities, the acceleration of tumor progression by N-Ras or H-Ras in combination with tumor suppressor deficiency needs to be investigated.

Each Ras family member is associated with different kinds of cancer. Moreover, mutant B-Raf-harboring cancers do not completely overlap with cancers carrying Ras mutations (e.g. mutant B-Raf has not been detected in myeloid malignancies where N-Ras is the most commonly mutated Ras gene; see Table 1), indicating that activation of the MAPK pathway alone is unlikely to promote cancer. In fact, it has been shown in mouse models [56,57] and cell culture [58] that activation of other Ras effector pathways is important for tumorigenesis. The ability of endogenously expressed, mutant Ras to activate certain effector pathways may vary between the three family members and could be influenced by factors such as subcellular localization of Ras and cell type. Additionally, the oncogenic mutations may confer different activity onto Ras and Raf, which may also depend on cell type. Understanding the difference in oncogenic activities between mutant K-Ras, N-Ras, H-Ras and B-Raf as well as the cellular context in which they are transforming should ultimately explain the tropism of these oncogenes. Finally, the development of preclinical mouse models of oncogenic Ras/Raf signalling will prove instrumental for developing novel therapeutics in a timely manner.

### Acknowledgements

We apologize to our colleagues whose data could not be discussed due to space restriction. We are grateful to Dr A. Cox and members of the Tuveson laboratory for critical comments on the manuscript. DAT is supported by US National Institutes of Health grants CA101973, CA111292, CA084291, CA105490 and the Lustgarten Foundation for Pancreatic Cancer Research. DAT is a group leader of Cancer Research UK.

### References and recommended reading

Papers of particular interest, published within the period of review, have been highlighted as:

- of special interest
  - of outstanding interest
1. Schubert S, Shannon K, Bollag G: **Hyperactive Ras in developmental disorders and cancer.** *Nat Rev Cancer* 2007, **7**:295-308.
  2. Gschwind A, Fischer OM, Ullrich A: **The discovery of receptor tyrosine kinases: targets for cancer therapy.** *Nat Rev Cancer* 2004, **4**:361-370.
  3. Bos JL: **ras oncogenes in human cancer: a review.** *Cancer Res* 1989, **49**:4682-4689.
  4. Downward J: **Targeting RAS signalling pathways in cancer therapy.** *Nat Rev Cancer* 2003, **3**:11-22.
  5. Brose MS, Volpe P, Feldman M, Kumar M, Rishi I, Gerrero R, Einhorn E, Herlyn M, Minna J, Nicholson A *et al.*: **BRAF and RAS mutations in human lung cancer and melanoma.** *Cancer Res* 2002, **62**:6997-7000.
  6. Davies H, Bignell GR, Cox C, Stephens P, Edkins S, Clegg S, Teague J, Woffendin H, Garnett MJ, Bottomley W *et al.*: **Mutations of the BRAF gene in human cancer.** *Nature* 2002, **417**:949-954.
  7. Pollock PM, Harper UL, Hansen KS, Yudt LM, Stark M, Robbins CM, Moses TY, Hostetter G, Wagner U, Kakareka J *et al.*: **High frequency of BRAF mutations in nevi.** *Nat Genet* 2003, **33**:19-20.
  8. Mercer KE, Pritchard CA: **Raf proteins and cancer: B-Raf is identified as a mutational target.** *Biochim Biophys Acta* 2003, **1653**:25-40.
  9. Frese KK, Tuveson DA: **Maximizing mouse cancer models.** *Nat Rev Cancer* 2007, **7**:645-658.
  10. Guerra C, Mijimolle N, Dhawahir A, Dubus P, Barradas M, Serrano M, Campuzano V, Barbacid M: **Tumor induction by an endogenous K-ras oncogene is highly dependent on cellular context.** *Cancer Cell* 2003, **4**:111-120.
  11. Tuveson DA, Shaw AT, Willis NA, Silver DP, Jackson EL, Chang S, Mercer KL, Grochow R, Hock H, Crowley D *et al.*: **Endogenous oncogenic K-ras(G12D) stimulates proliferation and widespread neoplastic and developmental defects.** *Cancer Cell* 2004, **5**:375-387.
  12. Jackson EL, Willis N, Mercer K, Bronson RT, Crowley D, Montoya R, Jacks T, Tuveson DA: **Analysis of lung tumor initiation and progression using conditional expression of oncogenic K-ras.** *Genes Dev* 2001, **15**:3243-3248.
  13. Hingorani SR, Petricoin EF, Maitra A, Rajapakse V, King C, Jacobetz MA, Ross S, Conrads TP, Veenstra TD, Hitt BA *et al.*: **Preinvasive and invasive ductal pancreatic cancer and its early detection in the mouse.** *Cancer Cell* 2003, **4**:437-450.
  14. Sarkisian CJ, Keister BA, Stairs DB, Boxer RB, Moody SE, Chodosh LA: **Dose-dependent oncogene-induced senescence *in vivo* and its evasion during mammary tumorigenesis.** *Nat Cell Biol* 2007, **9**:493-505.
- This study provides the first *in vivo* evidence for the cell biological responses to different expression levels of oncogenic Ras. High levels engaged the p19ARF-p53 tumor suppressor pathway to induce senescence, while low levels promoted hyperplastic growth of mammary epithelial cells.
15. Aguirre AJ, Bardeesy N, Sinha M, Lopez L, Tuveson DA, Horner J, Redston MS, DePinho RA: **Activated Kras and Ink4a/Arf deficiency cooperate to produce metastatic pancreatic ductal adenocarcinoma.** *Genes Dev* 2003, **17**:3112-3126.
  16. Hingorani SR, Wang L, Multani AS, Combs C, Deramandt TB, Hruban RH, Rustgi AK, Chang S, Tuveson DA: **Trp53R172H and KrasG12D cooperate to promote chromosomal instability and widely metastatic pancreatic ductal adenocarcinoma in mice.** *Cancer Cell* 2005, **7**:469-483.
  17. Bardeesy N, Cheng KH, Berger JH, Chu GC, Pahler J, Olson P, Hezel AF, Horner J, Lauwers GY, Hanahan D *et al.*: **Smad4 is**

- dispensable for normal pancreas development yet critical in progression and tumor biology of pancreas cancer.** *Genes Dev* 2006, **20**:3130-3146.
18. Ijichi H, Chytil A, Gorska AE, Aakre ME, Fujitani Y, Fujitani S, Wright CV, Moses HL: **Aggressive pancreatic ductal adenocarcinoma in mice caused by pancreas-specific blockade of transforming growth factor-beta signaling in cooperation with active Kras expression.** *Genes Dev* 2006, **20**:3147-3160.
  19. Izeradjene K, Combs C, Best M, Gopinathan A, Wagner A, Grady WM, Deng CX, Hruban RH, Adsay NV, Tuveson DA *et al.*: **Kras(G12D) and Smad4/Dpc4 haploinsufficiency cooperate to induce mucinous cystic neoplasms and invasive adenocarcinoma of the pancreas.** *Cancer Cell* 2007, **11**:229-243.
  20. Siveke JT, Einwachter H, Sipos B, Lubeseder-Martellato C, Kloppel G, Schmid RM: **Concomitant pancreatic activation of Kras(G12D) and Tgfa results in cystic papillary neoplasms reminiscent of human IPMN.** *Cancer Cell* 2007, **12**:266-279.
  21. Guerra C, Schuhmacher AJ, Canamero M, Grippo PJ, Verdaguer L, Perez-Gallego L, Dubus P, Sandgren EP, Barbacid M: **Chronic pancreatitis is essential for induction of pancreatic ductal adenocarcinoma by K-Ras oncogenes in adult mice.** *Cancer Cell* 2007, **11**:291-302.
  22. Carriere C, Seeley ES, Goetze T, Longnecker DS, Korc M: **The Nestin progenitor lineage is the compartment of origin for pancreatic intraepithelial neoplasia.** *Proc Natl Acad Sci U S A* 2007, **104**:4437-4442.
  23. Tuveson DA, Zhu L, Gopinathan A, Willis NA, Kachatrian L, Grochow R, Pin CL, Mitin NY, Taparowsky EJ, Gimotty PA *et al.*: **Mist1-KrasG12D knock-in mice develop mixed differentiation metastatic exocrine pancreatic carcinoma and hepatocellular carcinoma.** *Cancer Res* 2006, **66**:242-247.
  24. Kim CF, Jackson EL, Woolfenden AE, Lawrence S, Babar I, Vogel S, Crowley D, Bronson RT, Jacks T: **Identification of bronchioalveolar stem cells in normal lung and lung cancer.** *Cell* 2005, **121**:823-835.
  25. Iwanaga K, Yang Y, Raso MG, Ma L, Hanna AE, Thilaganathan N, Moghaddam S, Evans CM, Li H, Cai WW *et al.*: **Pten inactivation accelerates oncogenic K-ras-initiated tumorigenesis in a mouse model of lung cancer.** *Cancer Res* 2008, **68**:1119-1127.
  26. Jackson EL, Olive KP, Tuveson DA, Bronson R, Crowley D, Brown M, Jacks T: **The differential effects of mutant p53 alleles on advanced murine lung cancer.** *Cancer Res* 2005, **65**:10280-10288.
  27. Grady WM, Markowitz SD: **Genetic and epigenetic alterations in colon cancer.** *Annu Rev Genomics Hum Genet* 2002, **3**:101-128.
  28. Sansom OJ, Meniel V, Wilkins JA, Cole AM, Oien KA, Marsh V, Jamieson TJ, Guerra C, Ashton GH, Barbacid M *et al.*: **Loss of Apc allows phenotypic manifestation of the transforming properties of an endogenous K-ras oncogene in vivo.** *Proc Natl Acad Sci U S A* 2006, **103**:14122-14127.
  29. Calcagno SR, Li S, Colon M, Kreinest PA, Thompson EA, Fields AP, Murray NR: **Oncogenic K-ras promotes early carcinogenesis in the mouse proximal colon.** *Int J Cancer* 2008, **122**:2462-2470.
  30. Haigis KM, Kendall KR, Wang Y, Cheung A, Haigis MC, Glickman JN, Niwa-Kawakita M, Sweet-Cordero A, Sebolt-Leopold J, Shannon KM *et al.*: **Differential effects of oncogenic K-Ras and N-Ras on proliferation, differentiation and tumor progression in the colon.** *Nat Genet* 2008, **40**:600-608.  
Haigis *et al.* describe oncogene-specific effects in the colon, where K-Ras but not N-Ras induced hyperplasia, suggesting that Ras family members are oncogenic only in cell type-specific contexts.
  31. Dinulescu DM, Ince TA, Quade BJ, Shafer SA, Crowley D, Jacks T: **Role of K-ras and Pten in the development of mouse models of endometriosis and endometrioid ovarian cancer.** *Nat Med* 2005, **11**:63-70.
  32. Kirsch DG, Dinulescu DM, Miller JB, Grimm J, Santiago PM, Young NP, Nielsen GP, Quade BJ, Chaber CJ, Schultz CP *et al.*: **A spatially and temporally restricted mouse model of soft tissue sarcoma.** *Nat Med* 2007, **13**:992-997.
  33. Braun BS, Tuveson DA, Kong N, Le DT, Kogan SC, Rozmus J, Le Beau MM, Jacks TE, Shannon KM: **Somatic activation of oncogenic Kras in hematopoietic cells initiates a rapidly fatal myeloproliferative disorder.** *Proc Natl Acad Sci U S A* 2004, **101**:597-602.
  34. Chan IT, Kutok JL, Williams IR, Cohen S, Kelly L, Shigematsu H, Johnson L, Akashi K, Tuveson DA, Jacks T *et al.*: **Conditional expression of oncogenic K-ras from its endogenous promoter induces a myeloproliferative disease.** *J Clin Invest* 2004, **113**:528-538.
  35. Chan IT, Kutok JL, Williams IR, Cohen S, Moore S, Shigematsu H, Ley TJ, Akashi K, Le Beau MM, Gilliland DG: **Oncogenic K-ras cooperates with PML-RAR alpha to induce an acute promyelocytic leukemia-like disease.** *Blood* 2006, **108**:1708-1715.
  36. Parikh C, Subrahmanyam R, Ren R: **Oncogenic NRAS rapidly and efficiently induces CMML- and AML-like diseases in mice.** *Blood* 2006, **108**:2349-2357.
  37. Parikh C, Subrahmanyam R, Ren R: **Oncogenic NRAS, KRAS, and HRAS exhibit different leukemogenic potentials in mice.** *Cancer Res* 2007, **67**:7139-7146.
  38. Chin L, Pomerantz J, Polsky D, Jacobson M, Cohen C, Cordon-Cardo C, Horner JW 2nd, DePinho RA: **Cooperative effects of INK4a and ras in melanoma susceptibility in vivo.** *Genes Dev* 1997, **11**:2822-2834.
  39. Harada N, Oshima H, Katoh M, Tamai Y, Oshima M, Taketo MM: **Hepatocarcinogenesis in mice with beta-catenin and Ha-ras gene mutations.** *Cancer Res* 2004, **64**:48-54.
  40. Schuhmacher AJ, Guerra C, Sauzeau V, Canamero M, Bustelo XR, Barbacid M: **A mouse model for Costello syndrome reveals an Ang II-mediated hypertensive condition.** *J Clin Invest* 2008, **118**:2169-2179.  
This reference reports the generation of an endogenous H-Ras<sup>G12V</sup> germline mouse model, which did not develop cancer but displayed phenotypes resembling human Costello syndrome.
  41. Mercer K, Giblett S, Green S, Lloyd D, DaRocha Dias S, Plumb M, Marais R, Pritchard C: **Expression of endogenous oncogenic V600E-raf induces proliferation and developmental defects in mice and transformation of primary fibroblasts.** *Cancer Res* 2005, **65**:11493-11500.  
See Ref. [42\*]
  42. Dankort D, Filenova E, Collado M, Serrano M, Jones K, McMahon M: **A new mouse model to explore the initiation, progression, and therapy of BRAFV600E-induced lung tumors.** *Genes Dev* 2007, **21**:379-384.  
Refs. [41\*, 42\*\*] describe the generation of conditional oncogenic B-Raf mutant mice. Upon activation by Cre in the appropriate cell type, these mice developed haematopoietic and pulmonary malignancies.
  43. Collier LS, Carlson CM, Ravimohan S, Dupuy AJ, Largaespada DA: **Cancer gene discovery in solid tumours using transposon-based somatic mutagenesis in the mouse.** *Nature* 2005, **436**:272-276.
  44. Kerkhoff E, Fedorov LM, Siefken R, Walter AO, Papadopoulos T, Rapp UR: **Lung-targeted expression of the c-Raf-1 kinase in transgenic mice exposes a novel oncogenic character of the wild-type protein.** *Cell Growth Diff* 2000, **11**:185-190.
  45. Ceteci F, Ceteci S, Karreman C, Kramer BW, Asan E, Gotz R, Rapp UR: **Disruption of tumor cell adhesion promotes angiogenic switch and progression to micrometastasis in RAF-driven murine lung cancer.** *Cancer Cell* 2007, **12**:145-159.
  46. Lyustikman Y, Momota H, Pao W, Holland EC: **Constitutive activation of Raf-1 induces glioma formation in mice.** *Neoplasia* 2008, **10**:501-510.
  47. Le LQ, Parada LF: **Tumor microenvironment and neurofibromatosis type I. connecting the GAPS.** *Oncogene* 2007, **26**:4609-4616.
  48. Rubin JB, Gutmann DH: **Neurofibromatosis type 1 – a model for nervous system tumour formation?** *Nat Rev Cancer* 2005, **5**:557-564.

49. Cabrita MA, Christofori G: **Sprouty proteins, masterminds of receptor tyrosine kinase signaling.** *Angiogenesis* 2008, **11**:53-62.
50. Shaw AT, Meissner A, Dowdle JA, Crowley D, Magendantz M, Ouyang C, Parisi T, Rajagopal J, Blank LJ, Bronson RT *et al.*: **Sprouty-2 regulates oncogenic K-ras in lung development and tumorigenesis.** *Genes Dev* 2007, **21**:694-707.
51. Salojin K, Oravec T: **Regulation of innate immunity by MAPK dual-specificity phosphatases: knockout models reveal new tricks of old genes.** *J Leukoc Biol* 2007, **81**:860-869.
52. Mijimolle N, Velasco J, Dubus P, Guerra C, Weinbaum CA, Casey PJ, Campuzano V, Barbacid M: **Protein farnesyltransferase in embryogenesis, adult homeostasis, and tumor development.** *Cancer Cell* 2005, **7**:313-324.  
See Ref. [55\*\*]
53. Wahlstrom AM, Cutts BA, Karlsson C, Andersson KM, Liu M, Sjogren AK, Swolin B, Young SG, Bergo MO: **Rce1 deficiency accelerates the development of K-RAS-induced myeloproliferative disease.** *Blood* 2007, **109**:763-768.  
See Ref. [55\*\*]
54. Sjogren AK, Andersson KM, Liu M, Cutts BA, Karlsson C, Wahlstrom AM, Dalin M, Weinbaum C, Casey PJ, Tarkowski A *et al.*: **GGTase-I deficiency reduces tumor formation and improves survival in mice with K-RAS-induced lung cancer.** *J Clin Invest* 2007, **117**:1294-1304.  
See Ref. [55\*\*]
55. Wahlstrom AM, Cutts BA, Liu M, Lindskog A, Karlsson C, Sjogren AK, Andersson KM, Young SG, Bergo MO: **Inactivating Icm1 ameliorates K-RAS-induced myeloproliferative disease.** *Blood* 2008, **112**:1357-1365.  
Refs. [52\*\*,53\*\*,54\*\*,55\*\*] report the genetic ablation of Ras processing enzymes. In the case of GGTase-I and Icm1 deficiency, K-Ras<sup>G12D</sup>-driven tumorigenesis was impaired, while loss of Rce1 enhanced tumorigenicity.
56. Gupta S, Ramjaun AR, Haiko P, Wang Y, Warne PH, Nicke B, Nye E, Stamp G, Alitalo K, Downward J: **Binding of ras to phosphoinositide 3-kinase p110alpha is required for ras-driven tumorigenesis in mice.** *Cell* 2007, **129**:957-968.  
See Ref. [58\*]
57. Kissil JL, Walmsley MJ, Hanlon L, Haigis KM, Bender Kim CF, Sweet-Cordero A, Eckman MS, Tuveson DA, Capobianco AJ, Tybulewicz VL *et al.*: **Requirement for Rac1 in a K-ras induced lung cancer in the mouse.** *Cancer Res* 2007, **67**:8089-8094.  
See Ref. [58\*]
58. Lim KH, Baines AT, Fiordalisi JJ, Shipitsin M, Feig LA, Cox AD, Der CJ, Counter CM: **Activation of RalA is critical for Ras-induced tumorigenesis of human cells.** *Cancer Cell* 2005, **7**:533-545.  
The studies referenced in [56\*,57\*,58\*] showed the importance of different Ras effector pathways for Ras-mediated tumorigenesis, distinguishing these pathways as relevant therapeutic targets.



## **4. Materials and Methods**

### **4.1 DNA manipulation**

Standard procedures were used for DNA manipulations. A detailed description can be found in 'Current Protocols in Molecular Biology, Volume 1'. In brief, restriction digests were set up the following way:

1ul restriction enzyme (2-10 units, New England Biolabs)

1ul 10x buffer (New England Biolabs)

1ul 10x BSA (1ug/ul, New England Biolabs)

0.1-0.5ug DNA

H<sub>2</sub>O to a final volume of 10ul.

Restriction digests were incubated at 37°C for a minimum of an hour and separated on 1% TAE agarose gels. Gel extraction of DNA, Minipreps and Midipreps (QIAquick Gel Extraction Kit, QuickLyse Miniprep Kit, QIAfilter Midiprep Kit, respectively, all Qiagen) were performed according to the manufacturer's instructions. Ligations were set up the following way:

1ul Ligase (New England Biolabs)

1ul Ligase buffer (New England Biolabs)

Vector and Insert DNA at a ratio of 1:3

H<sub>2</sub>O to a final volume of 10ul.

Ligations were incubated at 16°C over-night, precipitated by adding 1ul Glycogen, 40ul H<sub>2</sub>O and 500ul N-Butanol, centrifuged and the pellet air-dried. DNA was resuspended in 10ul of H<sub>2</sub>O and 2ul were electroporated into electrocompetent E.coli (DH10a, either home-made or from Invitrogen) using a BioRad Micropulser and plated onto LB agar plates containing either

Ampicillin or Kanamycin (prepared by the media kitchens of the AFCRI or CRI). Bacteria were grown over-night at 37°C and colonies picked the next day for diagnostic analysis.

#### 4.2 Polymerase Chain Reaction (PCR)

For PCR reactions either the PCR core kit (Roche) or Phusion Hot Start High-Fidelity DNA Polymerase (New England Biolabs) were used following the manufacturer's instructions. 0.25ul of each 100uM primer solution were used per 20ul reaction. PCR programs were as follows:

1. initial denaturation: 96°C, 2 minutes
2. denaturation: 96°C, 30 seconds
3. annealing: 58-66°C, 30 seconds
4. extension: 72°C, 1-3 minutes

Repeat steps 2.-4. 34 times

5. final extension: 72°C, 5 minutes
6. 4°C, forever

Annealing temperature was pre-determined by a gradient PCR reaction with annealing temperatures ranging from 55°C to 68°C. Extension temperatures were chosen depending on the size of the fragment to be amplified. PCR reactions were run on a BioRad DNA Engine Dyad Peltier Thermal Cycler (BioRad).

#### 4.3 Colony lift

Nylon membranes were placed onto bacteria plates for 30 seconds followed by incubation on Whatman paper soaked with Denaturation solution (1.5M

NaCl, 0.5M NaOH), then Neutralization solution (1.5M NaCl, 0.5M Tris-HCl pH7.5) and finally 3xSSC for 5 minutes each. Membranes were air dried and DNA cross-linked by 240uJ/cm<sup>2</sup> UVC irradiation. Pre-hybridization, hybridization with radio-labeled probe and exposure to film was performed as for Southern blotting (see below).

#### 4.4 Plasmids

B-Raf was PCR amplified from mouse cDNA, a flag-tag or HA-tag introduced at the C-terminus and cloned into pBabe-puro or pWZL-hygro, respectively. The N-terminus of B-Raf was amplified using the following primers: braf-BamHI-fwd 5'-ccggatcccagtggtgtgtacgtaggaattggaagcatggcggcgctgagtggc-3' (BamHI restriction site is underlined) and braf-Clal-rev 5'-ggaattttcatcgatattcacagg-3' (Clal restriction site is underlined). The C-terminus of B-Raf was amplified using the following primers: braf-Clal-fwd 5'-cctgtgaatatcgatggaaaattcc-3' (Clal restriction site is underlined) and braf-flag-Sall-rev 5'-gggtcgaccactgtgctggcgaattgtcaCTTATCGTCGTCGTCATCCTTGT Aatcgtggactggaaacc-3' (Sall restriction site is underlined and flag tag is depicted by capital letters) or braf-HA-Sall-rev 5'-gggtcgaccactgtgctggcgaattgtcaTATCCGTATGATGTGCCGGATTATGCAatcgtggactggaaacc-3' (Sall restriction site is underlined and HA tag is depicted by capital letters). The B-Raf N-terminal and C-terminal fragments were digested with BamHI and Clal (partial digest as there is another BamHI site in the B-Raf cDNA) or Clal and Sall, respectively, and triple ligated into BamHI/Sall digested pBabe or pWZL using standard cloning procedures. To generate oncogenic mutant variants, the C-terminal Clal/Sall fragment was subcloned into pBluescript. The

mutations were introduced using a site-directed mutagenesis kit (Stratagene) following the manufacturer's recommendations and the mutated B-Raf fragments were cloned back into the pBabe or pWZL retroviral expression vectors. The following primers were used for the site directed mutagenesis: V600E-fwd 5'-gactttggctagccacagAgaatctcgggtg-3', V600E-rev 5'-ccaccgagatttcTctgtggctagaccaaagtc, G466V-fwd 5' cagagaattggatctgTgtcatttggaaactg-3' and G466V-rev 5'-cagttccaaatgacAcagatccaattctctg-3' (the introduced nucleotide changes are highlighted by capital letters).  $\Delta$ 3-B-Raf-pBabe,  $\Delta$ 3-B-Raf<sup>V600E</sup>-pBabe, and  $\Delta$ 3-B-Raf<sup>G466V</sup>-pBabe were generated by replacing the N-terminal BamHI-BamHI fragment of the full length cDNA with a sub-cloned N-terminal fragment lacking the 99 nucleotides in exon 3. This fragment was PCR amplified from mouse cDNA. All cloned cDNAs were sequenced to confirm that no unwanted nucleotide changes were introduced. Sequencing was performed by the Sequencing cores of the University of Pennsylvania and the Cambridge Research Institute. Expression vectors pEFm-A-Raf, pEFm-Raf1.6, pEFm-Raf1.6-K375M, and pEFm-Raf1.6-S338A were kindly provided by Dr. R. Marais. pBabe-Nras<sup>G12D</sup> was generated by Dr. C. Der and obtained from Addgene. pBabe-Hras<sup>G12V</sup> was generated by Dr. S. Lowe and obtained by Dr. D. Tuveson. pSuper-retro-scrambled and pSuper-retro-C-Raf were constructed by Dr. S. Hingorani and shRNA sequences were published previously (Hingorani et al., 2003).

#### 4.5 Cell lines and transfections

HEK293T and NIH3T3 cells were obtained from ATCC and cultured in DMEM (Invitrogen) containing 10% fetal calf serum (Hyclone), 100U/mL Penicillin and

100ug/mL Streptomycin (both Invitrogen). NHEM were obtained from PromoCell and cultured in Melanocyte Growth Medium (PromoCell). Melanoma and human melanocyte cell lines (1205Lu, 451Lu, A375P, Malme 3M, SKMeI5, WM35, WM115, WM164, WM278, WM793, WM902B, WM982A, WM1552c, SbCl2, SKMeI2, WM1346, WM1361A, Fom99) were a kind gift from Dr. M. Herlyn and cultured in DMEM containing 10% fetal calf serum, 100U/mL Penicillin and 100ug/mL Streptomycin or Melanocyte Growth Medium (Fom99). Melan-a cells were a kind gift from Dr. D. Bennett and cultured in RPMI (Invitrogen) containing 10% fetal calf serum, 100U/mL Penicillin and 100ug/mL Streptomycin and 200uM TPA (Sigma). All cell lines were propagated using standard cell culture techniques. HEK293T cells were plated 24 hours before transient transfection using Fugene 6 (Roche) or Lipofectamine 2000 (Invitrogen). Transfections were performed following the manufacturer's instructions. Transfected HEK293T cells were used for experiments 48 hours after transfection. NIH3T3 fibroblasts were infected with retroviruses produced in the Phoenix packaging cell line, in the presence of 8ug/ml polybrene and selected with 2ug/ml puromycin or 200ug/ml hygromycin 48 hours after infection. For some experiments, cells were treated with Sorafenib (LC Laboratories) in DMSO at the indicated concentrations.

#### 4.6 Embryonic stem cell culture and targeting

The 129Sv-derived embryonic stem (ES) cell line E14J was a kind gift from Dr. D. Adams. E14Js were cultured in Knock-out DMEM (Invitrogen) containing 15% ES cell tested fetal calf serum (Hyclone), 100U/mL Penicillin, 100ug/mL Streptomycin, 2mM L-Glutamine (all Invitrogen), 0.001% beta-

Mercaptoethanol and 1000U/ml leukemia-inhibitory factor (LIF, Chemicon). Cell culture plastics were pre-treated with 0.1% gelatin in PBS for 15 minutes and ES cells were cultured on a confluent layer of feeder cells. As feeder cells served growth arrested mouse embryonic fibroblasts derived from DR4 mice, which carry drug resistances for puromycin, hygromycin, G418, and 6-thioguanine (Tucker et al., 1997). For ES cell targeting, cells were electroporated in 0.4cm cuvettes with 50ug of linearized targeting vector using a Biorad – Gene Pulsar II Excel (BioRad) set to 25uF and 800V. Electroporated ES cells were grown in media containing 3ug/ml puromycin, 150ug/ml G418 or 2uM ganciclovir, depending on the selection cassette used for the targeting. 96 ES cell clones that survived selection were picked after 7 days, trypsinized and plated in 96 well plates with feeder cells. After 3 days, clones were split into two 96 well plates. Clones in one 96 well plate were overgrown for DNA isolation. Clones in the other 96 well plate were trypsinized after 3 days, 2x freezing media added (60% FCS, 20% DMSO, 20% ES cell media), overlaid with mineral oil and frozen at -80°C. Positively targeted ES cell clones were injected into blastocysts by the CRI transgenic core to generate chimeric animals.

#### 4.7 Mouse embryonic fibroblasts

Mouse breedings were set up and females were checked for vaginal plugs the following days. The morning vaginal plugs were discovered was counted as 0.5 dpc and embryos were isolated at 13.5-14.5 dpc. Embryos were washed in PBS and the amniotic sac, placenta and organs as well as the head, which was kept for genotyping the embryos, were removed. Embryos were then

finely chopped in 1ml of Trypsin using a razorblade and placed in a tissue culture incubator for 45 minutes. After incubation, Trypsin was quenched with 20ml of MEF media (DMEM containing 10% FCS, penicillin and streptomycin) and cultured for two days. MEF lines were split once and frozen down at passage 2. Experiments with MEFs were carried out at passages 3-5 before the cells experienced tissue culture shock and underwent replicative senescence. To ablate conditional knock-out alleles and induce expression of conditional oncogenic alleles, MEFs were infected with adenoviral-Cre (Ad-Cre) ( $\sim 0.5-1.5 \times 10^8$  PFU, Transgenic Core, University of Iowa) or empty adenoviral control (Ad-Mock). Cells were incubated for three days post-infection to allow recombination to occur.

#### 4.8 Proliferation, focus formation, soft agar and apoptosis assay

For proliferation assays,  $2.0-2.5 \times 10^4$  cells were plated in triplicates in 12 well plates and counted every day for 4 days (melan-a and NIH3T3 cells) or every other day for 7 days (WM793 cells and MEFs) using a Z2 Coulter Particle Count and Size Analyzer (Beckman Coulter). Alternatively, cells were incubated with 4 $\mu$ M BrdU for 6 hours and proliferating cells were detected using an anti-BrdU antibody (B&D) following the manufacturer's instructions. For focus formation,  $3 \times 10^5$  MEFs were plated in 6cm dishes or  $5 \times 10^3$  MEFs were plated onto a confluent layer of growth arrested MEFs in 6 well plates. Cells were fixed with 70% ethanol after 12-21 days and stained with Giemsa. For soft agar assays,  $5 \times 10^4$  cells were resuspended in 0.4% agar and plated over 0.8% agar. Colonies were stained with Giemsa after 3 weeks. For apoptosis assays, MEFs were treated with either 10ng/ml TNF $\alpha$  and 0.5 $\mu$ g/ml

cycloheximide or 5nM Staurosporine in DMEM containing 0.5% FCS for 8 hours. The fraction of dead cells was determined using the CellTiter-Glo Luminescence Cell Viability Assay (Promega) according to the manufacturer's recommendation and normalized to untreated control cells.

#### 4.9 Alkaline phosphatase staining

MEFs derived from R26-LSL-FlpERT2; PLAP mice were infected with Ad-Cre and incubated with 10-100nM 4-Hydroxytamoxifen (4-OHT, Sigma) in DMSO for three days. Cells were fixed with 0.5% glutaraldehyde in PBS for 10 minutes and endogenous alkaline phosphatase was inactivated by incubation in PBS at 65°C for 30 minutes. Next, cells were rinsed in AP solution (100mM Tris pH8.5, 100mM NaCl, 50mM MgCl<sub>2</sub>) followed by staining with BM Purple (Roche) in the dark for 24 hours. Cells were air-dried and photographed using a Nikon Eclipse 100 microscope (Nikon).

#### 4.10 Immunoprecipitation

Cells were washed twice with PBS and lysed in ice-cold RIPA lysis buffer (150mM NaCl, 50mM Tris-HCl pH7.4, 1mM EDTA, 1% Igepal CA-630). 400ug of total lysate were precleared for 20 minutes and then immunoprecipitated using 20ul of ANTI-FLAG M2 agarose beads (Sigma) or ANTI-HA agarose beads (Sigma) for 2 hours at 4°C. Beads were washed 4 times with RIPA lysis buffer and subjected to SDS-PAGE. For kinase assays, HA-B-Raf<sup>V600E</sup>, HA-B-Raf or myc-C-Raf were co-expressed with flag-B-Raf<sup>V600E</sup>. HA-tagged and myc-tagged components of the complexes were immunoprecipitated for 6 hours from 600ug of total lysate using ANTI-HA agarose beads or ANTI-myc



agarose beads, respectively. Complexes were eluted twice using 200ug/ml HA- or myc-peptide (both Sigma) in TBS for 30 minutes at 4°C, diluted with RIPA lysis buffer and subjected to a flag-IP overnight to isolate specific HA-tagged/flag-tagged or myc-tagged/flag-tagged protein complexes. Beads were washed four times with RIPA lysis buffer and used in a MAPK sandwich kinase assay with  $^{32}\text{P}$ - $\gamma$ -ATP, using MBP as final substrate (Millipore) according to the manufacturer's recommendations. Kinase reactions were analyzed by SDS-PAGE and autoradiography to detect  $^{32}\text{P}$ - $\gamma$ -labeled MBP. The beads from the flag-IP were used to detect the amount of immunoprecipitated flag-B-Raf<sup>V600E</sup> by Western blotting and the phospho-MBP signal was normalized to immunoprecipitated flag-B-Raf<sup>V600E</sup>.

#### 4.11 Western blotting

Protein lysates and immunoprecipitates were separated on precast NuPAGE Novex 4-12% Bis-Tris gradient gels (Invitrogen), transferred onto a PVDF membrane (Millipore) and incubated overnight with one of the following primary antibodies: HA (1:2000), flag (1:2000), phospho-ERK1/2 (1:5000), ERK1/2 (1:3000), phospho-MEK1/2 (1:2000), MEK1/2 (1:2000) (all Cell Signaling), C-Raf (1:2000), B-Raf (1:2000), actin (1:6000) (all Santa Cruz Biotechnologies) panRas (1:2000) (Calbiochem), phospho-S338-C-Raf (1:1000), myc (1:2000), A-Raf (1:2000), DUSP4 (1:1000), DUSP6 (1:1000), Sprouty 2 (1:1000) (Abcam) in 5% milk in TBST. Membranes were incubated with secondary HRP-antibodies in 5% milk in TBST (Jackson ImmunoResearch) for one hour followed by signal detection with enhanced chemiluminescence and x-ray film (both Amersham). Alternatively,

membranes were incubated with Alexa Fluor secondary antibodies (Invitrogen) for one hour, and scanned using Li-Cor Odyssey. Signal was quantified using Odyssey software.

#### 4.12 Quantification of amount of Raf molecules per cell

To determine the number of Raf molecules per cell, the same number of cells of each cell line was plated onto two plates. The next day, one plate was lysed in RIPA buffer, while the other plate was used to determine the cell number at the time-point the cells were lysed. Next, the protein concentrations of each lysate were determined and the amount of protein per cell and the number of cells per 20ug of total protein calculated. 20ug of total protein were then subjected to SDS-PAGE along with 4, 2, 1, 0.5, 0.2 ng of recombinant B-Raf and C-Raf (Millipore) as a standard reference. Western blots for B-Raf and C-Raf were performed, the signal for the B-Raf and C-Raf standards were quantified using Image scan software and standard curves calculated for B-Raf and C-Raf. These standard curves were used to calculate the amount of B-Raf or C-Raf protein per 20ug of total protein, which corresponded to a previously determined number of cells. From this the amount of B-Raf or C-Raf protein per cell was calculated. Finally, the number of molecules per cell was calculated using the following formula:

Avogadro's number / (weight of one B-Raf or C-Raf molecule in ng / ng of B-Raf or C-Raf per cell) = B-Raf or C-Raf molecules per cell.

Below as an example is the determination of B-Raf molecules per one WM793 melanoma cell: 1,907,000 cells were lysed in 100ul RIPA buffer. The protein concentration was determined as 2.012ug/ul, which corresponded to 0.1055ng total protein per cell and 189,600 cells per 20ug total protein. After Western blotting the amount of B-Raf per 20ug of total protein was calculated as 1.715803ng, which corresponded to  $9.0496 \times 10^{-6}$ ng of B-Raf molecules per cell. Using this number in the above equation gives the following:

$$6.02 \times 10^{23} / (9.6 \times 10^{13} / 9.0496 \times 10^{-6}) = 56,750 \text{ B-Raf molecules per cell.}$$

#### 4.13 RNA isolation and cDNA synthesis

RNA was isolated from mouse tissues with TRIzol reagent (Invitrogen). 2-4ug RNA were used for cDNA synthesis using Ready-To-Go You-Prime First-Strand Beads (Amersham Biosciences) following the manufacturer's recommendations.

#### 4.14 DNA isolation and Southern blotting

To isolate tail DNA, tails were incubated in 500ul tail buffer (50mM Tris-HCl pH8, 100mM EDTA, 100mM NaCl, 1% SDS, 0.5mg/ml Proteinase K) at 55°C overnight. 160ul 5M NaCl were added followed by centrifugation for 5 minutes, and 500ul of supernatant were transferred to a fresh tube. DNA was precipitated with 340ul of Isopropanol, collected by centrifugation and washed in 70% Ethanol. Pellets were air-dried and resuspended in TE. To isolate ES cell DNA, overgrown clones were washed with PBS and incubated in tail buffer at 37°C for one hour. Twice the volume of ice-cold 96% Ethanol

saturated with NaCl was added to each well and the plates were shaken on an orbital shaker until DNA precipitates appeared. DNA was collected with pipette tips, transferred to tubes containing 70% Ethanol, centrifuged, air-dried and resuspended in TE. For some gene targetings, ES cell clones were pre-screened by long range PCR using Phusion Taq polymerase (Phusion Hot Start High-Fidelity DNA Polymerase, New England Biolabs) following the manufacturer's recommendations. Typically, one primer for these PCR reactions was located within the selection cassette whereas the other primer bound outside the homology arm. Thus, with the PCR product spanning the homology arm, false positives could be distinguished from correctly targeted clones. For Southern blotting, ~10ug of genomic DNA were digested overnight with 3ul of the appropriate restriction enzyme(s). DNA digests were separated on 0.8% TAE agarose gels. Gels were depurinated in 0.25M HCl for 25 minutes and denatured in 1.5M NaCl, 0.5M NaOH for 25 minutes. DNA was then transferred onto positively charged Hybond N+ nylon membranes (Amersham) in 10x SSC overnight. After the DNA transfer, membranes were washed in 3x SSC, air-dried, and the DNA was cross-linked to membranes with 240 mJ/cm<sup>2</sup> UVC irradiation. Membranes were incubated in ExpressHyb hybridization solution (Clontech) at 65°C for 30 minutes followed by hybridization of radio-labeled probe overnight at 65°C. Probes were designed to bind outside of the homology arms to distinguish between random integrants and correctly targeted clones. Probes were radio-labeled using the Prime-It II Random Primer Labeling Kit (Stratagene) and denatured by boiling for 5 minutes. After hybridization, membranes were washed twice with 2x SSC, 0.2% SDS for 2 minutes at room temperature and once for 30 minutes

at 65°C. Air-dried membranes were exposed to X-ray film using intensifying screens at -80°C for up to 7 days.

#### 4.15 Mouse strains, genotyping and intranasal Ad-Cre instillation

Conditional B-Raf knock-out mice (B-Raf<sup>fl/fl</sup>) were generated by Dr. A. Silva (Chen et al., 2006) and kindly provided by Dr. M. Baccarini. Conditional C-Raf knock-out mice (Mikula et al., 2001) were created and provided by Dr. M. Baccarini. TyrCreERT2 mice were generated and provided by Dr. M. Bosenberg (Bosenberg et al., 2006) and LSL-Kras<sup>G12D</sup> mice were generated by Dr. D. Tuveson (Jackson et al., 2001). PLAP Flp reporter mice were created by Dr. S. Dymecki (Awatramani et al., 2001) and obtained from Jackson Laboratories. The generation of LSL-B-Raf<sup>V619E</sup> and R26-LSL-FlpERT2 mice is described in chapter 5.2. Initially, TyrCreERT2, PLAP, B-Raf<sup>fl/fl</sup> and C-Raf<sup>fl/fl</sup> mice were genotyped following the published PCR protocols. Later, genotyping was outsourced and all strains were genotyped by Transnetyx Inc. ([www.transnetyx.com](http://www.transnetyx.com)). For infection of mouse lungs with Ad-Cre, mice were anesthetized using Isoflurane.  $3 \times 10^8$  PFU of virus were precipitated in 500ul MEM (Invitrogen) and 2.4ul 2M CaCl<sub>2</sub>, according to the protocol used by the Jacks laboratory (DuPage et al., 2009; Jackson et al., 2001, <http://web.mit.edu/jacks-lab/>). 50ul of MEM containing Ad-Cre were placed drop-wise onto one nostril of anesthetized mice until all liquid was inhaled. This procedure was repeated once so that each mouse was infected with  $\sim 6 \times 10^7$  PFU of Ad-Cre. For induction of Cre activity, mice carrying inducible CreERT2 alleles were intraperitoneally injected with 2mg Tamoxifen

(Sigma) in corn oil for 3 consecutive days or 4-Hydroxytamoxifen (25mg/ml in DMSO) was topically administered with a brush on two consecutive days.

#### 4.16 Histology, immunohistochemistry and quantification of lung tumor burden

Tissues were fixed in Formalin over-night and stored in 70% Ethanol. Fixed tissues were embedded, cut and stained with H&E by the CRI Histopathology core. Immunohistochemistry for Ki-67, cleaved Caspase 3 and phospho-ERK was also performed by the CRI Histopathology core. To determine the lung tumor burden of mice, total lung areas and neoplastic areas were calculated using Image J (Rasband, 1997-2008) and disease burden was represented as percent of total area. For characterization of individual neoplasms, data was represented as neoplasms/lung area.

#### 4.17 Statistical analysis

All experiments were repeated at least three times and done in triplicates. Western blot experiments that showed modest changes were repeated five times and quantified each time. Data were accepted as reproducible when similar results with consistent changes were observed in all five experiments. Statistical analysis was performed using Student's *t*-test,  $P < 0.05$  was accepted as significant, \*  $P < 0.05$ , \*\*  $P < 0.01$ . Data are shown as mean, error bars represent the standard deviation.

## 5. Results and Discussion

5.1 C-Raf inhibits MAPK activation and transformation by  
B-Raf<sup>V600E</sup> (Molecular Cell, in press)

**C-Raf inhibits MAPK activation and transformation by B-Raf<sup>V600E</sup>**

Florian A. Karreth<sup>1,2</sup>, Gina M. DeNicola<sup>1</sup>, Stephen P. Winter<sup>1</sup>, and David A. Tuveson<sup>1</sup>

<sup>1</sup> Li Ka Shing Centre, Cambridge Research Institute, Cancer Research UK, Robinson Way, Cambridge CB2 0RE, United Kingdom

<sup>2</sup> University of Vienna, Dr. Bohrgasse, 1030 Vienna, Austria

Running title: C-Raf suppresses B-Raf<sup>V600E</sup>

Correspondence should be addressed to David A Tuveson.

Li Ka Shing Centre, Cambridge Research Institute, Cancer Research UK  
Robinson Way  
Cambridge CB2 0RE  
United Kingdom

Tel: +44 (0)1223 404300

Fax: +44 (0)1223 404199

e-mail: david.tuveson@cancer.org.uk



## **Summary**

Activating B-Raf mutations that deregulate the MAPK pathway commonly occur in cancer. Whether additional proteins modulate the enzymatic activity of oncogenic B-Raf is unknown. Here, we show that the proto-oncogene C-Raf paradoxically inhibits B-Raf<sup>V600E</sup> kinase activity through the formation of B-Raf<sup>V600E</sup>-C-Raf complexes. Although all Raf family members associate with oncogenic B-Raf, this inhibitory effect is specific to C-Raf. Indeed, a B-Raf<sup>V600E</sup> isoform with impaired ability to interact with C-Raf exhibits elevated oncogenic potential. Human melanoma cells expressing B-Raf<sup>V600E</sup> display a reduced C-Raf:B-Raf ratio and further suppression of C-Raf increases MAPK activation and proliferation. Conversely, ectopic C-Raf expression lowers ERK phosphorylation and proliferation. Moreover, both oncogenic Ras and Sorafenib stabilize B-Raf<sup>V600E</sup>-C-Raf complexes, thereby impairing MAPK activation. This inhibitory function of C-Raf on B-Raf<sup>V600E</sup>-mediated MAPK activation may explain the lack of co-occurrence of B-Raf<sup>V600E</sup> and oncogenic Ras mutations, and influence the successful clinical development of small molecule inhibitors for B-Raf<sup>V600E</sup>-driven cancers.

## **Introduction**

The mitogen-activated protein kinase (MAPK) pathway relays signals from the plasma membrane to the nucleus, thereby regulating the cell's response to extracellular stimuli. This response encompasses diverse cell biological processes such as proliferation, growth, differentiation and apoptosis (Robinson and Cobb, 1997; Wellbrock et al., 2004a). To ensure proper control of these processes, the MAPK pathway is tightly regulated. Upon ligand binding to receptor tyrosine kinases, the small G protein Ras becomes activated and signals to the MAPK pathway and to several other effector pathways. Active Ras recruits Raf serine/threonine kinases (A-Raf, B-Raf, and C-Raf) to the plasma membrane, where they become activated by regulatory phosphorylation and dephosphorylation events, conformational changes and binding to other proteins (Wellbrock et al., 2004a). Active Raf phosphorylates MEK (for MAPK and extracellular signal-regulated kinase (ERK) kinase), which subsequently phosphorylates ERK. ERK translocates to the nucleus where it initiates diverse gene expression programs by activating transcription factor families such as ETS and AP-1.

Since the MAPK pathway controls cellular processes that are often perturbed in human malignancy, it is not surprising that deregulation of the pathway is commonly observed in cancer. Indeed, activating Ras mutations are found in approximately 30% of human neoplasms (Bos, 1989). More recently, B-Raf mutations were reported in 7% of human cancers (Brose et al., 2002; Davies et al., 2002; Pollock and Meltzer, 2002), and two classes of B-Raf mutations have been identified. The majority of B-Raf mutations hyperactivate its kinase

function and B-Raf<sup>V600E</sup> represents the most prominent example of this class. In contrast, three tumor-associated mutations (G466V, G466E, G596R) weaken the catalytic activity of B-Raf. These mutants have been proposed to stimulate C-Raf activity through physical interaction, thereby hyperactivating the MAPK pathway (Garnett et al., 2005; Wan et al., 2004). A link between mutations activating the MAPK pathway and cancer development was provided by genetically engineered mouse models. Mice expressing endogenous oncogenic Kras or B-Raf develop preneoplasms in several tissues (Karreth and Tuveson, 2009). Cells isolated from these mice display activation of the MAPK pathway and are partially transformed (Mercer et al., 2005; Tuveson et al., 2004). Interestingly, despite possessing oncogenic potential *in vivo* (Kerkhoff et al., 2000) and *in vitro* (Heidecker et al., 1990; Stanton et al., 1989), activating mutations in C-Raf that lead to abnormal MAPK signaling are extremely rare and have only been observed in two cases of AML thus far (Zebisch et al., 2006).

Raf proteins associate in response to Ras stimulation and complexes containing either two copies of the same Raf protein or one copy of two different Raf proteins have been observed (Farrar et al., 1996; Luo et al., 1996; Weber et al., 2001). Indeed, wildtype B-Raf can signal to MEK/ERK by binding and activating C-Raf (Garnett et al., 2005), and B-Raf–C-Raf complexes possess higher kinase activity toward MEK than complexes containing only B-Raf or C-Raf (Rushworth et al., 2006). Additionally, impaired activity B-Raf mutants that require C-Raf to relay signals to MEK and ERK constitutively bind and activate C-Raf (Wan et al., 2004), leading to MAPK

hyperactivation (Garnett et al., 2005; Wan et al., 2004). Together, these findings imply that association of Raf proteins plays an important role in regulating MAPK signal intensity and may participate in controlling the biological output of MAPK activation.

A crucial role for C-Raf in the activation of the MAPK pathway by B-Raf mutants with impaired catalytic function has been established. However, whether C-Raf is able to modulate B-Raf<sup>V600E</sup>-mediated signaling is unknown. Here we report that C-Raf surprisingly inhibits B-Raf<sup>V600E</sup>-induced MAPK activation and transformation through formation of a B-Raf<sup>V600E</sup>-C-Raf complex with reduced kinase activity. Furthermore, oncogenic Ras stimulates activation of C-Raf and association with B-Raf<sup>V600E</sup> to diminish MAPK signaling and proliferation, providing a rationale for the lack of co-occurrence of oncogenic Ras and B-Raf<sup>V600E</sup> mutations in cancer. Finally, incubation of B-Raf<sup>V600E</sup>-expressing cells with the Raf kinase inhibitor Sorafenib results in stabilization of the C-Raf:B-Raf complex, providing additional insight into the mechanism of action of this and potentially other Raf kinase inhibitors.

## **Results**

### **Effects of C-Raf on MAPK pathway activation by oncogenic B-Raf mutants**

To study modulation of oncogenic B-Raf signaling by C-Raf, mutant B-Raf and C-Raf were transiently expressed in HEK293T cells and ERK activation was examined. Concomitant expression of B-Raf<sup>G466V</sup> and C-Raf promoted MAPK activation (Fig. 1A). In contrast, co-expression of B-Raf<sup>V600E</sup> and C-Raf resulted in a marked decrease of phosphorylated ERK (pERK) levels compared to expression of B-Raf<sup>V600E</sup> alone (Fig. 1A), suggesting a suppressive effect of C-Raf on B-Raf<sup>V600E</sup>. We next determined whether C-Raf activity is required for suppression by co-expressing C-Raf mutants with severely reduced kinase activity with B-Raf<sup>V600E</sup>. While C-Raf<sup>K375M</sup> failed to suppress B-Raf<sup>V600E</sup> signaling, B-Raf<sup>V600E</sup>-mediated ERK activation was reduced by C-Raf<sup>S338A</sup> (Fig. 1B). Interestingly, C-Raf<sup>S338A</sup> but not C-Raf<sup>K375M</sup> co-operated with B-Raf<sup>G466V</sup> to promote MAPK pathway activation (Fig. 1B and Garnett et al., 2005), suggesting that Ras-induced phosphorylation of C-Raf at Ser338 is not required for suppression of B-Raf<sup>V600E</sup> and co-operation with B-Raf<sup>G466V</sup>. The extent of interaction between C-Raf<sup>K375M</sup> and B-Raf has been reported to be reduced, while binding of C-Raf<sup>S338A</sup> to B-Raf is not affected by the mutation (Rushworth et al., 2006). Similarly, binding of C-Raf<sup>K375M</sup>, but not C-Raf<sup>S338A</sup>, to B-Raf<sup>V600E</sup> was markedly impaired (Fig. 1C), suggesting that binding to C-Raf is required, while C-Raf kinase activity is dispensable for suppression of B-Raf<sup>V600E</sup>. Since C-Raf<sup>K375M</sup> did not bind and suppress B-Raf<sup>V600E</sup>, we reasoned that the direct association of C-Raf with B-Raf<sup>V600E</sup> inhibits the activity of B-Raf<sup>V600E</sup>. To investigate this hypothesis, flag-tagged B-Raf<sup>V600E</sup> was co-expressed with HA-tagged B-Raf<sup>V600E</sup> or myc-

tagged C-Raf. To measure the kinase activity of different Raf complexes, sequential immunoprecipitation of associated Raf proteins was performed followed by MEK-ERK-MBP *in vitro* kinase assays using the purified complexes. The kinase activity of B-Raf<sup>V600E</sup>-B-Raf<sup>V600E</sup> complexes was comparable to the activity of B-Raf<sup>V600E</sup>-B-Raf<sup>WT</sup> complexes (data not shown). Notably, the kinase activity of B-Raf<sup>V600E</sup>-C-Raf complexes was significantly reduced (Fig. 1D). Thus, C-Raf has an unexpected inhibitory function on MAPK pathway activation by associating with B-Raf<sup>V600E</sup>, thereby reducing the kinase activity of the complex.

#### Suppression of B-Raf<sup>V600E</sup> signaling is specific to C-Raf and not due to activation of negative feedback loops

We next determined whether wildtype B-Raf and A-Raf possess suppressive activities similar to C-Raf. Interestingly, co-expression of wildtype B-Raf did not suppress B-Raf<sup>V600E</sup> (Fig. 2A). Conversely, wildtype B-Raf enhanced MAPK activation by B-Raf<sup>G466V</sup> to similar levels as C-Raf (Fig. 2A). B-Raf<sup>V600E</sup> was not inhibited by co-expression of A-Raf (Fig. 2B), indicating that C-Raf is the only Raf protein capable of suppressing B-Raf<sup>V600E</sup>. Intriguingly, A-Raf failed to co-operate with B-Raf<sup>G466V</sup> to promote MAPK pathway activation (Fig. 2B). The binding efficiency of A-Raf to B-Raf<sup>V600E</sup> was similar to that of C-Raf (Fig. 2C); hence, the lack of a suppressive function of A-Raf was not due to reduced complex formation of A-Raf with B-Raf<sup>V600E</sup>. Thus, suppression of B-Raf<sup>V600E</sup> signaling is specific to C-Raf, while both C- and B-Raf can cooperate with B-Raf<sup>G466V</sup>. To exclude the possibility that co-expression of oncogenic B-Raf and C-Raf activates negative feedback loops and thus leading to reduced

pERK expression, we analyzed phosphorylation of MEK to more accurately determine the activity of B-Raf mutants. Similar to the results regarding pERK, co-expression of C-Raf and B-Raf<sup>V600E</sup> diminished MEK activation, while concomitant expression of C-Raf and B-Raf<sup>G466V</sup> further induced phosphorylation of MEK when compared to expression of the respective B-Raf mutants alone (Fig. 2D). Finally, expression levels of dual specificity phosphatases (DUSP4 and DUSP6) as well as Sprouty 2, known negative modulators of the MAPK pathway, were unchanged upon expression of B-Raf<sup>V600E</sup> or B-Raf<sup>G466V</sup> alone or in combination with C-Raf (Fig. 2E). Therefore, modulation of oncogenic B-Raf-induced MAPK pathway activation by C-Raf is not mediated by activation of negative feedback loops.

#### Interaction of C-Raf and oncogenic B-Raf<sup>V600E</sup> impairs cellular transformation

We identified a murine splice form of B-Raf (termed  $\Delta$ 3-B-Raf) that lacked 33 amino acids within exon 3. The sequence of  $\Delta$ 3-B-Raf has been noted in Genbank for mouse (e.g. NM\_139294) and rat (e.g. XM\_231692).  $\Delta$ 3-B-Raf interacts with C-Raf less efficiently (Suppl. Fig. 1-3) and was utilized to study the effect of B-Raf–C-Raf interaction on cellular transformation by oncogenic B-Raf. Decreased basal and Hras<sup>G12V</sup>-induced binding of  $\Delta$ 3-B-Raf<sup>G466V</sup> to C-Raf was accompanied by reduced activation of the MAPK pathway (Suppl. Fig. 4A, B). Moreover, stimulation of proliferation and anchorage-independent growth in soft agar by  $\Delta$ 3-B-Raf<sup>G466V</sup> was less pronounced when compared to B-Raf<sup>G466V</sup> (Suppl. Fig. 4C, D). These findings further support the notion that complex formation of C-Raf and B-Raf<sup>G466V</sup> promotes activation of the MAPK pathway.

We next determined whether reduced interaction with C-Raf increased the oncogenic potential of B-Raf<sup>V600E</sup>. First, expression in HEK293T cells showed that, in contrast to impaired activity mutants (Garnett et al., 2005), B-Raf<sup>V600E</sup> or  $\Delta$ 3-B-Raf<sup>V600E</sup> only very inefficiently interact with endogenous C-Raf (Fig. 3A). Co-expression with Hras<sup>G12V</sup> induced association of full length B-Raf<sup>V600E</sup> and, to a lesser extent, of  $\Delta$ 3-B-Raf<sup>V600E</sup> with C-Raf (Fig. 3A). Strikingly, Hras<sup>G12V</sup>-mediated complex formation of C-Raf with B-Raf<sup>V600E</sup> diminished B-Raf<sup>V600E</sup>-driven phosphorylation of ERK, and reduction of pERK levels was less pronounced in cells expressing  $\Delta$ 3-B-Raf<sup>V600E</sup> compared to full length B-Raf<sup>V600E</sup> (19% vs. 26% reduction, Fig. 3A). Ectopic expression of B-Raf<sup>V600E</sup> has been shown to transform the immortalized melanocyte cell line melan-a (Wellbrock et al., 2004b), confirming B-Raf's oncogenic potential in melanoma (Davies et al., 2002). Therefore, full length B-Raf<sup>V600E</sup> and  $\Delta$ 3-B-Raf<sup>V600E</sup> were stably expressed in melan-a cells to assess the role of B-Raf<sup>V600E</sup>-C-Raf complex formation on cellular transformation.  $\Delta$ 3-B-Raf<sup>V600E</sup> expression stimulated ERK activation and TPA-independent proliferation more efficiently than B-Raf<sup>V600E</sup> (Fig. 3B and 3C). Moreover, anchorage-independent growth promoted by B-Raf<sup>V600E</sup> was further increased by  $\Delta$ 3-B-Raf<sup>V600E</sup> (Fig. 3D). Similar increases in transformation potential conferred by  $\Delta$ 3-B-Raf<sup>V600E</sup> were observed in NIH3T3 fibroblasts (data not shown). Together, these data demonstrate that C-Raf-mediated inhibition of B-Raf<sup>V600E</sup>-stimulated MAPK signaling and cell transformation is proportional to the efficiency of B-Raf<sup>V600E</sup>-C-Raf complex formation.



## Human melanoma cells circumvent suppression of B-Raf<sup>V600E</sup> by reducing the C-Raf:B-Raf ratio

To investigate whether the antagonistic function of C-Raf towards B-Raf<sup>V600E</sup> was apparent in melanoma, the relative amounts of C-Raf and B-Raf were assessed in a panel of human melanoma cell lines and compared to a human melanocyte cell line (normal human epidermal melanocytes, NHEM). All investigated melanoma cell lines harboring B-Raf<sup>V600E</sup> displayed a reduced C-Raf:B-Raf ratio when compared to NHEM (Fig. 4A). In contrast, Nras mutant cells exhibited similar C-Raf levels but lower B-Raf levels than NHEM, resulting in an increased C-Raf:B-Raf ratio (Fig. 4A). These results indicate that the reduction of C-Raf levels relative to B-Raf is specific to melanoma cells harboring B-Raf<sup>V600E</sup> and does not occur in cell lines that activate the MAPK pathway through other means. To assess whether relative Raf levels in NHEM are representative of melanocytes, expression of B-Raf and C-Raf was compared to another human melanocytes cell line, Fom99. C-Raf expression in Fom99 melanocytes was increased compared to NHEM, resulting in a higher C-Raf:B-Raf ratio in these cells (Suppl. Fig. 5A). Thus, the reduction of the C-Raf:B-Raf ratios in B-Raf<sup>V600E</sup> mutant melanoma cell lines compared to melanocytes is a general finding. For the observed reduction of the C-Raf:B-Raf ratio in B-Raf<sup>V600E</sup> melanoma cells to be biologically relevant, C-Raf and B-Raf molecules should be present at comparable levels in such cells. To address this, the quantity of B-Raf and C-Raf molecules per cell was determined in several melanoma cell lines using recombinant B-Raf and C-Raf as reference standards (Suppl. Fig. 5B). Importantly, the amounts of B-Raf and C-Raf molecules expressed per cell were similar in all investigated

cell lines (Suppl. Fig. 5C). Finally, A-Raf expression was not significantly changed and did not correlate with B-Raf mutation status (Suppl. Fig. 5D), which is consistent with the lack of suppressive activity towards B-Raf<sup>V600E</sup>. Thus, by altering the C-Raf to B-Raf stoichiometry, human melanoma cells harboring B-Raf<sup>V600E</sup> may circumvent suppression of B-Raf<sup>V600E</sup>-induced MAPK activation.

#### Altering C-Raf expression levels in melanoma cell lines carrying B-Raf<sup>V600E</sup> impacts on MAPK signaling and proliferation

To analyze whether further reducing the expression levels of C-Raf affects on MAPK activation and cell proliferation in human B-Raf<sup>V600E</sup> and Nras mutant melanoma cell lines, C-Raf was depleted using RNAi. C-Raf protein levels were decreased significantly following knock-down, while B-Raf levels were unchanged (Fig. 4B). Interestingly, abrogation of C-Raf expression in the B-Raf<sup>V600E</sup> expressing cell lines WM793, WM164, and WM983A promoted increased ERK phosphorylation (Fig. 4B). In contrast, decreased pERK levels were observed upon C-Raf depletion in the N-Ras-mutant cell line SKMel2 (Fig. 4B), consistent with published data (Dumaz et al., 2006). Next, the effect of enhanced MAPK signaling on proliferation of melanoma cells was determined by labeling shRNA-treated cells with BrdU. C-Raf depletion was accompanied by a moderate increase in proliferation of WM793, WM164, and WM983A cells, whereas Nras mutant cells exhibited reduced proliferation upon C-Raf depletion (Fig. 4C). Since C-Raf expression is reduced in many B-Raf mutant human melanoma cell lines, we sought to determine the effect of increased C-Raf levels on MAPK pathway activation and proliferation in

such cells. Consistent with our prior findings regarding the properties of C-Raf in B-Raf<sup>V600E</sup> melanoma cells, we found that multiple melanoma cell lines would not support the stable ectopic expression of C-Raf. Therefore, the melanoma cell line WM793 was examined immediately following transfection with C-Raf, demonstrating that increased C-Raf levels can directly inhibit both the MAPK pathway (Fig. 4D) and cellular proliferation (Fig. 4E). Therefore, C-Raf possesses a suppressive function in B-Raf<sup>V600E</sup> melanoma cells.

#### Oncogenic Ras impairs B-Raf<sup>V600E</sup> signaling through activation of C-Raf

In human cancer, oncogenic Ras and B-Raf<sup>V600E</sup> mutations do not co-occur, while tumors harboring Ras and non-V600E B-Raf mutations have been reported (Thomas et al., 2007). Intriguingly, B-Raf<sup>V600E</sup>-C-Raf association was increased upon Hras<sup>G12V</sup> co-expression (Fig. 2B). Hence, we hypothesized that oncogenic Ras could inhibit B-Raf<sup>V600E</sup>-mediated MAPK signaling by activating C-Raf and promoting B-Raf<sup>V600E</sup>-C-Raf interaction. Accordingly, Hras<sup>G12V</sup> was expressed in NIH3T3 fibroblasts either alone or together with B-Raf<sup>V600E</sup>. Expression of Hras<sup>G12V</sup> resulted in elevated levels of pS338-C-Raf, confirming increased C-Raf activation by Hras<sup>G12V</sup> (Fig. 5A). In addition, B-Raf-C-Raf complexes and pERK levels were more abundant in cells expressing Hras<sup>G12V</sup> (Fig. 5A). Thus, oncogenic Ras induces MAPK signaling in fibroblasts through C-Raf activation and induction of B-Raf-C-Raf complexes. In contrast, Hras<sup>G12V</sup>-mediated induction of B-Raf-C-Raf complexes in NIH3T3 fibroblasts expressing B-Raf<sup>V600E</sup> correlated with diminished MAPK pathway activation (Fig. 5B). Moreover, increased proliferation conferred by either B-Raf<sup>V600E</sup> or Hras<sup>G12V</sup> was negated by

concomitant expression of both oncogenes in NIH3T3 cells (Fig. 5C). To ascertain that complex formation is not due to overexpression of oncogenic B-Raf, similar experiments were performed in WM793 melanoma cells that express endogenous B-Raf<sup>V600E</sup>. Consistent with the data obtained in NIH3T3 fibroblasts, expression of Nras<sup>G12D</sup> in WM793 cells stimulated B-Raf–C-Raf interaction and resulted in reduced pERK levels (Fig. 5D). Moreover, WM793 cells expressing Nras<sup>G12V</sup> proliferated less than cells transfected with a vector control (Fig. 5E). Similarly, ectopic expression of Hras<sup>G12V</sup> in WM793 melanoma cells increased B-Raf–C-Raf complex formation, which correlated with decreased levels of pERK and proliferation (Suppl. Fig. 6A, B), indicating that different Ras oncoproteins are capable of antagonizing B-Raf<sup>V600E</sup>. These findings provide a potential explanation for the exclusivity of Ras and B-Raf<sup>V600E</sup> mutations in human cancers.

#### Sorafenib stabilizes B-Raf<sup>V600E</sup>–C-Raf complexes

Raf kinase inhibitors have been developed as targeted therapeutics for melanoma, and therefore we investigated whether such compounds could influence B-Raf<sup>V600E</sup>–C-Raf complex formation. Indeed, treatment of HEK293T cells expressing flag-B-Raf<sup>V600E</sup> and myc-C-Raf with the Raf inhibitor Sorafenib at concentrations that inhibited MAPK signaling (0.3-3  $\mu$ M) resulted in increased formation of B-Raf<sup>V600E</sup>–C-Raf complexes (Fig. 6A, B). Surprisingly, low concentrations of Sorafenib increased rather than inhibited ERK phosphorylation (Fig. 6A, B). To exclude overexpression artifacts as a possible explanation for this observation, the response to Sorafenib was examined in WM164, A375P and SKMel2 melanoma cells and mouse

embryonic fibroblasts expressing endogenous B-Raf<sup>V619E</sup>. We found similar patterns of B-Raf<sup>V600E</sup>-C-Raf complex stabilization and pERK inhibition at high doses of Sorafenib in all examined cell lines. (Suppl. Fig. 6). However, increased pERK levels at low doses of Sorafenib were only observed in B-Raf<sup>V600E</sup> mutant cells (WM164, A375P, and MEFs) but not in SKMeI2 cells, which carry an N-Ras mutation (Supp. Fig. 6). To determine whether stabilization of B-Raf<sup>V600E</sup>-C-Raf complexes leads to inhibition of MAPK activation, the sensitivity of  $\Delta$ 3-B-Raf<sup>V600E</sup> to Sorafenib was assessed. Sorafenib increased association of C-Raf with  $\Delta$ 3-B-Raf<sup>V600E</sup> in a dose-dependent manner; however, the amount of complexes was lower compared to Sorafenib-induced full length B-Raf<sup>V600E</sup>-C-Raf complexes (Fig. 6C). Moreover, cells expressing  $\Delta$ 3-B-Raf<sup>V600E</sup> were more resistant to high concentrations of Sorafenib than FL-B-Raf<sup>V600E</sup>-expressing cells. While treatment with 3uM Sorafenib significantly reduced pERK levels compared to the 0.3uM dose when FL-B-Raf<sup>V600E</sup> was expressed, no pronounced decrease in pERK levels was observed in  $\Delta$ 3-B-Raf<sup>V600E</sup>-expressing cells at these concentrations (Fig. 6D). Thus, promoting suppression of B-Raf<sup>V600E</sup> through stabilization of B-Raf<sup>V600E</sup>-C-Raf complexes may be an additional mode of action of Sorafenib. We reasoned that the increased pERK levels noted at low doses of Sorafenib may be due to induction of active protein complexes containing only B-Raf<sup>V600E</sup>. To examine this, HA-B-Raf<sup>V600E</sup> and flag-B-Raf<sup>V600E</sup> were co-expressed and cells treated with increasing concentrations of Sorafenib. Indeed, Sorafenib induced HA-B-Raf<sup>V600E</sup>-flag-B-Raf<sup>V600E</sup> complexes in a dose-dependent manner (Fig. 6E). Elevation of pERK levels correlated with HA-B-Raf<sup>V600E</sup>-flag-B-Raf<sup>V600E</sup> complex formation in response

to low doses Sorafenib (0.003-0.03uM). Interestingly, high doses of the Raf inhibitor could not diminish pERK levels below vehicle-treated control levels in cells expressing B-Raf<sup>V600E</sup> alone (Fig. 6E). These findings suggest that Sorafenib-induced stabilization of B-Raf<sup>V600E</sup>-C-Raf complexes with low kinase activity contributes to the therapeutic activity of this small molecule inhibitor.

## **Discussion**

Activating mutations in Ras and B-Raf are commonly found in cancer and lead to deregulation of the MAPK pathway. Investigating this aberrant regulation of the MAPK signaling cascade in cancer could identify useful therapeutic targets to combat the disease. In this study, we report a suppressive function of the proto-oncogene C-Raf on oncogenic B-Raf<sup>V600E</sup>.

We found that C-Raf suppresses B-Raf<sup>V600E</sup> through the formation of B-Raf<sup>V600E</sup>-C-Raf complexes that display markedly decreased kinase activity, leading to impaired activation of MEK/ERK. This finding was surprising because B-Raf-C-Raf complexes were reported to possess higher kinase activity towards MEK than B-Raf-B-Raf and C-Raf-C-Raf complexes (Rushworth et al., 2006). A potential explanation could be the restriction of B-Raf<sup>V600E</sup> protein dynamics and therefore catalytic activity by its association with C-Raf. As wildtype A-Raf or B-Raf bind to B-Raf<sup>V600E</sup> but don't inhibit the activity of B-Raf<sup>V600E</sup>, such complexes are likely distinct in their quaternary structure or contain different additional binding partners compared to the B-Raf<sup>V600E</sup>-C-Raf complexes. Whether C-Raf has a similar inhibitory influence on wildtype B-Raf-mediated MAPK activation in cells is incompletely understood. Indeed, genetic ablation of C-Raf increases B-Raf activity and phosphorylation of MEK in fibroblasts (Mikula et al., 2001), indicating that C-Raf may negatively modulate MAPK signaling under certain conditions. These data suggest that the composition and abundance of Raf complexes play pivotal roles in regulating the extent of MAPK pathway activation under normal and pathological conditions. The relative cellular amounts of B-Raf

and C-Raf may affect the formation of Raf complexes and thus the susceptibility of certain cell types to transformation by different oncogenic B-Raf mutants. This is supported by the fact that the occurrence of the V600E mutation is relatively rare in cancers that more commonly carry impaired activity B-Raf mutations, such as the lung (see COSMIC database for B-Raf mutation data in cancer; <http://www.sanger.ac.uk/genetics/CGP/cosmic/>).

C-Raf has been previously demonstrated to antagonize other serine/threonine kinases through physical interaction. Binding of C-Raf to the proapoptotic kinases MST2 (O'Neill et al., 2004) and ASK1 (Chen et al., 2001) prevents their activation and protects cells from apoptosis. Moreover, C-Raf inhibits Rok- $\alpha$ , thereby regulating cell motility and death (Piazzolla et al., 2005). Similar to MST2 (O'Neill et al., 2004), suppression of B-Raf<sup>V600E</sup> is specific to C-Raf as wildtype B-Raf could not inhibit B-Raf<sup>V600E</sup>. C-Raf exerts its inhibitory functions on MST2, ASK1 and Rok- $\alpha$  independent of its kinase activity and MEK/ERK signaling. To address whether C-Raf kinase activity is required for suppression of B-Raf<sup>V600E</sup>, we determined MAPK activation by B-Raf<sup>V600E</sup> in the presence of two C-Raf mutants with severely impaired catalytic activity. Interestingly, suppression of B-Raf<sup>V600E</sup> by wildtype and mutant C-Raf correlated with the efficiency of complex formation rather than C-Raf activity. Moreover, we did not observe changes in Ser/Thr phosphorylation of immunoprecipitated B-Raf<sup>V600E</sup> when co-expressed with C-Raf (data not shown) and thus kinase activity appears to be dispensable for the antagonistic effect of C-Raf. Reduced binding of C-Raf<sup>K375M</sup> to B-Raf has been noted before (Rushworth et al., 2006) and could be due to a conformational change



induced by the K375M mutation, thereby impairing interaction. In contrast, the association of C-Raf with MST2, ASK1, and ROK- $\alpha$  is unaffected by the K375M mutation. Whether the catalytic lysine at position 375 of C-Raf is crucial for complex formation with B-Raf remains to be determined. Therefore, these findings suggest that the interaction of C-Raf with B-Raf<sup>V600E</sup> directly lowers the kinase activity of B-Raf<sup>V600E</sup>.

We found that the C-Raf expression levels are reduced relative to B-Raf levels in human melanoma cell lines expressing B-Raf<sup>V600E</sup>. Interestingly, cells derived from early tumor stages (radial and vertical growth phase) contained decreased C-Raf protein levels, while metastasis-derived cell lines harbored increased B-Raf protein levels and therefore a reduced C-Raf:B-Raf ratio. Previously, C-Raf mRNA levels were found to be lower in B-Raf<sup>V600E</sup> melanoma cells compared to cells expressing wildtype B-Raf, suggesting transcriptional regulation as a potential mechanism of C-Raf reduction (Pavey et al., 2004). We have confirmed that the B-Raf mRNA levels are higher than that of C-Raf in B-Raf<sup>V600E</sup> expressing melanoma cells (data not shown), although translational and post-translational processes may also participate in our findings. Nonetheless, the reduced ratio of C-Raf:B-Raf protein levels in B-Raf<sup>V600E</sup>-expressing melanoma cells relative to melanocytes is likely to alleviate suppression of B-Raf<sup>V600E</sup>. This hypothesis is substantiated by our observation that C-Raf and B-Raf molecules are present at near-equimolar amounts in these cells. Therefore, changes in the stoichiometry could impact the formation of Raf complexes. Further evidence for a suppressive function of C-Raf in B-Raf<sup>V600E</sup>-expressing human melanoma cell lines comes from the

observation that stable cell lines expressing ectopic C-Raf or ectopic Ras could not be isolated. Invariably, expression of these cDNAs was rapidly downregulated or lost, indicating that B-Raf<sup>V600E</sup>-C-Raf complex formation by forced expression of high C-Raf or Ras levels is not tolerated by these cells. Together, these findings support the premise that B-Raf<sup>V600E</sup>-expressing cells circumvent C-Raf's antagonistic function by reducing C-Raf levels relative to B-Raf, thereby creating an intracellular environment that facilitates hyperactivation of the MAPK pathway and cellular transformation.

B-Raf<sup>V600E</sup> and oncogenic Ras mutations are mutually exclusive in human cancer, which has previously been attributed to redundant MAPK pathway activation by the two oncogenes. We demonstrate here that oncogenic Ras activates C-Raf, leading to an interaction with B-Raf<sup>V600E</sup> and inhibition of its catalytic activity. Suppression of MAPK pathway activation by two oncogenic Ras mutants (Hras<sup>G12V</sup> and Nras<sup>G12D</sup>) was observed in melanoma cells and fibroblasts expressing B-Raf<sup>V600E</sup>, indicating that Ras-mediated inhibition of B-Raf<sup>V600E</sup> is not limited to one specific cell type or Ras protein. Indeed, mutual exclusivity of B-Raf<sup>V600E</sup> and oncogenic Ras appears to be a universal phenomenon, irrespective of cancer type. Interestingly, non-B-Raf<sup>V600E</sup> mutations co-occur with Ras mutations (Thomas et al., 2007), consistent with the increased association of B-Raf<sup>G466V</sup> with C-Raf and ERK activation upon expression of Hras<sup>G12V</sup> as observed in this study. C-Raf activation by impaired activity mutant B-Raf occurs independently of Ras (Garnett et al., 2005); however, we propose that C-Raf activation is further increased by oncogenic Ras, thereby enhancing MAPK signaling. Thus, co-occurrence of oncogenic

Ras and impaired activity mutant B-Raf cooperates to deregulate the MAPK pathway, resulting in signal intensities that may enhance oncogenesis of certain tumor types.

Sorafenib inhibits C-Raf more potently than B-Raf and B-Raf<sup>V600E</sup> (Wilhelm et al., 2004). While high doses of Sorafenib inhibited MAPK signaling, lower doses partially rescued C-Raf-induced suppression of B-Raf<sup>V600E</sup> signaling (Fig. 6). Importantly, cells expressing either  $\Delta 3$ -B-Raf<sup>V600E</sup> or no ectopic C-Raf were more resistant to Sorafenib at high doses. Therefore, the Sorafenib-mediated interaction of C-Raf with B-Raf<sup>V600E</sup> and the consequential decrease in catalytic activity may be an additional mode of action of Sorafenib. Increased MAPK pathway activation at low concentrations may be due to Sorafenib-induced association of B-Raf<sup>V600E</sup> with wildtype or mutant B-Raf, which could augment B-Raf<sup>V600E</sup> activity. Indeed, B-Raf<sup>V600E</sup>-B-Raf<sup>V600E</sup> complexes were induced at lower concentrations of Sorafenib than B-Raf<sup>V600E</sup>-C-Raf complexes. When Sorafenib-induced formation of B-Raf<sup>V600E</sup>-B-Raf<sup>V600E</sup> complexes was determined, only the amount of HA-tagged B-Raf<sup>V600E</sup> bound to flag-tagged B-Raf<sup>V600E</sup> was examined, whereas complexes consisting of only one species of tagged B-Raf<sup>V600E</sup> were disregarded. The actual amount of complexes containing only B-Raf<sup>V600E</sup> is therefore much higher than indicated by the experimental approach. Moreover, low levels of Sorafenib did not increase pERK levels in N-Ras mutant SKMel2 cells (Suppl. Fig. 7), indicating that mutant N-Ras-induced activation of the MAPK pathway is not enhanced by stabilization of wildtype B-Raf-B-Raf complexes. Thus, low concentrations of Sorafenib may promote rather than inhibit B-Raf<sup>V600E</sup>

signaling through stabilization of B-Raf<sup>V600E</sup>-B-Raf<sup>V600E</sup> complexes. Indeed, Sorafenib has performed poorly in clinical trials thus far and showed equal efficacy in B-Raf<sup>V600E</sup> and B-Raf<sup>WT</sup> tumors (Eisen et al., 2006). Tumors carrying impaired activity mutant B-Raf, however, were not evaluated and may be more responsive to pan-Raf inhibitors such as Sorafenib. Therefore, determining the B-Raf mutational status could be imperative for the right choice of treatment. Our finding that proto-oncogenic C-Raf exhibits suppressive activity towards B-Raf<sup>V600E</sup> should encourage investigations into the development of inhibitors that efficiently and selectively stabilize B-Raf<sup>V600E</sup>-C-Raf complexes for the treatment of cancers harboring this mutation.

## **Experimental Procedures**

### **Plasmids**

B-Raf was PCR amplified from mouse cDNA, a flag-tag or HA-tag introduced at the C-terminus and cloned into pBabe-puro or pWZL-hygro, respectively. Mutant variants were generated using a site-directed mutagenesis kit (Stratagene).

### **Cell lines and transfections**

HEK293T and NIH3T3 cells were obtained from ATCC and cultured in DMEM (Invitrogen) containing 10% fetal calf serum (Hyclone), 100U/mL Penicillin and 100ug/mL Streptomycin (both Invitrogen). NHEM were obtained from PromoCell and cultured in Melanocyte Growth Medium (PromoCell). Melanoma cell lines were a kind gift from M. Herlyn (Wistar Institute, Philadelphia) and cultured in DMEM containing 10% fetal calf serum, 100U/mL Penicillin and 100ug/mL Streptomycin. Melan-a cells were a kind gift from D. Bennett (London) and cultured in RPMI (Invitrogen) containing 10% fetal calf serum, 100U/mL Penicillin and 100ug/mL Streptomycin and 200uM TPA (Sigma). HEK293T cells were plated 24 hours before transient transfection using Fugene 6 (Roche) or Lipofectamine 2000 (Invitrogen). Transfected HEK293T cells were used for experiments 48 hours after transfection. NIH3T3 fibroblasts were infected with retroviruses produced in the Phoenix packaging cell line, in the presence of 8ug/ml polybrene and selected with puromycin or hygromycin 48 hours after infection. For knock-down experiments, we used the pSuper-retro-puro vector containing short

hairpins targeting human C-Raf and a scrambled control. shRNA sequences were published previously (Hingorani et al., 2003).

### Immunoprecipitation

Cells were washed twice with PBS and lysed in ice-cold RIPA lysis buffer. 400ug of total lysate were precleared for 20 minutes and then immunoprecipitated with 20ul of ANTI-FLAG M2 agarose beads (Sigma) or ANTI-HA agarose beads (Sigma) for 2 hours at 4°C. Beads were washed 4 times with RIPA lysis buffer and subjected to SDS-PAGE. For kinase assays, HA-B-Raf<sup>V600E</sup>, HA-B-Raf, myc-C-Raf, or myc-C-Raf<sup>K375M</sup> were co-expressed with flag-B-Raf<sup>V600E</sup>. HA-tagged and myc-tagged components of the complexes were immunoprecipitated for 6 hours from 600ug of total lysate using ANTI-HA agarose beads or ANTI-myc agarose beads, respectively. Complexes were eluted twice using 200ug/ml HA- or myc-peptide in TBS for 30 minutes at 4°C, diluted with RIPA lysis buffer and subjected to a flag-IP overnight to isolate specific HA-tagged/flag-tagged or myc-tagged/flag-tagged protein complexes. Beads were washed four times with RIPA lysis buffer and used in a MAPK sandwich kinase assay with <sup>32</sup>P-γ-ATP, using MBP as final substrate (Millipore) according to the manufacturer's recommendations. Kinase reactions were analyzed by SDS-PAGE and autoradiography to detect <sup>32</sup>P-γ-labeled MBP. The beads from the flag-IP were used to detect the amount of immunoprecipitated flag-B-Raf<sup>V600E</sup> by Western blotting and the phospho-MBP signal was normalized to immunoprecipitated flag-B-Raf<sup>V600E</sup>.

### Western blotting

Protein lysates and immunoprecipitates were separated on precast NuPAGE Novex 4-12% Bis-Tris gradient gels (Invitrogen), transferred onto a PVDF membrane (Millipore) and incubated overnight with one of the following primary antibodies: HA, flag, phospho-ERK1/2, ERK1/2, phospho-MEK1/2, MEK1/2 (all Cell Signaling), C-Raf, B-Raf, actin (all Santa Cruz Biotechnologies) panRas (Calbiochem), phospho-S338-C-Raf, myc, A-Raf, DUSP4, DUSP6, Sprouty 2 (both Abcam). Membranes were incubated with secondary HRP-antibodies (Jackson ImmunoResearch) for one hour followed by signal detection with enhanced chemiluminescence and x-ray film (both Amersham). Alternatively, membranes were incubated with Alexa Fluor secondary antibodies (Invitrogen) for one hour, and scanned using Li-Cor Odyssey. Signal was quantified using Odyssey software.

#### Proliferation and soft agar assays

$2.0-2.5 \times 10^4$  cells were plated in triplicates in 12 well plates and counted every day for 4 days for proliferation of melan-a and NIH3T3 cells or counted every other day for 7 days for proliferation of WM793 cells. Alternatively, cells were incubated with BrdU for 6 hours and proliferating cells detected using an anti-BrdU antibody (B&D) following the manufacturer's instructions. For soft agar assays,  $5 \times 10^4$  cells were resuspended in 0.4% agar and plated over 0.8% agar. Colonies were stained with Giemsa after 3 weeks.

#### RNA isolation, cDNA synthesis, and PCR analysis

RNA was isolated from mouse tissues with TRIzol reagent (Invitrogen). 2-4ug RNA were used for cDNA synthesis using Ready-To-Go You-Prime First-

Strand Beads (Amersham Biosciences) following the manufacturer's recommendations. For PCR analysis of exon 3, primers binding to exon 2 and 4 were designed.

#### Statistical analysis

All experiments were repeated at least three times and done in triplicates. Western blot experiments that showed modest changes were repeated five times and quantified each time. Data were accepted as reproducible when similar results with consistent changes were observed in all five experiments. Statistical analysis was performed using Student's *t*-test,  $P < 0.05$  was accepted as significant, \*  $P < 0.05$ , \*\*  $P < 0.01$ . Data are shown as mean, error bars represent the standard deviation.



## **Acknowledgements**

We thank members of the Tuveson laboratory for helpful discussions and M. Baccarini for suggestions on the manuscript. We are grateful to M. Herlyn, D. Bennett, C. Pritchard, M. McMahon, and R. Marais for cell lines and expression vectors. FAK was supported by a Boehringer Ingelheim Fonds PhD student fellowship. DAT is a group leader of Cancer Research UK, and this research was funded by the University of Cambridge and Cancer Research UK, The Li Ka Shing Foundation and Hutchison Whampoa. Earlier work was funded in part by the Samuel Waxman Foundation.

## **References**

- Bos, J. L. (1989). ras oncogenes in human cancer: a review. *Cancer Res* 49, 4682-4689.
- Brose, M. S., Volpe, P., Feldman, M., Kumar, M., Rishi, I., Gerrero, R., Einhorn, E., Herlyn, M., Minna, J., Nicholson, A., *et al.* (2002). BRAF and RAS mutations in human lung cancer and melanoma. *Cancer Res* 62, 6997-7000.
- Chen, J., Fujii, K., Zhang, L., Roberts, T., and Fu, H. (2001). Raf-1 promotes cell survival by antagonizing apoptosis signal-regulating kinase 1 through a MEK-ERK independent mechanism. *Proc Natl Acad Sci U S A* 98, 7783-7788.
- Davies, H., Bignell, G. R., Cox, C., Stephens, P., Edkins, S., Clegg, S., Teague, J., Woffendin, H., Garnett, M. J., Bottomley, W., *et al.* (2002). Mutations of the BRAF gene in human cancer. *Nature* 417, 949-954.
- Diaz, B., Barnard, D., Filson, A., MacDonald, S., King, A., and Marshall, M. (1997). Phosphorylation of Raf-1 serine 338-serine 339 is an essential regulatory event for Ras-dependent activation and biological signaling. *Mol Cell Biol* 17, 4509-4516.
- Dumaz, N., Hayward, R., Martin, J., Ogilvie, L., Hedley, D., Curtin, J. A., Bastian, B. C., Springer, C., and Marais, R. (2006). In melanoma, RAS mutations are accompanied by switching signaling from BRAF to CRAF and disrupted cyclic AMP signaling. *Cancer Res* 66, 9483-9491.
- Eisen, T., Ahmad, T., Flaherty, K. T., Gore, M., Kaye, S., Marais, R., Gibbens, I., Hackett, S., James, M., Schuchter, L. M., *et al.* (2006). Sorafenib in advanced melanoma: a Phase II randomised discontinuation trial analysis. *Br J Cancer* 95, 581-586.
- Farrar, M. A., Alberol, I., and Perlmutter, R. M. (1996). Activation of the Raf-1 kinase cascade by coumermycin-induced dimerization. *Nature* 383, 178-181.
- Garnett, M. J., Rana, S., Paterson, H., Barford, D., and Marais, R. (2005). Wild-type and mutant B-RAF activate C-RAF through distinct mechanisms involving heterodimerization. *Mol Cell* 20, 963-969.
- Heidecker, G., Huleihel, M., Cleveland, J. L., Kolch, W., Beck, T. W., Lloyd, P., Pawson, T., and Rapp, U. R. (1990). Mutational activation of c-raf-1 and definition of the minimal transforming sequence. *Mol Cell Biol* 10, 2503-2512.
- Hingorani, S. R., Jacobetz, M. A., Robertson, G. P., Herlyn, M., and Tuveson, D. A. (2003). Suppression of BRAF(V599E) in human melanoma abrogates transformation. *Cancer Res* 63, 5198-5202.
- Karreth, F. A., and Tuveson, D. A. (2009). Modelling oncogenic Ras/Raf signalling in the mouse. *Curr Opin Genet Dev* 19, 4-11.
- Kerkhoff, E., Fedorov, L. M., Siefken, R., Walter, A. O., Papadopoulos, T., and Rapp, U. R. (2000). Lung-targeted expression of the c-Raf-1 kinase in transgenic mice exposes a novel oncogenic character of the wild-type protein. *Cell Growth Differ* 11, 185-190.
- Luo, Z., Tzivion, G., Belshaw, P. J., Vavvas, D., Marshall, M., and Avruch, J. (1996). Oligomerization activates c-Raf-1 through a Ras-dependent mechanism. *Nature* 383, 181-185.
- Mercer, K., Giblett, S., Green, S., Lloyd, D., DaRocha Dias, S., Plumb, M., Marais, R., and Pritchard, C. (2005). Expression of endogenous oncogenic V600EB-raf induces proliferation and developmental defects in mice and transformation of primary fibroblasts. *Cancer Res* 65, 11493-11500.

Mikula, M., Schreiber, M., Husak, Z., Kucerova, L., Ruth, J., Wieser, R., Zatloukal, K., Beug, H., Wagner, E. F., and Baccarini, M. (2001). Embryonic lethality and fetal liver apoptosis in mice lacking the c-raf-1 gene. *Embo J* 20, 1952-1962.

O'Neill, E., Rushworth, L., Baccarini, M., and Kolch, W. (2004). Role of the kinase MST2 in suppression of apoptosis by the proto-oncogene product Raf-1. *Science* 306, 2267-2270.

Pavey, S., Johansson, P., Packer, L., Taylor, J., Stark, M., Pollock, P. M., Walker, G. J., Boyle, G. M., Harper, U., Cozzi, S. J., *et al.* (2004). Microarray expression profiling in melanoma reveals a BRAF mutation signature. *Oncogene* 23, 4060-4067.

Piazzolla, D., Meissl, K., Kucerova, L., Rubiolo, C., and Baccarini, M. (2005). Raf-1 sets the threshold of Fas sensitivity by modulating Rok-alpha signaling. *J Cell Biol* 171, 1013-1022.

Pollock, P. M., and Meltzer, P. S. (2002). A genome-based strategy uncovers frequent BRAF mutations in melanoma. *Cancer Cell* 2, 5-7.

Robinson, M. J., and Cobb, M. H. (1997). Mitogen-activated protein kinase pathways. *Curr Opin Cell Biol* 9, 180-186.

Rushworth, L. K., Hindley, A. D., O'Neill, E., and Kolch, W. (2006). Regulation and role of Raf-1/B-Raf heterodimerization. *Mol Cell Biol* 26, 2262-2272.

Stanton, V. P., Jr., Nichols, D. W., Laudano, A. P., and Cooper, G. M. (1989). Definition of the human raf amino-terminal regulatory region by deletion mutagenesis. *Mol Cell Biol* 9, 639-647.

Thomas, R. K., Baker, A. C., Debiasi, R. M., Winckler, W., Laframboise, T., Lin, W. M., Wang, M., Feng, W., Zander, T., MacConaill, L., *et al.* (2007). High-throughput oncogene mutation profiling in human cancer. *Nat Genet* 39, 347-351.

Tuveson, D. A., Shaw, A. T., Willis, N. A., Silver, D. P., Jackson, E. L., Chang, S., Mercer, K. L., Grochow, R., Hock, H., Crowley, D., *et al.* (2004). Endogenous oncogenic K-ras(G12D) stimulates proliferation and widespread neoplastic and developmental defects. *Cancer Cell* 5, 375-387.

Wan, P. T., Garnett, M. J., Roe, S. M., Lee, S., Niculescu-Duvaz, D., Good, V. M., Jones, C. M., Marshall, C. J., Springer, C. J., Barford, D., and Marais, R. (2004). Mechanism of activation of the RAF-ERK signaling pathway by oncogenic mutations of B-RAF. *Cell* 116, 855-867.

Weber, C. K., Slupsky, J. R., Kalmes, H. A., and Rapp, U. R. (2001). Active Ras induces heterodimerization of cRaf and BRaf. *Cancer Res* 61, 3595-3598.

Wellbrock, C., Karasarides, M., and Marais, R. (2004a). The RAF proteins take centre stage. *Nat Rev Mol Cell Biol* 5, 875-885.

Wellbrock, C., Ogilvie, L., Hedley, D., Karasarides, M., Martin, J., Niculescu-Duvaz, D., Springer, C. J., and Marais, R. (2004b). V599EB-RAF is an oncogene in melanocytes. *Cancer Res* 64, 2338-2342.

Wilhelm, S. M., Carter, C., Tang, L., Wilkie, D., McNabola, A., Rong, H., Chen, C., Zhang, X., Vincent, P., McHugh, M., *et al.* (2004). BAY 43-9006 exhibits broad spectrum oral antitumor activity and targets the RAF/MEK/ERK pathway and receptor tyrosine kinases involved in tumor progression and angiogenesis. *Cancer Res* 64, 7099-7109.

Zebisch, A., Staber, P. B., Delavar, A., Bodner, C., Hiden, K., Fischereeder, K., Janakiraman, M., Linkesch, W., Auner, H. W., Emberger, W., *et al.* (2006). Two transforming C-RAF germ-line mutations identified in patients with therapy-related acute myeloid leukemia. *Cancer Res* 66, 3401-3408.

## **Figures**

Figure 1: C-Raf inhibits B-Raf<sup>V600E</sup> kinase activity. (A) Effect of C-Raf on ERK activation mediated by B-Raf mutants. Levels of pERK in HEK293T cells expressing flag-B-Raf<sup>V600E</sup> or flag-B-Raf<sup>G466V</sup> alone or together with myc-C-Raf were determined by Western blotting. Densitometric analyses for pERK levels are shown. (B) Effect of C-Raf mutants with impaired kinase activity on ERK activation by B-Raf<sup>V600E</sup> or B-Raf<sup>G466V</sup>. Levels of pERK in B-Raf mutant cells expressing either wildtype C-Raf, C-Raf<sup>K375M</sup> or C-Raf<sup>S338A</sup> were determined by Western blotting. (C) Reduced association of C-Raf<sup>K375M</sup> with B-Raf<sup>V600E</sup>. C-Raf, C-Raf<sup>K375M</sup> or C-Raf<sup>S338A</sup> were co-immunoprecipitated with B-Raf<sup>V600E</sup> and levels of bound protein assessed by Western blotting. (D) B-Raf<sup>V600E</sup>-C-Raf complexes display reduced kinase activity. Schematic depicts the sequential immunoprecipitation approach. Amount of MBP phosphorylation with <sup>32</sup>P-γ-ATP by B-Raf<sup>V600E</sup>-B-Raf<sup>V600E</sup> complexes or B-Raf<sup>V600E</sup>-C-Raf complexes was determined by SDS-PAGE and autoradiography. Equal levels of input proteins were verified by Western blotting.

Figure 2: B-Raf<sup>V600E</sup> signaling is not inhibited by A-Raf, wildtype B-Raf or activation of negative feedback loops. (A) Effect of wildtype B-Raf on ERK activation mediated by B-Raf mutants. Levels of pERK in cells expressing flag-B-Raf<sup>V600E</sup> or flag-B-Raf<sup>G466V</sup> with or without HA-B-Raf<sup>WT</sup> were determined by Western blotting. (B) Effect of A-Raf on ERK activation mediated by B-Raf mutants. Levels of pERK in cells expressing flag-B-Raf<sup>V600E</sup> or flag-B-Raf<sup>G466V</sup> with or without myc-A-Raf were determined by Western blotting. (C) A-Raf

forms complexes with B-Raf<sup>V600E</sup>. myc-C-Raf or myc-A-Raf were immunoprecipitated from HEK293T cells co-expressing flag-B-Raf<sup>V600E</sup> and levels of bound B-Raf<sup>V600E</sup> determined by Western blotting. (D) C-Raf decreases MEK activation by B-Raf<sup>V600E</sup> and augments MEK activation by B-Raf<sup>G466V</sup>. Levels of pMEK in cells expressing flag-B-Raf<sup>V600E</sup> or flag-B-Raf<sup>G466V</sup> with or without myc-C-Raf were determined by Western blotting. (E) Negative feedback loops are not activated upon co-expression of B-Raf<sup>V600E</sup> and C-Raf. C-Raf was expressed in cells expressing B-Raf mutants and levels of DUSP4, DUSP6 and Sprouty 2 were analyzed by Western blotting. Lysates of Hras<sup>G12V</sup>-transformed NIH3T3 fibroblasts served as positive controls.

Figure 3: Reduced interaction with C-Raf promotes transformation by  $\Delta 3$ -B-Raf<sup>V600E</sup>. (A) Hras<sup>G12V</sup>-induced association of C-Raf with full length (FL-) B-Raf<sup>V600E</sup> and  $\Delta 3$ -B-Raf<sup>V600E</sup> in HEK293T cells. Immunoprecipitated amounts of C-Raf as well as levels of pERK, B-Raf, C-Raf, and Hras<sup>G12V</sup> in the lysates were determined by Western blotting. (B) Stable expression of FL-B-Raf<sup>V600E</sup> and  $\Delta 3$ -B-Raf<sup>V600E</sup> in melan-a cells, and associated pERK levels. (C) Proliferation of melan-a cells expressing FL-B-Raf<sup>V600E</sup> and  $\Delta 3$ -B-Raf<sup>V600E</sup> cultured in the absence of TPA.  $\Delta 3$ -B-Raf<sup>V600E</sup> cells proliferate faster than FL-B-Raf<sup>V600E</sup> cells (\*  $P=0.0009$ , \*\*  $P=0.001$ , \*\*\*  $P=0.0006$ ). (D) Anchorage-independent growth of melan-a cells expressing FL-Raf<sup>V600E</sup> and  $\Delta 3$ -B-Raf<sup>V600E</sup>.  $\Delta 3$ -B-Raf<sup>V600E</sup> expressing melan-a cells form significantly more colonies in soft agar. The mean and standard deviation of one representative experiment done in triplicate is shown in (C) and (D).

Figure 4: C-Raf levels in melanoma cell lines modulate B-Raf<sup>V600E</sup> signaling and proliferation. (A) B-Raf<sup>V600E</sup> mutant human melanoma cell lines display a reduced C-Raf:B-Raf ratio. Evaluation of C-Raf and B-Raf protein levels in early stage- and metastases-derived B-Raf<sup>V600E</sup> mutant as well as Nras mutant melanoma cells (upper panel). Quantification of expression levels and C-Raf:B-Raf ratio is shown in lower panel. C-Raf levels are reduced relative to B-Raf in B-Raf<sup>V600E</sup> mutant melanoma cell lines and slightly increased in Nras mutant melanoma cells. (B) C-Raf depletion increases ERK activation in B-Raf<sup>V600E</sup> mutant melanoma cells. Western blot displaying knock-down efficiency of C-Raf and accompanying increase of pERK levels is shown. (C) C-Raf depletion increases proliferation of B-Raf<sup>V600E</sup> mutant melanoma cells. Cells were labelled with BrdU for 6 hours and proliferating cells detected with an anti-BrdU antibody. (D) Ectopic expression of myc-C-Raf in WM793 melanoma cells diminished pERK levels. (E) WM793 cells transfected in (D) demonstrated decreased proliferation following C-Raf transfection. The mean and standard deviation of one representative experiment done in triplicate is shown in (C) and (E, \*\*  $P=0.0014$ , \*\*\*  $P=0.0003$ ).

Figure 5: Oncogenic Ras promotes association of C-Raf and B-Raf<sup>V600E</sup> and inhibition of MAPK signaling. (A) Hras<sup>G12V</sup> activates endogenous C-Raf and induces complex formation with endogenous B-Raf in NIH3T3 fibroblasts. Western blot shows Hras<sup>G12V</sup>-induced C-Raf<sup>S338</sup> phosphorylation, B-Raf-C-Raf association and MAPK activation in NIH3T3 fibroblasts. (B) Hras<sup>G12V</sup> antagonizes ERK activation in co-transfected HA-B-Raf<sup>V600E</sup> NIH3T3 fibroblasts. Western blots display Hras<sup>G12V</sup>-induced HA-B-Raf<sup>V600E</sup>-C-Raf

association and decreased pERK levels in B-Raf<sup>V600E</sup> expressing NIH3T3 fibroblasts. (C) Decreased proliferation of HA-B-Raf<sup>V600E</sup>; Hras<sup>G12V</sup> co-expressing fibroblasts depicted in (B). Cells were labelled with BrdU and proliferating cells were detected using an anti-BrdU antibody. (D) Nras<sup>G12D</sup> induces B-Raf–C-Raf complex formation and decreases pERK in B-Raf<sup>V600E</sup> mutant WM793 melanoma cells. (E) Expression of Nras<sup>G12D</sup> reduces proliferation of WM793 melanoma cells (\*  $P=0.025$ , \*\*  $P=0.0009$ ). The mean and standard deviation of one representative experiment done in triplicate is shown in (C) and (D).

Figure 6: Sorafenib stabilizes Raf complexes. (A, B) Treatment of HEK293T cells expressing ectopic B-Raf<sup>V600E</sup> and C-Raf with Sorafenib increases B-Raf<sup>V600E</sup>–C-Raf complex formation. Western blot of co-immunoprecipitated C-Raf and input proteins (A) and quantification of relative amounts of pERK and B-Raf<sup>V600E</sup>-bound C-Raf (B) are shown. (C, D) Full length or alternatively spliced B-Raf<sup>V600E</sup> were co-expressed with C-Raf in HEK293T cells and incubated with increasing concentrations of Sorafenib. (C) Comparison of Sorafenib-induced binding of C-Raf to FL-B-Raf<sup>V600E</sup> or  $\Delta 3$ -B-Raf<sup>V600E</sup>. Amount of immunoprecipitated C-Raf was normalized to C-Raf bound to FL-B-Raf<sup>V600E</sup> in untreated cells. (D) Inhibition of ERK activation by Sorafenib. pERK levels were normalized to untreated cells expressing FL-B-Raf<sup>V600E</sup> but no ectopic C-Raf. (E) Sorafenib enhances B-Raf<sup>V600E</sup>–B-Raf<sup>V600E</sup> association. HEK293T cells expressing flag-B-Raf<sup>V600E</sup> and HA-B-Raf<sup>V600E</sup> were treated with increasing concentrations of Sorafenib followed by assessment of HA-B-Raf<sup>V600E</sup> binding to flag-B-Raf<sup>V600E</sup> and activation of ERK. (F) Model of

suppression of B-Raf<sup>V600E</sup> signaling by C-Raf. (I) In normal cells, Ras stimulates MAPK signaling through activation of both B-Raf and C-Raf. (II) In B-Raf<sup>V600E</sup> mutant cells, C-Raf forms complexes with B-Raf<sup>V600E</sup> leading to reduced signaling. Complex formation can be promoted by oncogenic Ras-induced C-Raf activation or Sorafenib.



## **Supplemental Information**

### **Reduced C-Raf affinity of alternatively spliced $\Delta 3$ -B-Raf**

To address whether suppression of B-Raf<sup>V600E</sup>-mediated MAPK activation impaired cell transformation, we employed an alternatively spliced isoform of B-Raf, termed  $\Delta 3$ -B-Raf.  $\Delta 3$ -B-Raf is formed through ‘intra-exonal’ splicing, leading to a protein lacking 33 amino acids within exon 3 (Suppl. Fig. 1A).  $\Delta 3$ -B-Raf is ubiquitously expressed in mice, independent of background strain and gender (Suppl. Fig. 1B); however,  $\Delta 3$ -B-Raf is not expressed in humans likely due to the lack of a splice donor consensus sequence (Suppl. Fig. 1C and data not shown).  $\Delta 3$ -B-Raf bound itself as well as full length B-Raf (FL-B-Raf) with similar efficiency (Suppl. Fig. 2A). Moreover, binding of  $\Delta 3$ -B-Raf to Ras, MEK, and 14-3-3 proteins was comparable to FL-B-Raf (data not shown). Furthermore, both basal and Hras<sup>G12V</sup>-induced kinase activities of  $\Delta 3$ -B-Raf and FL-B-Raf were comparable (Suppl. Fig. 2B). When stably expressed in NIH3T3 cells, FL-B-Raf induced slightly higher pERK levels than  $\Delta 3$ -B-Raf (Suppl. Fig. 2C), and resulted in a slight but significant increase in cell proliferation (Suppl. Fig. 2D). The most striking difference between  $\Delta 3$ -B-Raf and FL-B-Raf regarded the association with C-Raf. We transiently expressed  $\Delta 3$ -B-Raf and FL-B-Raf in HEK293T cells together with Hras<sup>G12V</sup> to induce MAPK signaling. Hras<sup>G12V</sup> expression led to B-Raf–C-Raf association and activation of ERK (Suppl. Fig. 3A and Weber et al., 2001). Interestingly,  $\Delta 3$ -B-Raf–C-Raf complex formation was reduced by approximately 45%

(Suppl. Fig. 3A and 3B), and correlated with less efficient phosphorylation of ERK (Suppl. Fig. 3A).

Splicing occurs in the regulatory, N-terminal part of B-Raf by utilization of alternative splice donor and acceptor sites within exon 3, removing a serine-rich peptide (SRP) from full length B-Raf. Intra-exonic splicing is a rare alternative splicing event, which has also been observed for human thrombopoietin and fibronectin genes (Chang et al., 1995; Sasaki et al., 1999; Vibe-Pedersen et al., 1986). Alternative splicing of ectopically introduced B-Raf cDNA did not occur, implying that the 99 nucleotides are recognized as an intron only in the presence of constitutive introns, similar to the thrombopoietin gene (Romano et al., 2001). It has been suggested by Romano *et al.* that the assembly of the splicing machinery on constitutive introns is required for intra-exonic splicing to occur. Alternative splicing has been observed for B-Raf exons 10 and 8b, which alters the kinase activity of the different isoforms (Barnier et al., 1995; Papin et al., 1998). These splice forms locate to the hinge region between conserved regions 2 and 3 (CR2 and CR3) and are therefore likely to modify the conformation of active B-Raf. Alternative splicing of the N-terminal regulatory region had no effect on kinase activity (Suppl. Fig. 2B). Moreover, binding of B-Raf to Ras was not disrupted despite the proximity of the SRP to the Ras binding domain (data not shown). Expression of alternatively spliced  $\Delta 3$ -B-Raf<sup>V600E</sup> cDNAs with lower affinity for C-Raf in fibroblasts and melanocytes led to increased MAPK activation and cell transformation, supporting the finding that B-Raf<sup>V600E</sup> suppression by C-Raf is dependent on B-Raf–C-Raf interaction.

## **References**

- Barnier, J. V., Papin, C., Eychene, A., Lecoq, O., and Calothy, G. (1995). The mouse B-raf gene encodes multiple protein isoforms with tissue-specific expression. *J Biol Chem* 270, 23381-23389.
- Chang, M. S., McNinch, J., Basu, R., Shutter, J., Hsu, R. Y., Perkins, C., Mar, V., Suggs, S., Welcher, A., Li, L., and et al. (1995). Cloning and characterization of the human megakaryocyte growth and development factor (MGDF) gene. *J Biol Chem* 270, 511-514.
- Papin, C., Denouel-Galy, A., Laugier, D., Calothy, G., and Eychene, A. (1998). Modulation of kinase activity and oncogenic properties by alternative splicing reveals a novel regulatory mechanism for B-Raf. *J Biol Chem* 273, 24939-24947.
- Romano, M., Marcucci, R., and Baralle, F. E. (2001). Splicing of constitutive upstream introns is essential for the recognition of intra-exonic suboptimal splice sites in the thrombopoietin gene. *Nucleic Acids Res* 29, 886-894.
- Sasaki, Y., Takahashi, T., Miyazaki, H., Matsumoto, A., Kato, T., Nakamura, K., Iho, S., Okuno, Y., and Nakao, K. (1999). Production of thrombopoietin by human carcinomas and its novel isoforms. *Blood* 94, 1952-1960.
- Vibe-Pedersen, K., Magnusson, S., and Baralle, F. E. (1986). Donor and acceptor splice signals within an exon of the human fibronectin gene: a new type of differential splicing. *FEBS Lett* 207, 287-291.
- Weber, C. K., Slupsky, J. R., Kalmes, H. A., and Rapp, U. R. (2001). Active Ras induces heterodimerization of cRaf and BRaf. *Cancer Res* 61, 3595-3598.

## **Supplementary Figures**

Supplementary Figure 1: Expression of  $\Delta 3$ -B-Raf. (A) Schematic outline illustrating alternative splicing of exon 3 of murine B-Raf. (B) Reverse Transcriptase PCR analysis of full length and  $\Delta 3$ -B-Raf expression in mouse tissues from C57Bl/6 and 129/SvJae mice using intron-spanning primers in exons 2 and 4. The upper band represents full length B-Raf, whereas the lower band represents  $\Delta 3$ -B-Raf. (C) Reverse Transcriptase PCR analysis of full length and  $\Delta 3$ -B-Raf expression in human tissues. br, brain; he, heart; li, liver; lu, lung; ki, kidney; sp, spleen; st, stomach; in, intestines; pa, pancreas; th, thymus; mu, muscle; sk, skin; le, leukocytes.

Supplementary Figure 2: Effects of alternative splicing. (A) Western blot showing Hras<sup>G12V</sup>-induced formation of  $\Delta 3$ -B-Raf and FL-B-Raf complexes in HEK293T cells. White arrowhead denotes FL-B-Raf, black arrowhead denotes  $\Delta 3$ -B-Raf, and asterisk denotes background band. (B) Basal and Hras<sup>G12V</sup>-induced B-Raf kinase activity of FL-B-Raf and  $\Delta 3$ -B-Raf in HEK293T cells. (C) Western blot displaying phosphorylation of ERK in NIH3T3 fibroblasts stably expressing FL-B-Raf and  $\Delta 3$ -B-Raf. (D) Proliferation curve of NIH3T3 fibroblasts stably expressing FL-B-Raf and  $\Delta 3$ -B-Raf. The mean and standard deviation of one representative experiment done in triplicate is shown in (B) and (D).

Supplementary Figure 3: Alternative splicing impairs B-Raf–C-Raf complex formation and MAPK activation. (A) Western blot showing co-

immunoprecipitation of C-Raf with FL-B-Raf and  $\Delta 3$ -B-Raf in response to Hras<sup>G12V</sup> activation as well as phosphorylation of ERK in total lysates. (B) Quantification of Hras<sup>G12V</sup>-promoted FL-B-Raf–C-Raf and  $\Delta 3$ -B-Raf–C-Raf complexes.

Supplementary Figure 4: Reduced interaction with C-Raf impairs transformation by  $\Delta 3$ -B-Raf<sup>G466V</sup>. (A) Hras<sup>G12V</sup>-induced association of C-Raf with FL-B-Raf<sup>G466V</sup> and  $\Delta 3$ -B-Raf<sup>G466V</sup> in HEK293T cells. Immunoprecipitated amounts of C-Raf as well as levels of pERK, B-Raf, C-Raf, and Hras<sup>G12V</sup> in the lysates were determined by Western blotting. (B) Stable expression of FL-B-Raf<sup>G466V</sup> and  $\Delta 3$ -B-Raf<sup>G466V</sup> in NIH3T3 fibroblasts, and associated pERK levels were assessed by Western blotting. (C) Proliferation curves of NIH3T3 fibroblasts expressing FL-B-Raf<sup>G466V</sup> and  $\Delta 3$ -B-Raf<sup>G466V</sup>. FL-B-Raf<sup>G466V</sup> cells proliferate faster than  $\Delta 3$ -B-Raf<sup>G466V</sup> cells (\*  $P=0.022$ , \*\*  $P=0.007$ ). (D) Anchorage-independent growth of NIH3T3 fibroblasts expressing FL-B-Raf<sup>G466V</sup> and  $\Delta 3$ -B-Raf<sup>G466V</sup>. FL-B-Raf<sup>G466V</sup> expressing cells form approximately 2.5 fold more colonies in soft agar. The mean and standard deviation of one representative experiment done in triplicate is shown in (C, \*  $P<0.05$ , \*\*  $P<0.01$ ) and (D).

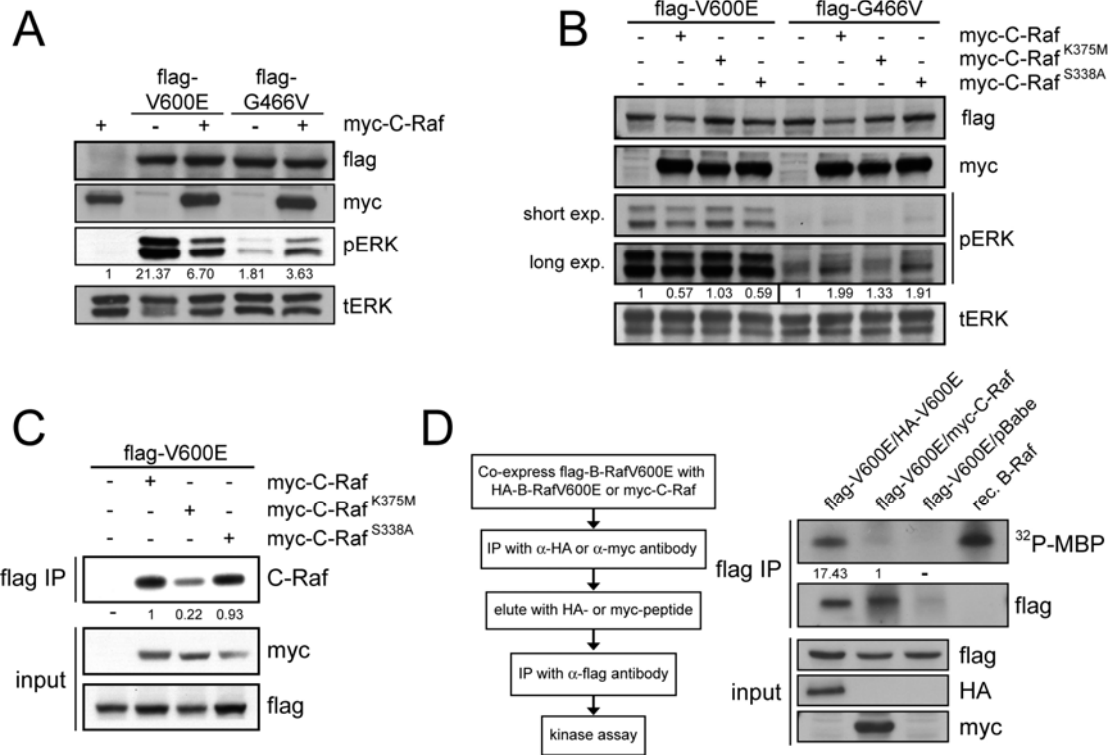
Supplementary Figure 5: Expression of Raf proteins in human melanoma cell lines. (A) Western blot displaying expression of C-Raf and B-Raf in human melanocyte cell lines NHEM and Fom99-1. (B, C) Estimation of the number of B-Raf and C-Raf molecules in a panel of melanoma cell lines. Recombinant

B-Raf and C-Raf were run on the same Western blot as reference standards.

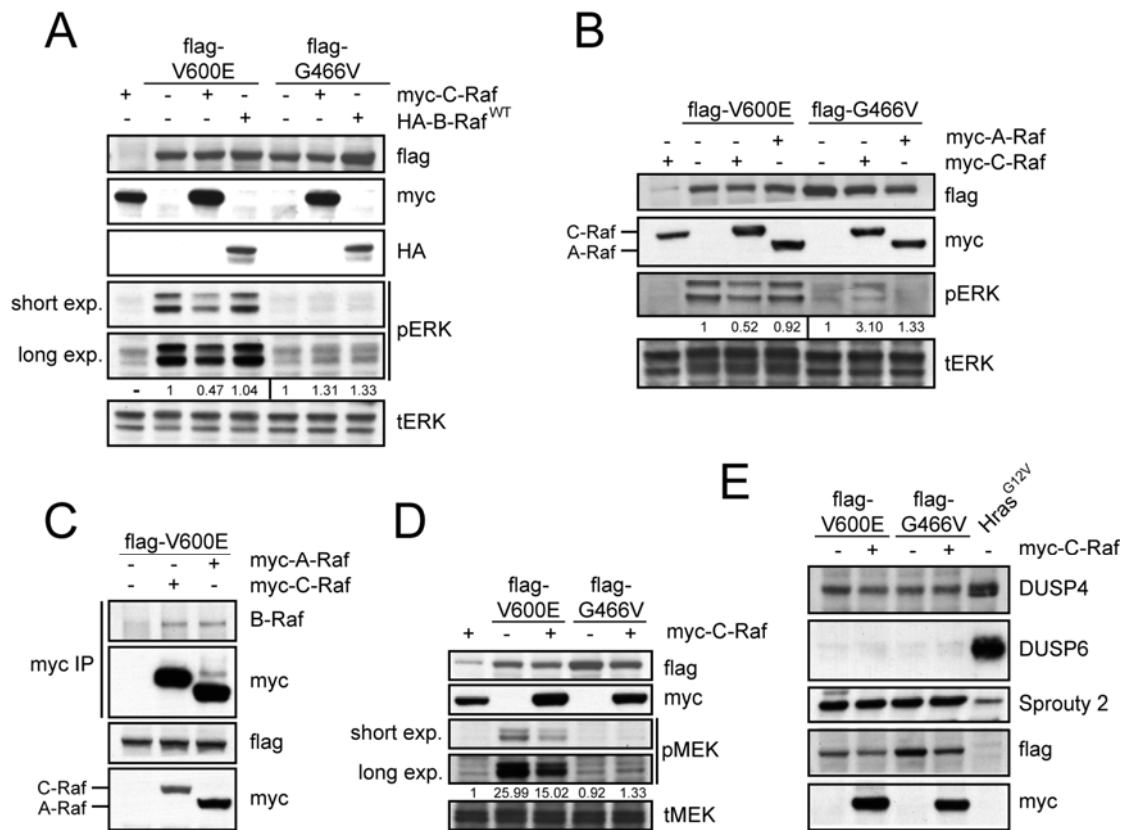
(D) Expression of A-Raf in melanoma cell lines.

Supplementary Figure 6: Hras<sup>G12V</sup> antagonizes B-Raf<sup>V600E</sup>. (A) Hras<sup>G12V</sup> inhibits ERK activation in B-Raf<sup>V600E</sup> mutant cells. Western blot displaying Hras<sup>G12V</sup>-induced B-Raf<sup>V600E</sup>-C-Raf complex formation and decreased pERK levels in WM793 melanoma cells. (B) Decreased proliferation of WM793 melanoma cells in response to Hras<sup>G12V</sup> expression. Cells were labelled with BrdU and proliferating cells were detected using an anti-BrdU antibody. The mean and standard deviation of one representative experiment done in triplicate is shown in (B).

Supplementary Figure 7: Response to Sorafenib in melanoma cell lines. When treated with increasing doses of Sorafenib, B-Raf<sup>V600E</sup> expressing cell lines A375P and WM164 display increased B-Raf-C-Raf complex formation as well as increased pERK levels at low doses of Sorafenib and decreased pERK at the highest dose of Sorafenib. Mouse embryonic fibroblasts expressing endogenous B-Raf<sup>V619E</sup> showed similar kinetics of C-Raf binding and pERK level changes in response to Sorafenib. In Nras mutant SKMel2 cells, pERK levels were not increased at low doses of Sorafenib but B-Raf-C-Raf complexes were induced.

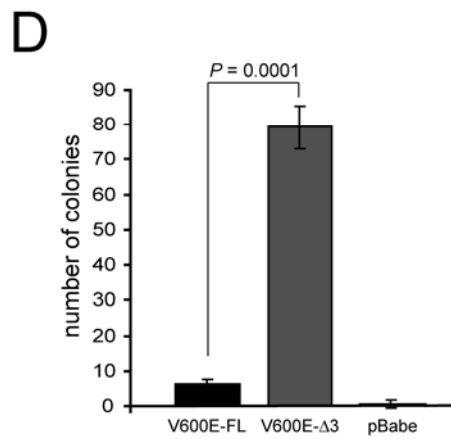
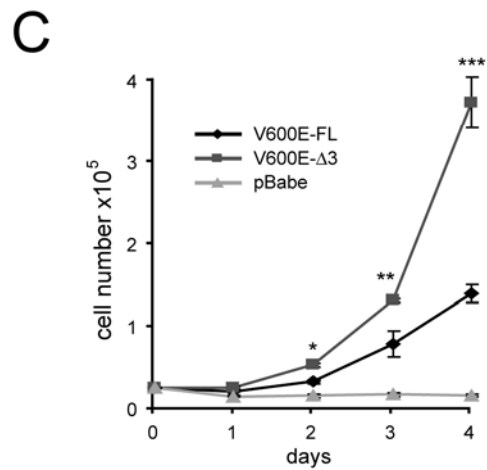
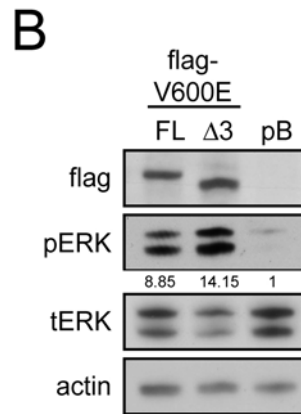
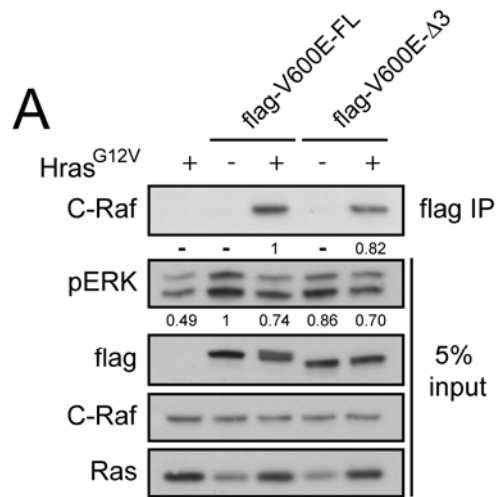


Karreth et al.  
Figure 1

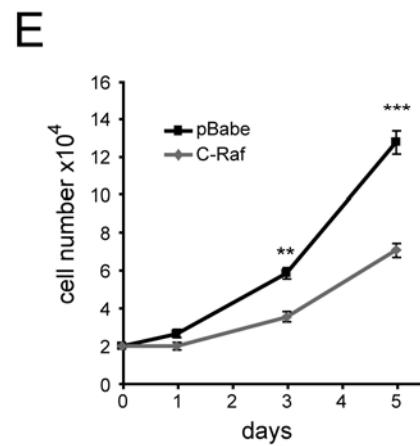
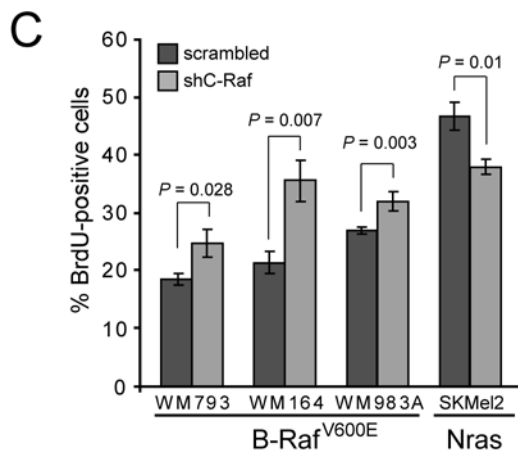
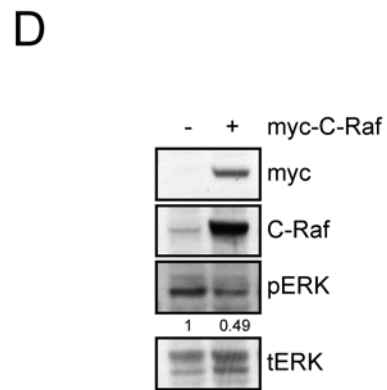
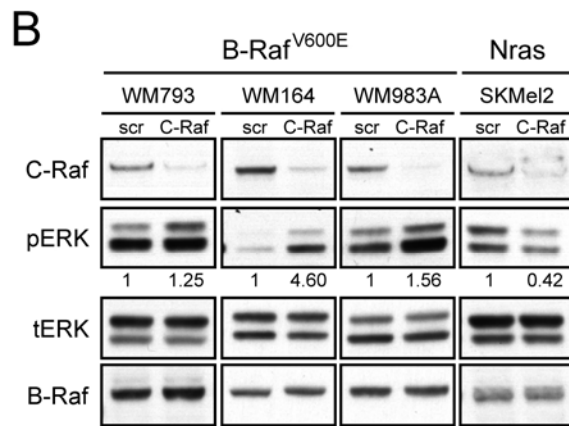
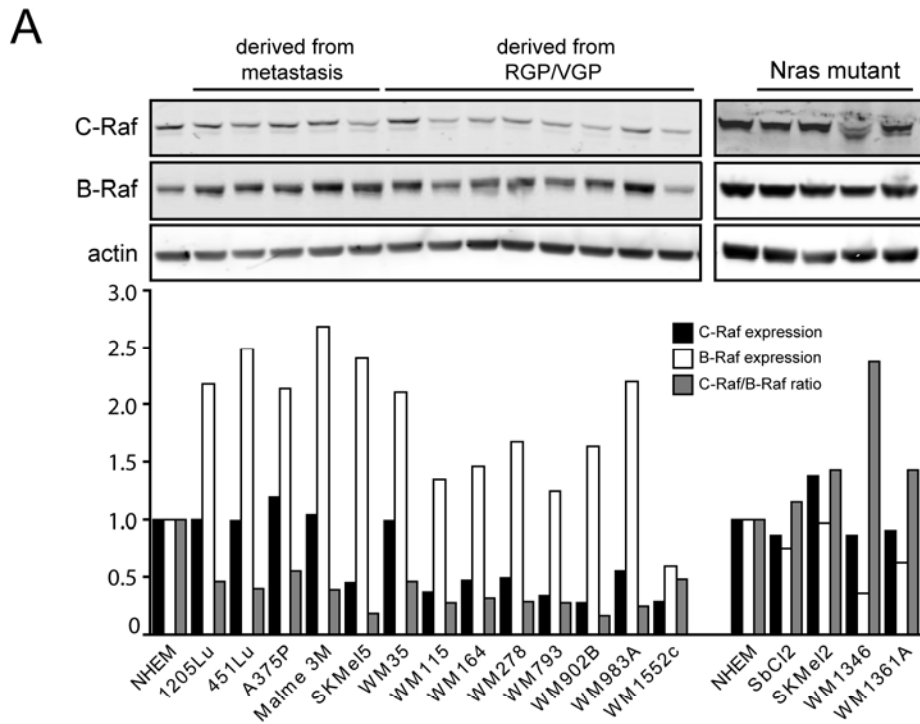


Karreth et al.  
Figure 2

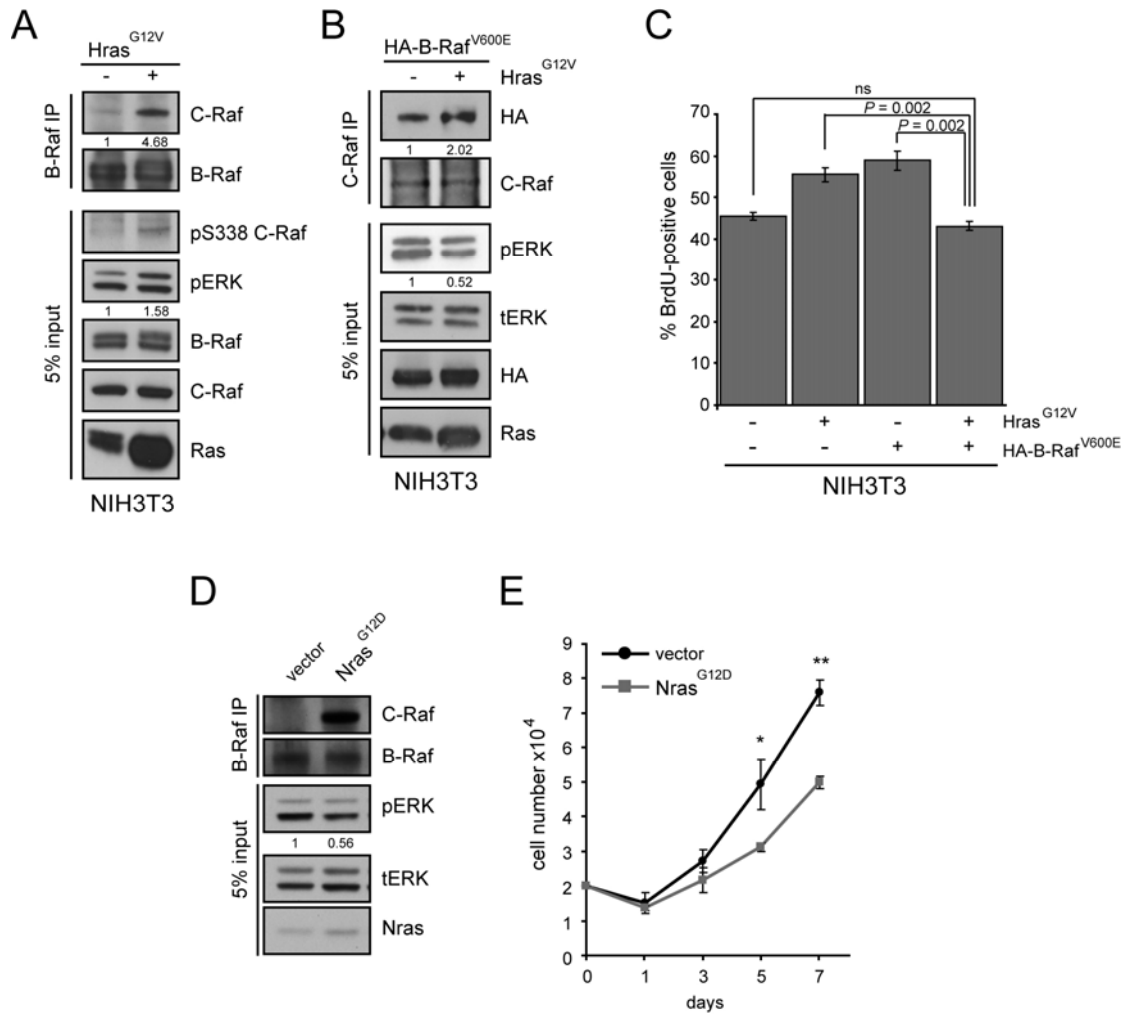




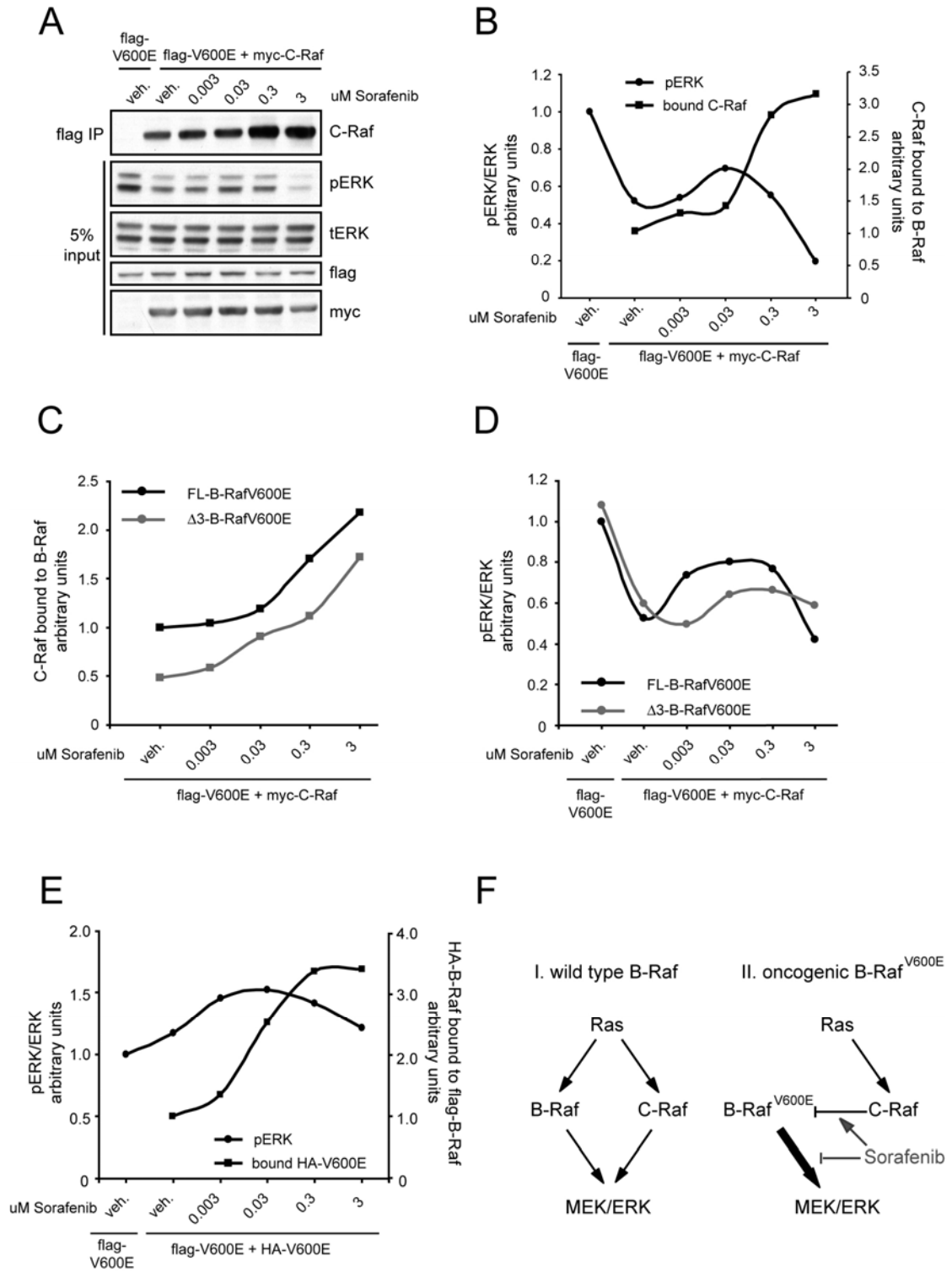
Karreth et al.  
Figure 3



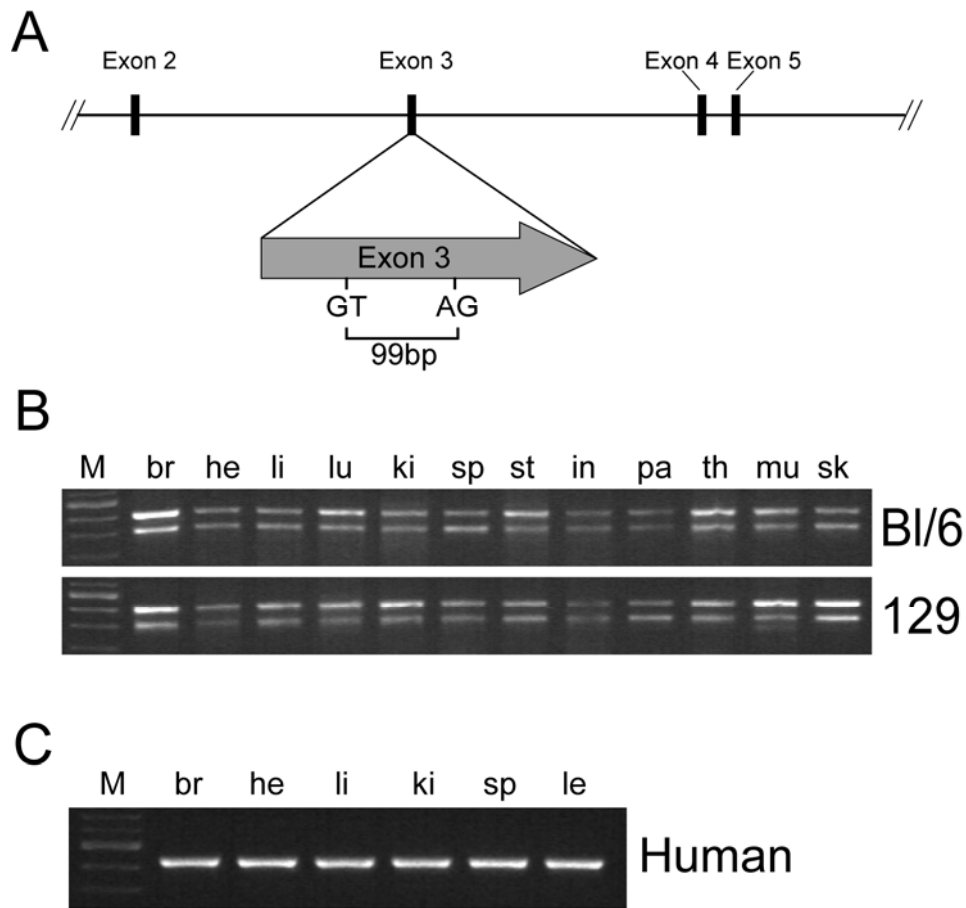
Karreth et al.  
Figure 4



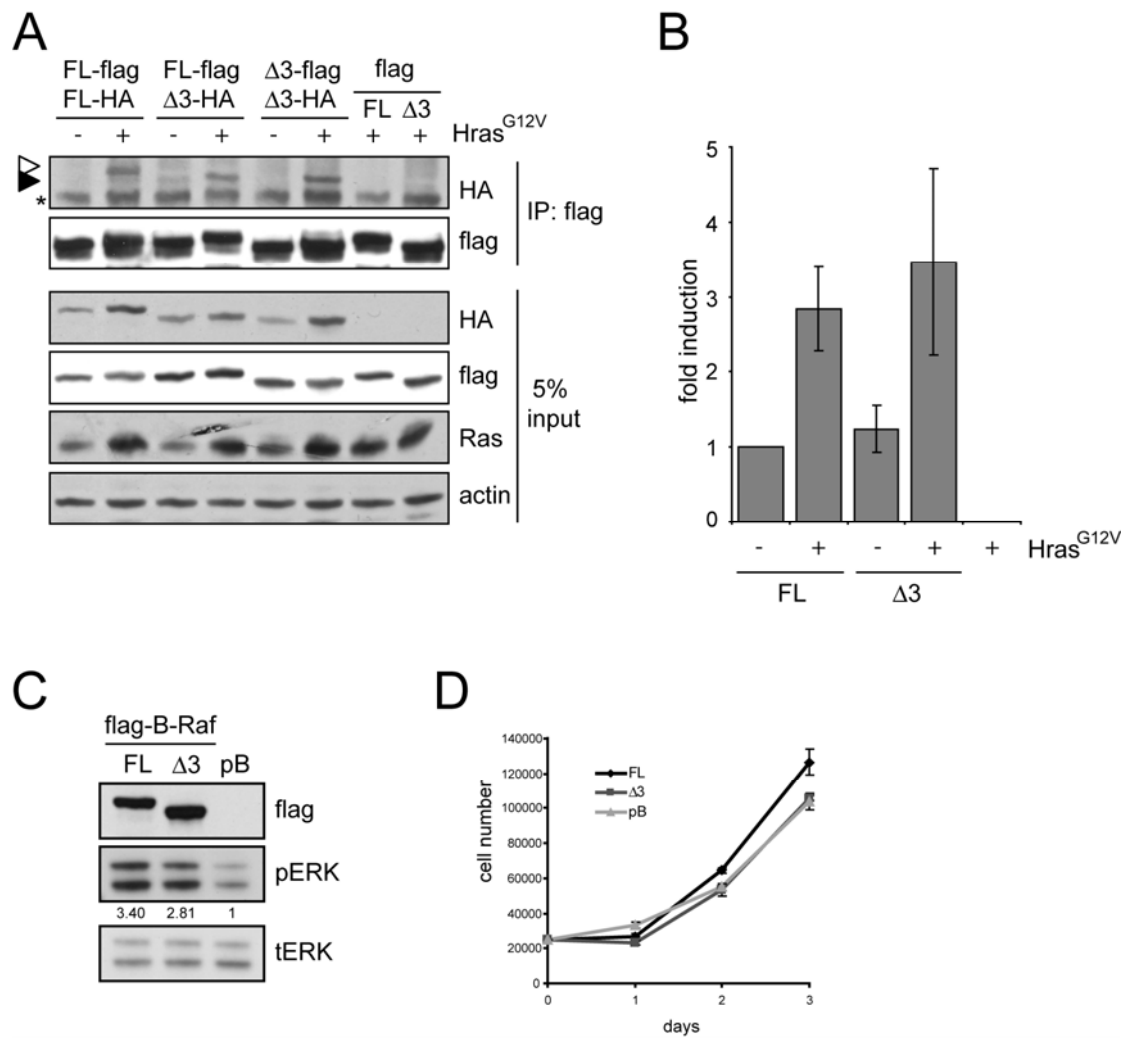
Karreth et al.  
Figure 5



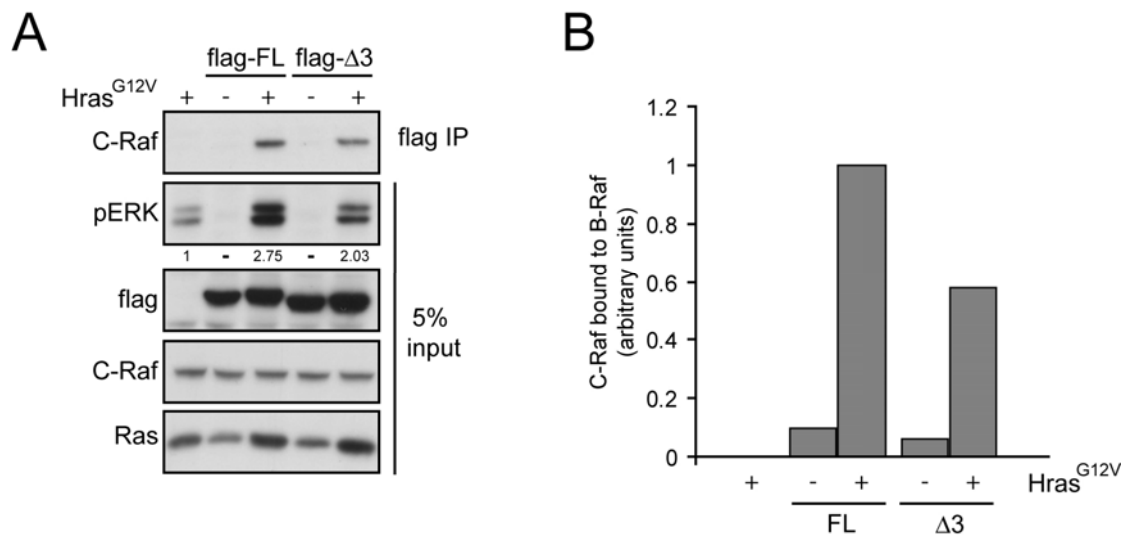
Karreth et al.  
Figure 6



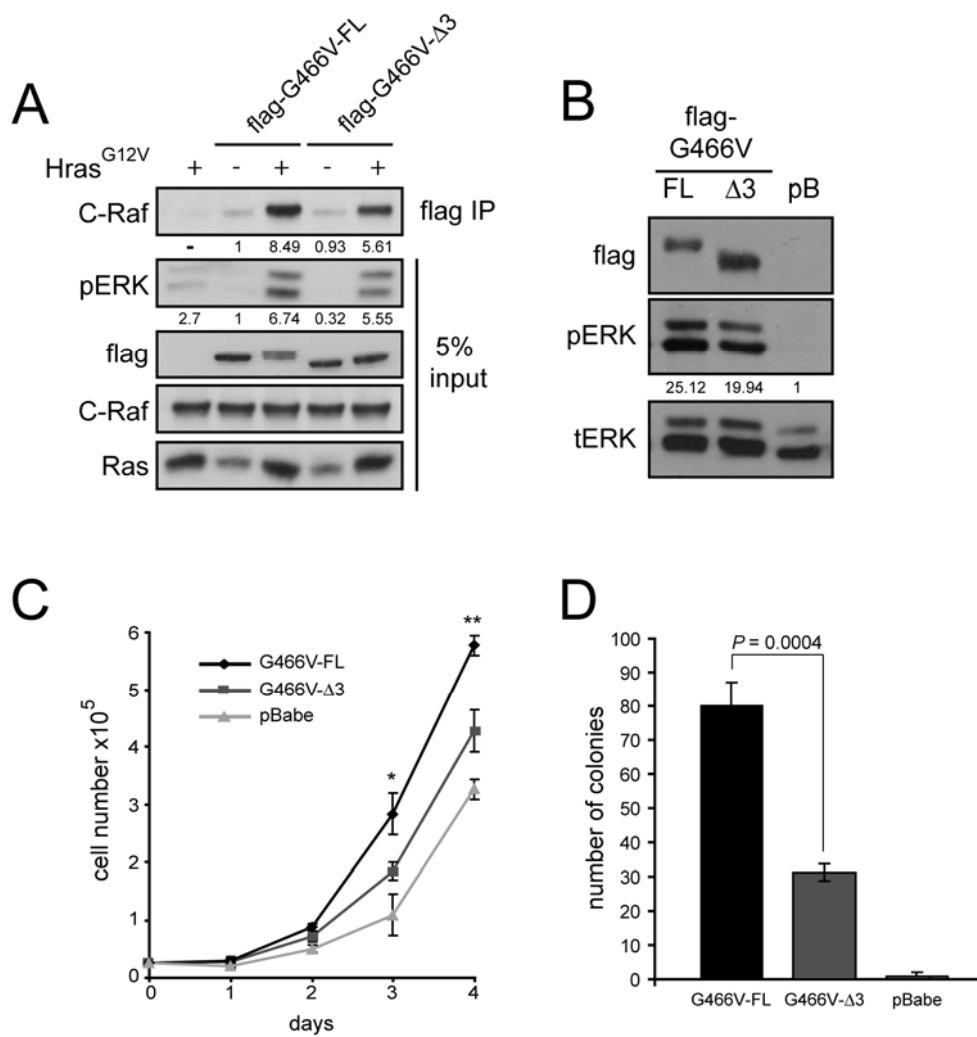
Karreth et al.  
Supplementary Figure 1



Karreth et al.  
Supplementary Figure 2

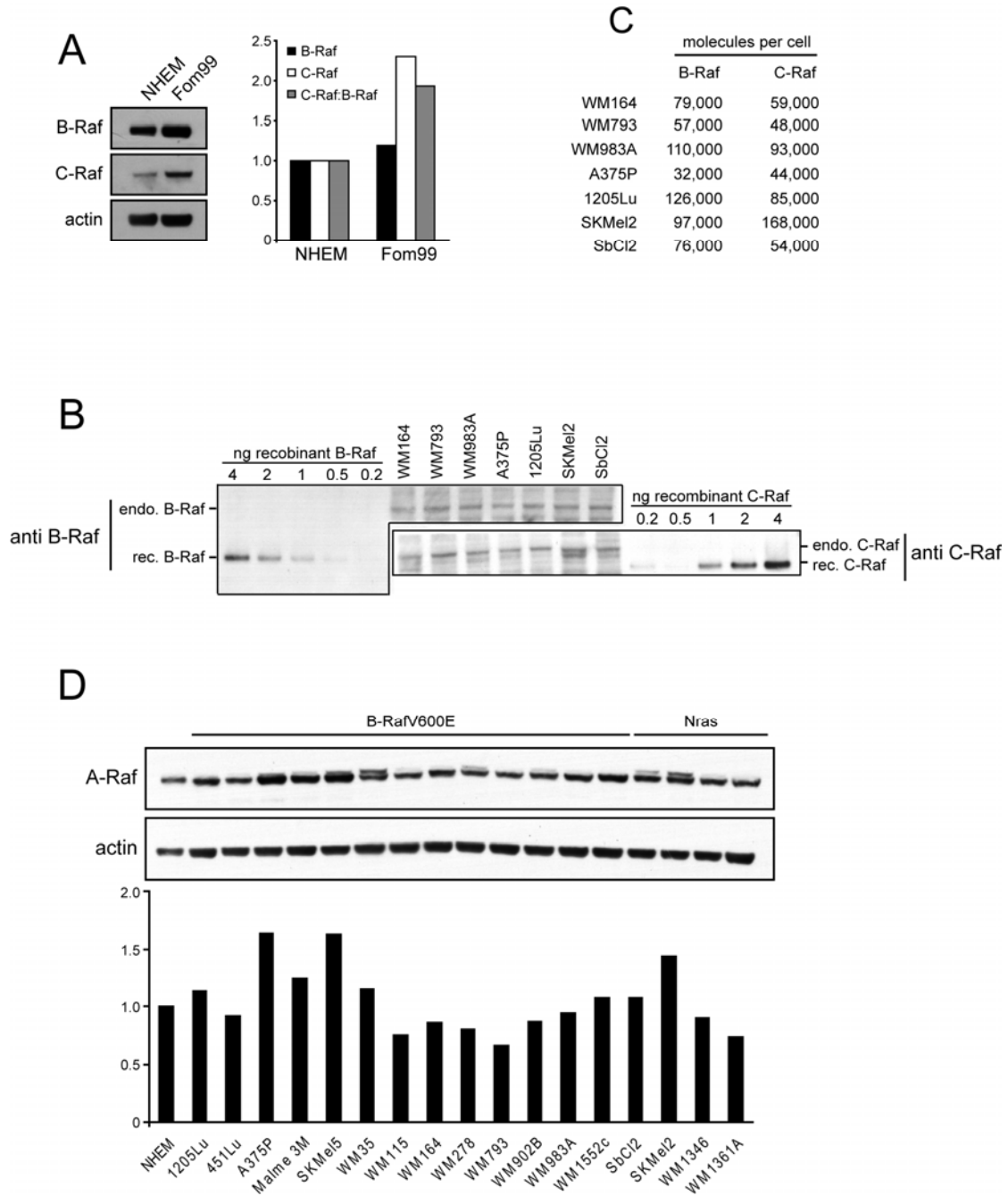


Karreth et al.  
Supplementary Figure 3

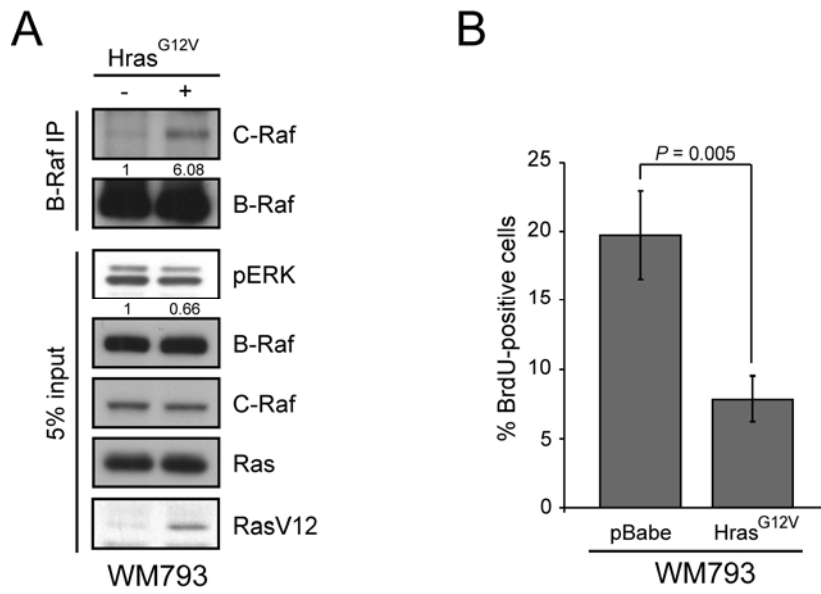


Karreth et al.  
Supplementary Figure 4

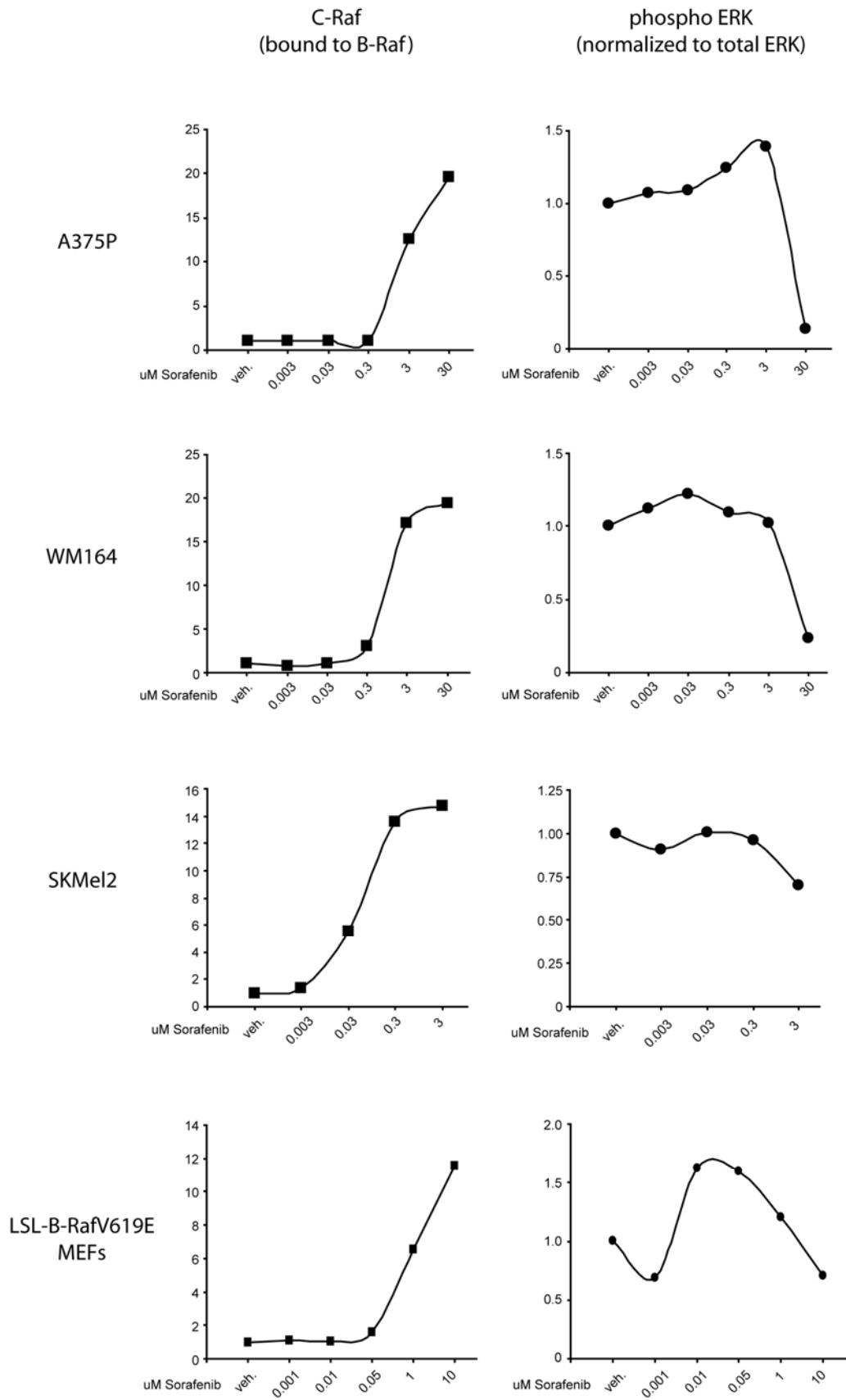




Karreth et al.  
Supplementary Figure 5



Karreth et al.  
Supplementary Figure 6



Karreth et al.  
Supplementary Figure 7

### 5.1.1 Additional data not included in the manuscript

Given the high content of putative phospho-residues (15 Serines and two Threonines) within the SRP, phosphorylation of the SRP could contribute to B-Raf–C-Raf complex formation. Thus, whether post-translational modification of the Serine-rich peptide (SRP) deleted in  $\Delta 3$ -B-Raf could regulate B-Raf–C-Raf heterodimerization was assessed. When flag-tagged B-Raf isoforms were separated on 3-7% gradient gels, a slower migrating band in FL-B-Raf samples was observed in response to H-Ras<sup>G12V</sup> (Fig. 5.1.1A), suggesting H-Ras<sup>G12V</sup>-mediated post-translational modification of B-Raf. Importantly, the slower migrating band was not observed when cells were co-transfected with  $\Delta 3$ -B-Raf and H-Ras<sup>G12V</sup> (Fig. 5.1.1A). Moreover, no slower migrating FL-B-Raf band was detected after incubation of protein lysates with calf intestinal phosphatase, indicating that full length B-Raf is subjected to post-translational phosphorylation in response to H-Ras<sup>G12V</sup> (Fig. 5.1.1B). It was determined whether H-Ras<sup>G12V</sup>-mediated B-Raf phosphorylation is regulated by a feedback loop involving the MAPK pathway. Cells co-expressing FL-B-Raf and H-Ras<sup>G12V</sup> were treated with the MEK inhibitor U0126 and assayed for the appearance of the slower migrating, phosphorylated B-Raf band by Western blot. No alteration of B-Raf phosphorylation in response to MEK inhibition was observed (Fig. 5.1.1C), suggesting that feedback-regulation does not play a role in B-Raf phosphorylation. To assess whether SRP phosphorylation contributes to regulation of B-Raf–C-Raf dimerization, four phospho-mutants of B-Raf were generated in which the following amino acids of the SRP were mutated to Alanines: PM1, S<sup>108</sup>-S<sup>110</sup>-S<sup>111</sup>-S<sup>112</sup>-S<sup>114</sup>; PM2, T<sup>117</sup>-T<sup>119</sup>-S<sup>120</sup>-S<sup>121</sup>; PM3, S<sup>122</sup>-S<sup>123</sup>-S<sup>124</sup>-S<sup>125</sup>; PM4, S<sup>127</sup>-S<sup>131</sup>-S<sup>132</sup>-S<sup>134</sup> (Fig. 5.1.1D, lower panel).

No slower migrating, phosphorylated B-Raf was observed when phospho-mutants PM1, PM2, and PM3 were co-expressed with H-Ras<sup>G12V</sup> (Fig. 5.1.1D, upper panel). In contrast, PM4 was still phosphorylated in response to H-Ras<sup>G12V</sup>, albeit at lower levels (Fig. 5.1.1D, upper panel), indicating that Serines 127, 131, 132 and 134 are not subjected to H-Ras<sup>G12V</sup>-mediated phosphorylation. To determine the functional significance of SRP phosphorylation, the effect of B-Raf phospho-mutants on MAPK pathway activation was examined. Interestingly, pERK levels in phospho-mutant expressing cells were similar to wildtype, full length B-Raf (Fig. 5.1.1E). Accordingly, B-Raf phospho-mutants associated with C-Raf as efficiently as wildtype B-Raf (Fig. 5.1.1E), suggesting that B-Raf–C-Raf dimerization is not regulated by phosphorylation within the SRP.

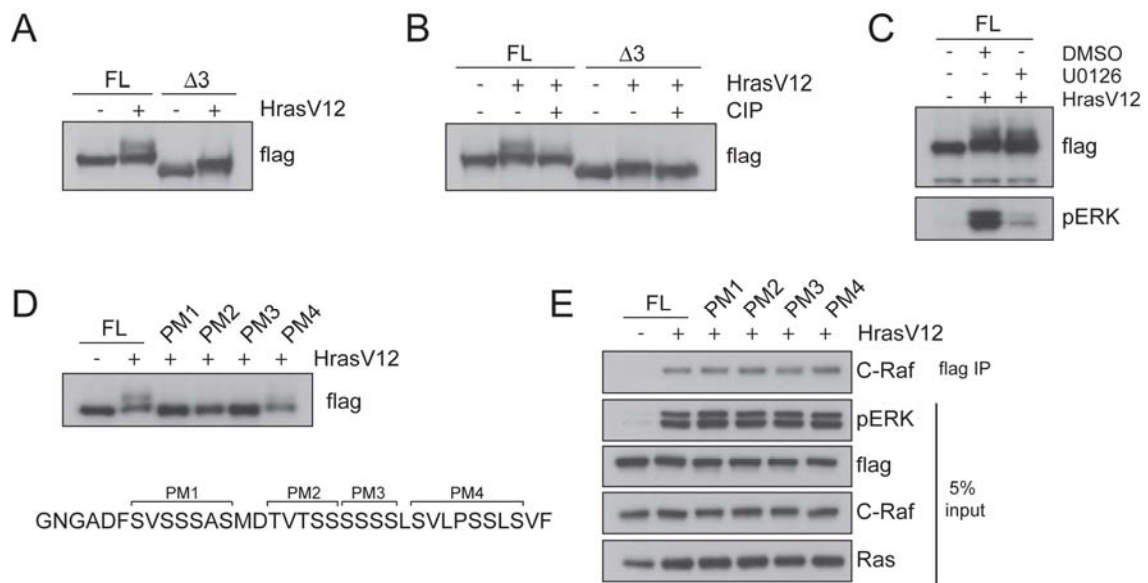


*Figure 5.1.1: Phosphorylation of SRP (A) Western blot showing H-Ras<sup>G12V</sup>-induced migratory shift of FL-B-Raf but not Δ3-B-Raf. (B) The migratory shift is due to phosphorylation. Protein lysates were incubated with calf intestinal phosphatase (CIP) and subjected to Western blot analysis using anti-flag*

antibodies. (C) FL-B-Raf phosphorylation is not regulated by a feedback loop. HEK293T cells were incubated with the MEK inhibitor U0126 or DMSO for 24 hours, followed by Western analysis. (D) Phospho-mutants of FL-B-Raf were co-expressed with H-Ras<sup>G12V</sup> in HEK293T cells and analyzed by Western blotting. The FL-B-Raf migratory shift was abolished in phospho-mutants 1, 2 and 3 (upper panel). Schematic representation of B-Raf phospho-mutants (lower panel). (E) C-Raf co-immunoprecipitation from cells expressing either FL-B-Raf or phospho-mutant isoforms of B-Raf in the presence of H-Ras<sup>G12V</sup>. B-Raf was immunoprecipitated with anti-flag antibodies and bound C-Raf detected with anti-C-Raf antibodies. 5% of input was used to detect pERK, flag-tagged B-Raf and Ras, as well as C-Raf as loading control.

## **5. Results and Discussion**

### 5.2 Generation of a conditional and reversible oncogenic B-Raf mutant mouse model (unpublished data)

### 5.2.1 The rationale and strategy for generating a LSL-B-Raf<sup>V619E</sup> mouse

B-Raf mutations occur frequently in human cancer and are also found at a high percentage in benign hyperplasias such as nevi (Brose et al., 2002; Davies et al., 2002; Pollock et al., 2003; Pollock and Meltzer, 2002). Most notably, B-Raf mutations are present in 60-70% of melanomas. To study the biology and oncogenic potential of B-Raf mutations *in vivo*, a mouse model of oncogenic B-Raf was generated. Historically, oncogenes have been ectopically expressed in mice as transgenes using strong promoters. The expression levels of such transgenes depend not only on the promoter used, but are also influenced by the integration site in the genome, the number of integrated copies and methylation of the promoter. These factors all contribute to abnormal regulation of transgene expression, which typically results in non-physiological expression levels. Importantly, different expression levels of oncogenes have profoundly varying biological outputs. Ectopic expression of oncogenic Ras in primary mouse embryonic fibroblasts results in a premature growth arrest termed oncogene-induced senescence (Serrano et al., 1997). In contrast, expression of oncogenic K-Ras from its endogenous promoter at physiological levels increases proliferation and results in immortalization of primary mouse embryonic fibroblasts (Tuveson et al., 2004). Moreover, an elegant study by Chodosh and colleagues showed that high levels of oncogenic H-Ras<sup>G12V</sup> in the mammary epithelium induce senescence, while low levels of expression promote proliferation (Sarkisian et al., 2007). Similarly, endogenous expression of oncogenic B-Raf results in immortalization of MEFs (Mercer et al., 2005), while overexpression in human diploid fibroblasts induces senescence (Kuilman et al., 2008). Whether



oncogene-induced senescence as caused by overexpression of oncogenic Ras in primary cell culture exists as a potent barrier to tumor progression *in vivo* is currently under debate. In addition, high expression levels of myc result in apoptosis of pancreatic  $\beta$ -cells; however, low levels of myc have the opposite effect and induce proliferation of such cells (Murphy et al., 2008). These data emphasize the importance of physiological expression of oncogenes to draw biologically relevant conclusions. Thus, the oncogenic B-Raf allele was designed to be expressed from its endogenous promoter.

In human cancer, over 30 B-Raf missense mutations have been identified. The vast majority of cancer cases harbor a Valine-for-Glutamic acid substitution at residue 600, which renders B-Raf constitutively active. This Valine residue in humans corresponds to Valine 619 in mice. Given its predominance in cancer, the oncogenic B-Raf allele was designed to carry the V619E mutation.

Global expression of oncogenes could be detrimental to mouse development. Indeed, widespread expression of K-Ras<sup>G12D</sup> in LSL-K-Ras<sup>G12D</sup>; CMV-Cre mice leads to embryonic lethality (Tuveson et al., 2004). Therefore, oncogenic B-Raf<sup>V619E</sup> was designed to be conditionally expressed in the cell type of choice. The previously constructed endogenous oncogenic LSL-K-Ras<sup>G12D</sup> allele employs a transcriptional and translational STOP cassette. This STOP cassette contains a puromycin resistance selection cassette, four SV40 polyadenylation signals as well as a strong Kozak sequence followed by a stop codon. Additionally, the STOP cassette is flanked by loxP sites. LoxP sites

are recognized by Cre recombinase, which deletes the intervening sequence. This loxP-STOP-loxP (LSL) cassette can be placed between the promoter and the coding sequence of a gene to prevent transcription of the gene. Cre-mediated excision of the LSL will result in expression of the gene only in cells that express Cre recombinase. The LSL cassette was placed in the 5' region of the B-Raf gene to prevent global expression of oncogenic B-Raf<sup>V619E</sup>. By crossing LSL-B-Raf<sup>V619E</sup> mice to mouse strains expressing Cre recombinase under the control of tissue specific promoters, expression of B-Raf<sup>V619E</sup> can be directed to certain cell types.

Whether continuous expression of 'druggable' oncogenes is required for tumor maintenance is of crucial importance for drug development efforts. If an oncogene was no longer required for the survival and tumorigenicity of cancer cells, then pharmacological inhibition of this oncogene in an established tumor would be futile. The issue of oncogene addiction has been addressed using mouse models: withdrawal of oncogenic Ras or myc resulted in tumor regression (Chin et al., 1999; Fisher et al., 2001; Jain et al., 2002; Pelengaris et al., 2002). To assess whether continuous expression is required for tumor maintenance, FRT sites were introduced into the oncogenic B-Raf<sup>V619E</sup> allele to additionally create a conditional knock-out of B-Raf<sup>V619E</sup>. FRT sites are 34bp DNA stretches similar to loxP sites; however, they are recognized by a different enzyme, Flp recombinase. Using this approach, expression of oncogenic B-Raf<sup>V619E</sup> is restricted to cells expressing Cre recombinase. Once neoplasms have developed, Flp recombinase expression can be induced in tumor cells resulting in genetic depletion of B-Raf<sup>V619E</sup> and tumor maintenance

in the absence of the initiating oncogene can be examined. This strategy is outlined in Figure 5.2.1.

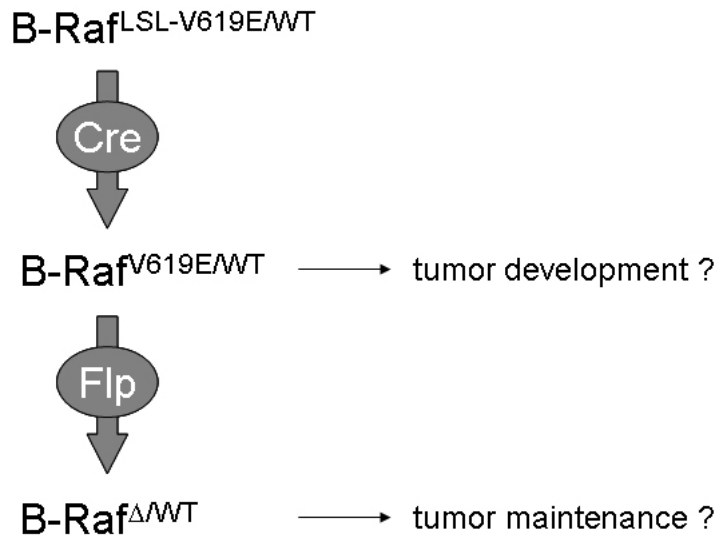


*Figure 5.2.1: Conditional and reversible activation of oncogenic B-Raf. Only wildtype B-Raf is expressed in B-Raf<sup>LSL-V619E/WT</sup> mice. Upon Cre-mediated deletion of the LSL cassette B-Raf<sup>V619E</sup> is expressed from the endogenous promoter at physiological levels. B-Raf<sup>V619E</sup> can be conditionally deleted by induction of Flp expression and activity.*

### 5.2.2 Design of the LSL-B-Raf<sup>V619E</sup> allele and targeting strategy

The murine B-Raf gene may contain an alternative promoter in intron 2 that drives expression of a truncated B-Raf protein. In fact, some B-Raf antibodies recognize several potential murine B-Raf proteins between 60 and 96kDa. To prevent expression of truncated oncogenic B-Raf<sup>V619E</sup>, the LSL had to be introduced immediately upstream of exon 3 rather than in between the B-Raf promoter and exon 1. Therefore, the LSL cassette was knocked-in into intron

2 and the V619E mutation was introduced into exon 15. A schematic outline of the LSL-B-Raf<sup>V619E</sup> allele is depicted in Figure 5.2.2. The murine B-Raf gene encompasses 18 exons and is 115kb in size. Exon 3 and exon 15 are approximately 50kb apart. Therefore, the LSL cassette and the V619E mutation could not be constructed into a single targeting vector and they had to be targeted independently. First, ES cells were targeted with a targeting vector containing the LSL, selected using puromycin and screened for correct targeting. The LSL targeting was performed first to prevent expression of oncogenic B-Raf in ES cells. Expression of oncogenic B-Raf is, of course, undesirable as it could lead to loss of pluripotency and the inability to contribute to the germline of chimeric mice. In fact, expression of oncogenic K-Ras<sup>G12D</sup> and resulting hyperactivation of the MAPK pathway induced differentiation of ES cells (D. Tuveson, unpublished observation). LSL-positive clones were then electroporated with a second targeting vector carrying mutant exon 15 as well as a FRT-flanked neomycin / HSV Thymidine kinase (Neo-TK) selection cassette. Double targeted ES cells were subjected to G418 selection and surviving clones were examined for correct integration of the Neo-TK cassette as well as for the presence of the mutation in exon 15. Finally, double positive ES cell clones were electroporated with a Flp recombinase expression vector to transiently express the enzyme and remove the Neo-TK cassette. ES cells were grown in ganciclovir to select for cells that had removed the Neo-TK cassette and surviving clones were screened for the presence of only one FRT site in intron 14.

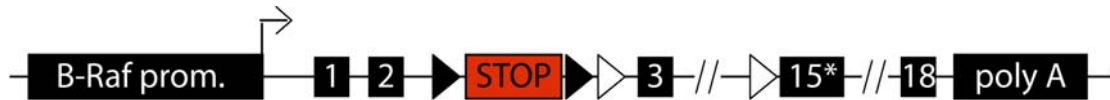


Figure 5.2.2: Schematic outline of the *B-Raf*<sup>V619E</sup> allele. The LSL cassette was introduced into intron 2. Black triangles represent *loxP* sites, white triangles represent *FRT* sites. Wildtype exon 15 was replaced by mutant exon 15 (depicted as 15\*) coding for the V619E mutation. Black numbered boxes represent exons.

### 5.2.3 Design, cloning and targeting of the LSL-FRT targeting vector

This targeting vector only needed to contain the LSL cassette immediately 5' of exon 3. The LSL cassette contains a puromycin resistance gene and, thus no additional selection cassette was required. All elements of the LSL cassette are outlined in Figure 5.2.3. To be able to conditionally delete the *B-Raf*<sup>V619E</sup> allele after Cre-mediated activation, a *FRT* site was inserted between the LSL cassette and exon 3. The second *FRT* site will be part of the second targeting vector containing mutant exon 15.

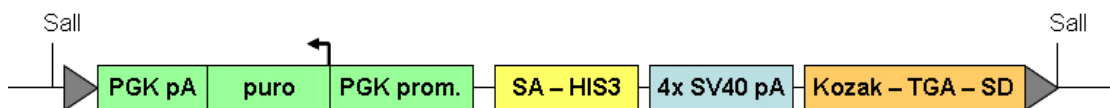


Figure 5.2.3: The *LoxP*-*STOP*-*LoxP* cassette. The LSL is flanked by *loxP* sites (gray triangles) and contains a puromycin resistance gene (*puro*), which is expressed from the ubiquitously active *PGK* promoter and transcription of *puro* is terminated by a *PGK* poly-adenylation signal (all in light green). Downstream of the *puro* cassette is a splice acceptor (*SA*) followed by a

*buffer sequence (HIS3, both in yellow). Transcripts driven from upstream promoters are spliced into the splice acceptor. These transcripts are then terminated by the four SV40 poly-adenylation sites (light blue), thereby preventing expression of downstream genomic coding sequences. Additionally, the LSL contains a Kozak sequence followed by a stop codon (TGA) and a splice donor (SD). Should a transcript escape termination by the four SV40 polyAs this sequence serves as a backup 'trap' to prevent expression of downstream genes. The Kozak sequence has a translational start codon (ATG) and serves as a ribosome binding site. Translation is then stopped by the stop codon that follows the Kozak sequence. The splice donor assures that downstream transcripts are spliced to the Kozak – stop codon sequence.*

To clone the homology arms, a C57Bl/6 BAC (RP24-387G20, BACPAC Resources, Children's Hospital Oakland Research Institute) containing the B-Raf genomic locus was digested with BamHI and separated on a 0.8% TAE agarose gel. Due to the numerous fragments resulting from this digest, the DNA ran as a smear. 6-10kb DNA fragments were excised from the gel and cloned into FK12-pBS. FK12-pBS is a version of pBluescript where the XhoI site in the multiple cloning site of pBluescript was destroyed by cutting with XhoI, fill-in of the overhangs using Klenow polymerase followed by blunt end ligation. Clones (termed BAC3-FK12-pBS) containing the desired 8.4kb fragment, which includes an intronic XhoI site upstream of B-Raf exon 3 were identified by colony lift. BAC3-FK12-pBS was end-sequenced using T3 and T7 primers and the exon 3 was sequenced to confirm correct cloning. A KpnI-

Xho-Sal-FRT-Xho-NotI polylinker was cloned into pBluescript using KpnI and NotI to generate FK20-pBS. The LSL cassette was then cloned into the SalI site of FK20-pBS. Subsequently, the LSL-FRT fragment was cloned into BAC3-FK12-pBS with XhoI to generate the LSL-FRT targeting vector. The lack of unwanted nucleotide changes in the FRT site, exon 3 and intron-exon boundaries was confirmed by sequencing.

E14J ES cells were targeted with 50ug of NotI linearized LSL-FRT targeting vector (Figure 5.2.4) and selected in puromycin for one week. 96 clones were picked, expanded and screened for the presence of the LSL cassette by long range PCR and Southern blotting. 58 clones were positively targeted and two clones were further expanded for subsequent targeting of exon 15.

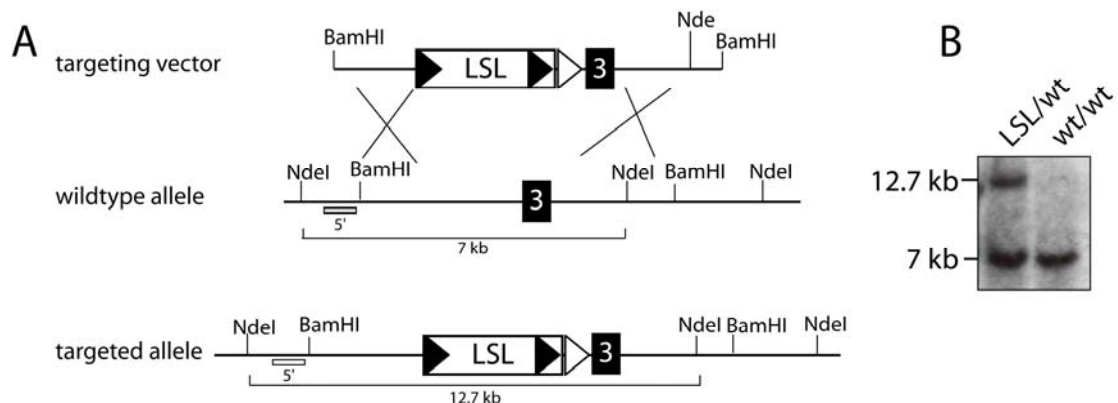


*Figure 5.2.4: Targeting of the LSL cassette (A) LSL-FRT targeting strategy. Black triangles, loxP sites; white triangle, FRT site; black box, exon 3. Positions of restriction sites used to isolate the homology arms (BamHI) and for Southern blotting (NdeI) are shown. Thin white bar labeled "5'" represents the location of the Southern blot probe used and the size of the Southern blot*

*fragments of the wildtype and targeted allele are depicted below the alleles.*

*(B) Southern blot of a wildtype and a targeted ES cell clone.*

#### 5.2.4 Design, cloning and targeting of the V619E-Neo-TK targeting vector

This targeting vector was designed to have two elements: the mutation in exon 15 and a Neo-TK selection cassette flanked by FRT sites for positive/negative selection. In order to get integration into the genome of both the selection cassette and the mutated exon, these elements should be as close to each other as possible. The closest suitable and unique restriction site to clone the selection cassette was a BamHI site approximately 1350bp upstream of exon 15. The FRT site left behind after removal of the NeoTK cassette in ES cells serves as the second FRT site to create the conditional B-Raf<sup>V619E</sup> knock-out allele.

A 9.8kb fragment containing exons 14, 15, and 16 from a C57Bl/6 BAC (RP24-387G20, BACPAC Resources, Children's Hospital Oakland Research Institute) containing the B-Raf genomic locus served as homology arms. The fragment was isolated with Sall and XbaI and cloned into pBluescript to generate BAC15-pBS in a fashion similar to the LSL-FRT targeting vector's homology arms. This plasmid was end-sequenced using T3 and T7 primers and the exons 14, 15, and 16 were sequenced to confirm correct cloning. Next, a BamHI-AvrII fragment containing B-Raf exon 15 was sub-cloned into pBluescript (BamHI-SpeI), mutated using the site directed mutagenesis kit (Stratagene), and, using BamHI and XbaI, cloned into BamHI-AvrII of BAC15-pBS. Finally, a FRT-Neo-TK-FRT selection cassette (E. Brown, AFCRI) was



introduced into the BamHI site to generate the V619E-Neo-TK targeting vector. The lack of unwanted nucleotide changes in the FRT sites, exons 14-16 and intron-exon boundaries was confirmed by sequencing.

LSL-FRT clones #12 and #15 were targeted with 50ug of NotI linearized V619E-NeoTK targeting vector (Figure 5.2.5A) and selected in neomycin for one week. 48 clones were picked for each LSL-FRT clone, expanded and screened for the presence of the Neo-TK cassette by long range PCR and Southern blotting (Figure 5.2.5B). A total of 41 clones were positively targeted and ten clones were further expanded for sequencing of exon 15. Seven of these clones carried the mutation in exon 15 (Figure 5.2.5C).

Since transgenic expression of HSV Thymidine kinase was associated with male infertility in mice (Braun et al., 1990), the Neo-TK selection cassette was removed in 3 LSL-FRT / V619E-Neo-TK double positive ES cell clones. This was achieved by electroporation of a Flp recombinase expression vector and selection of cells in ganciclovir. Twelve clones were picked for each of the three LSL-FRT / V619E-Neo-TK double positive ES cell clones and screened for the presence of only one FRT site in intron 14. Approximately 50% of clones were positive for the '1-FRT' PCR reaction (Figure 5.2.5D). Negative clones were tested by Southern blot for recombination between the 5' FRT site that was introduced into intron 2 with the LSL-FRT targeting vector and the 3' FRT site of the FRT-Neo-TK-FRT cassette in intron 14. This recombination reaction confirmed that both the LSL and the V619E mutation were indeed targeted to the same chromosome (Figure 5.2.5E).

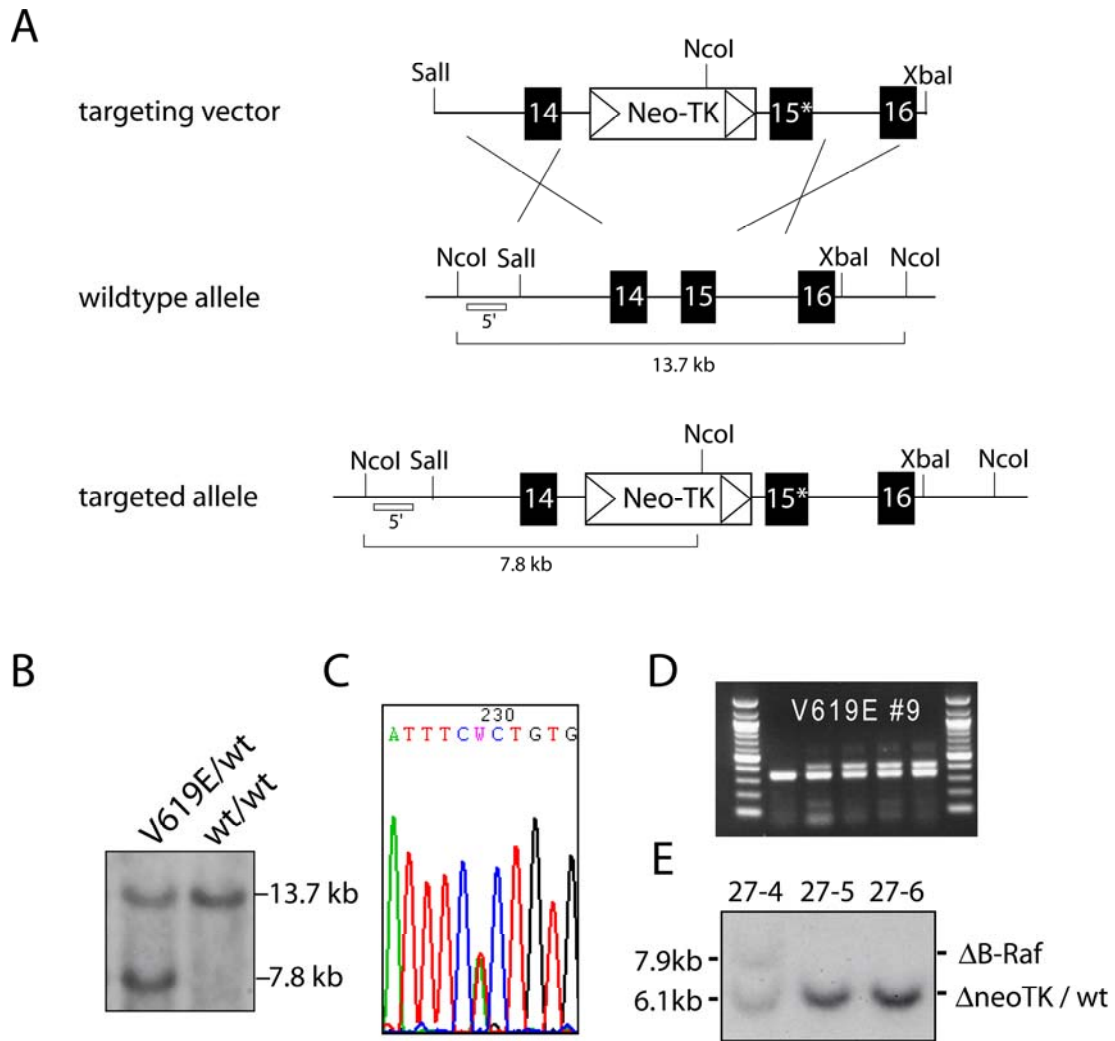


*Figure 5.2.5: Targeting of the V619E mutation (A) LSL-FRT targeting strategy. White triangles, FRT sites; numbered black boxes show exons. Positions of restriction sites used to isolate the homology arms (Sall and Xbal) and for Southern blotting (Ncol) are shown. Thin white bar labeled "5'" represents the location of the Southern blot probe used and the size of the Southern blot fragments of the wildtype and targeted allele are depicted below the alleles. (B) Southern blot of a wildtype and a targeted ES cell clone. (C) Sequencing of a double positive LSL-FRT / V619E-NeoTK clone. Note that the wildtype (green, A) and mutant exons (red, T) are present. (D) PCR of individual Flp-electroporated LSL-FRT / V619E-NeoTK clones from parental clone #9. The*

lower band represents wildtype intron 14, the upper band represents intron 14 containing one FRT site after removal of the Neo-TK cassette. (E) Southern blot using EcoRV to test individual Flp-electroporated LSL-FRT / V619E-NeoTK clones from parental clone #27 for targeting in cis (see text for description). Subclone 27-4 has exons 3-14 deleted ( $\Delta B$ -Raf), indicating that the parental clone #27 was targeted in cis with the LSL cassette and the V619E mutation.

#### 5.2.5 LSL-B-Raf<sup>V619E</sup> MEFs and mice

Two clones were expanded and injected into blastocysts by the CRI transgenic core. High contribution chimeras were crossed to C57Bl/6 mice and both clones transmitted the mutant B-Raf allele through the germline. To test the functionality of the allele, mouse embryonic fibroblasts (MEFs) were isolated from LSL-B-Raf<sup>V619E</sup> embryos. MEFs were infected with Ad-Cre to remove the LSL cassette and induce B-Raf<sup>V619E</sup> expression. Upon B-Raf<sup>V619E</sup> expression, MEFs expressed higher levels of pERK compared to Ad-Mock infected cells and were able to form foci (Figure 5.2.6A, B), similar to oncogenic B-Raf mutant MEFs generated by Dr. R. Marais' and Dr. C. Pritchard's groups (Mercer et al., 2005). B-Raf<sup>V619E</sup> MEFs changed their morphology and looked similar to MEFs expressing endogenous K-Ras<sup>G12D</sup> (Figure 5.2.6D and Tuveson et al., 2004). Importantly, the transformed morphology of B-Raf<sup>V619E</sup>-expressing cells was reversed upon infection with an Ad-Flp virus (Figure 5.2.6D). Recombination of the LSL cassette upon Ad-Cre infection and conditional knock-out of B-Raf<sup>V619E</sup> was confirmed by PCR analysis (Figure 5.2.6E). Furthermore, while expression of B-Raf<sup>V619E</sup>

prevents the senescence of MEFs, senescence is induced by subsequent infection with Ad-Flp (Figure 5.2.6F), suggesting that deletion of the oncogenic B-Raf allele returns MEFs to an untransformed state. Together, these data indicate that activation and inactivation of endogenous oncogenic B-Raf<sup>V619E</sup> was successful *in vitro*. To test the LSL-B-Raf<sup>V619E</sup> allele *in vivo*, mice were crossed to the melanocyte-specific, inducible TyrCreERT2 strain (Bosenberg et al., 2006), to activate oncogenic B-Raf in melanocytes. LSL-B-Raf<sup>V619E</sup>; TyrCreERT2 mice were treated with 3 x 2mg Tamoxifen at 4 weeks after birth and aged to assess melanocytic hyperplasia development. In two similar mouse models, this approach led to hyper-pigmentation of the skin due to melanocyte hyper-proliferation within a few weeks (Dankort et al., 2009; Dhomen et al., 2009). In one model, melanocytic hyperplasias progressed to melanoma (Dhomen et al., 2009). In Tamoxifen-treated LSL-B-Raf<sup>V619E</sup>, TyrCreERT2 mice, hyper-pigmentation of the tail skin (Figure 5.2.6C) was observed after 4-6 weeks. Thus, Cre-mediated activation of B-Raf<sup>V619E</sup> results in skin hyper-pigmentation, verifying that this targeting strategy induces a similar phenotype as two alternative B-Raf mouse models of melanoma (Dankort et al., 2009; Dhomen et al., 2009). Tamoxifen-treated LSL-B-Raf<sup>V619E</sup>; TyrCreERT2 mice are currently being aged to determine whether hyperplasias progress to melanoma without genetically-engineered, concomitant loss of a tumor suppressor gene such as p16INK4A or PTEN. Somatic loss of these tumor suppressor genes commonly occurs in melanoma and this has been shown to cooperate with B-Raf<sup>V600E</sup> to accelerate melanomagenesis (Dankort et al., 2009; Dhomen et al., 2009). Expression of endogenous oncogenic B-Raf has been shown to induce lung

tumorigenesis (Dankort et al., 2007), and it is currently being tested, whether conditional deletion of oncogenic B-Raf<sup>V619E</sup> in lung neoplasms leads to tumor regression.

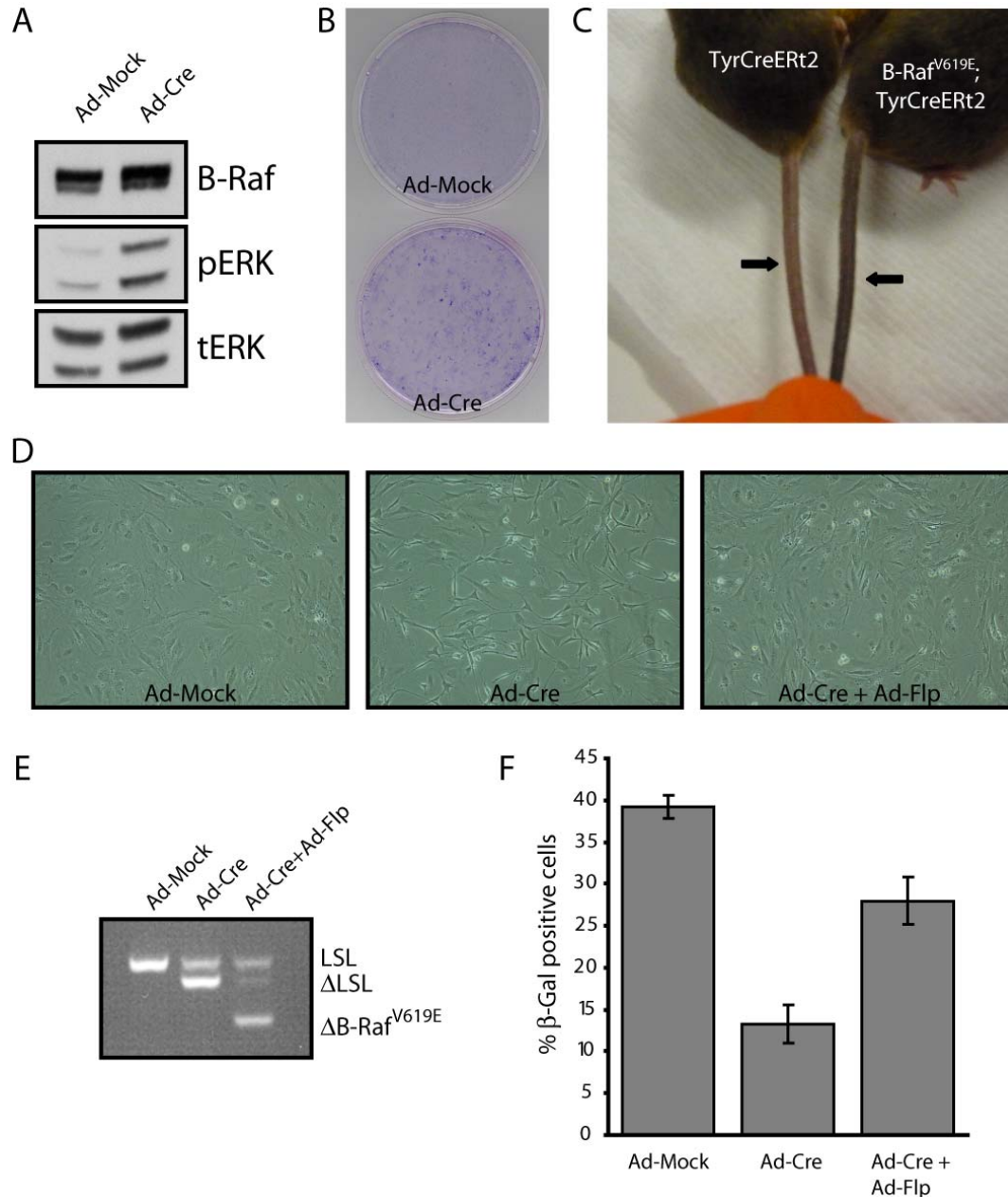


Figure 5.2.6: Characterization of LSL-B-Raf<sup>V619E</sup> MEFs and mice (A) Western blot of Ad-Mock and Ad-Cre infected LSL-B-Raf<sup>V619E</sup> MEFs. Deletion of the LSL cassette by Ad-Cre results in twice as much B-Raf expression and increased pERK levels. (B) Focus formation of Ad-Mock and Ad-Cre infected LSL-B-Raf<sup>V619E</sup> MEFs. (C) B-Raf<sup>V619E</sup>; TyrCreERT2 and TyrCreERT2 littermates

were *i.p.* injected with 3 x 2mg Tamoxifen in corn oil to induce B-Raf<sup>V619E</sup> expression in melanocytes. Note hyper-pigmentation of tail skin of B-Raf<sup>V619E</sup>; TyrCreERT2 mouse. Pictures were taken 10 weeks post Tamoxifen administration. (D) Cell morphology of Ad-Mock, Ad-Cre and Ad-Cre + Ad-Flp infected LSL-B-Raf<sup>V619E</sup> MEFs. (E) PCR reaction detecting the presence/absence of the LSL (LSL,  $\Delta$ LSL, respectively) and conditional knock-out of B-Raf<sup>V619E</sup> ( $\Delta$ B-Raf<sup>V619E</sup>) in Ad-Mock, Ad-Cre, and Ad-Cre + Ad-Flp infected LSL-B-Raf<sup>V619E</sup> MEFs. (F) Senescence-associated  $\beta$ -Galactosidase staining to detect senescent primary MEFs at passage 9. Cells not expressing B-Raf<sup>V619E</sup> (Ad-Mock and Ad-Cre + Ad-Flp) enter senescence, while B-Raf<sup>V619E</sup> MEFs are protected from senescence.

#### 5.2.6 Generation of R26-LSL-FlpERT2 mice

In order to inactivate oncogenic B-Raf<sup>V619E</sup>, the Flp recombinase must be present in B-Raf mutant cells. Moreover, Flp has to remain dormant until B-Raf<sup>V619E</sup> is supposed to be inactivated. Therefore, a mouse models that expresses a Flp-ERT2 fusion protein under the control of the rosa26 promoter was generated. ERT2 is the mutant ligand binding domain of the human estrogen receptor and is bound to heat shock proteins in the cytosol. If the ERT2 domain is fused to a recombinase, the recombinase will be inactive until ERT2 binds to its ligand, Tamoxifen, which triggers a release from heat shock proteins and allows enzymatic activity of the recombinase. The rosa26 promoter is ubiquitously expressed, making this FlpERT2 allele a useful reagent for various cancer models. However, to limit FlpERT2 expression to cells that express the oncogene of choice, a LSL cassette was inserted

between the rosa26 promoter and the FlpERT2 coding sequence. In addition to studying oncogene addiction, this allele is suitable to investigate sequential gene targeting such as oncogene activation followed by tumor suppressor inactivation in developed tumors. The design and targeting strategy of FlpERT2 allele are shown in Figure 5.2.7A.

To generate the FlpERT2 allele, Flp was amplified from pCAGGS-Flpe using an upstream primer containing a NheI and a Sall site as well as a viral splice acceptor and a downstream primer containing a BamHI site: SA-Flp-up 5'-gcGCTAGC**gtcgcac**agggcgagtagtccagggttccttgatgatgcatactatcctgtcccttttttccacagccatggctccaag-3' (NheI site is in capital letters, Sall site is in bold, SV40 splice acceptor is underlined) and SA-Flp-dwn 5'-cagcagaggatcctatgcgtc-3' (BamHI site is underlined). In parallel, ERt2-SV40pA was amplified from a CreERT2 plasmid (provided by Dr. P. Chambon) using an upstream primer containing a BamHI site and a downstream primer containing a NheI site: ERt2-SV40pA-up 5'-gacgcataggatcctctgctg-3' (BamHI site is underlined) and ERt2-SV40pA-dwn 5'-gcgctagcccagacatgataagatac-3' (NheI site is underlined). The SA-Flp and ERt2-SV40pA PCR products were digested with NheI/BamHI and BamHI/NheI and triple ligated into modified pBluescript containing a NheI site. Flp was fused to the ERt2 in a similar fashion as previously published (Hunter et al., 2005), suggesting that this fusion protein is likely to be functional. The SA-Flp-ERt2-SV40pA sequence was verified by sequencing followed by cloning into the NheI site of a rosa26 genomic fragment in pBluescript. Finally, the LSL cassette was inserted into the Sall site to generate the R26-LSL-FlpERT2 targeting vector.

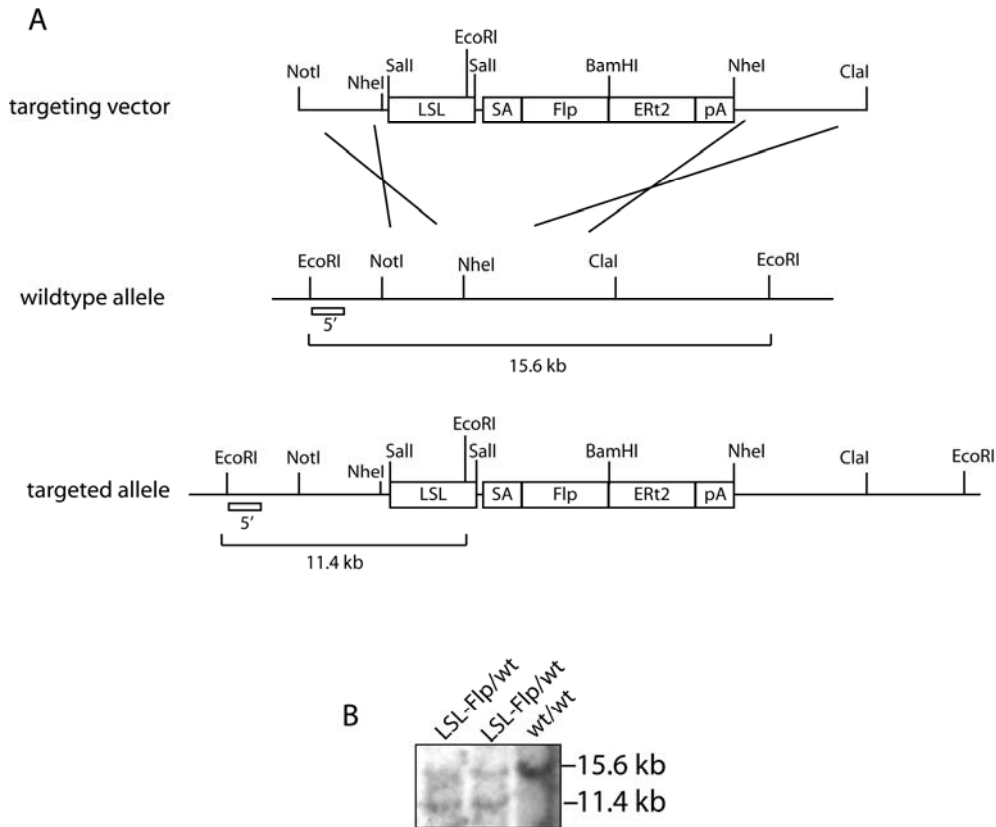


*Figure 5.2.7: Targeting of the LSL-FlpERT2 allele (A) LSL-FlpERT2 targeting strategy. NotI and ClaI restriction sites mark the borders of the homology arms. EcoRI was used to digest genomic DNA for Southern blotting. Thin white bar labeled “5’ ” represents the location of the Southern blot probe used and the size of the Southern blot fragments of the wildtype and targeted allele are shown below the alleles. (B) Southern blot of a wildtype and two targeted ES cell clones.*

E14J ES cells were targeted with 50ug of NotI linearized R26-LSL-FlpERT2 targeting vector, selected in puromycin, 48 clones picked and screened for the presence of the LSL-FlpERT2 allele by Southern blotting (Figure 5.2.7B). Two positive clones were expanded and injected into blastocysts. High contribution chimeras were crossed to C57Bl/6 mice and agouti offspring were genotyped



for the LSL-FlpERT2 allele. F1 LSL-FlpERT2 mice were crossed to a Flp-reporter strain (placental alkaline phosphatases, PLAP, Awatramani et al., 2001) and MEFs isolated. Double mutant MEFs were infected with Ad-Cre to delete the LSL cassette and treated with 10 and 100nM 4-Hydroxytamoxifen (4-OHT) for 3 days to induce Flp activity, which drives PLAP expression. Staining of MEFs for alkaline phosphatase revealed that only Ad-Cre infected, 4-OHT treated cells were positive for PLAP (Figure 5.2.8), indicating that the LSL-FlpERT2 allele works under these conditions. LSL-FlpERT2 mice were then crossed to Ub-CreERT2 (E. Brown, AFCRI) mice and treated with Tamoxifen to remove the LSL cassette in the germline and generate FlpERT2 mice. FlpERT2 mice were crossed to PLAP mice, treated with Tamoxifen and are currently being examined for *in vivo* activity of the FlpERT2 allele.

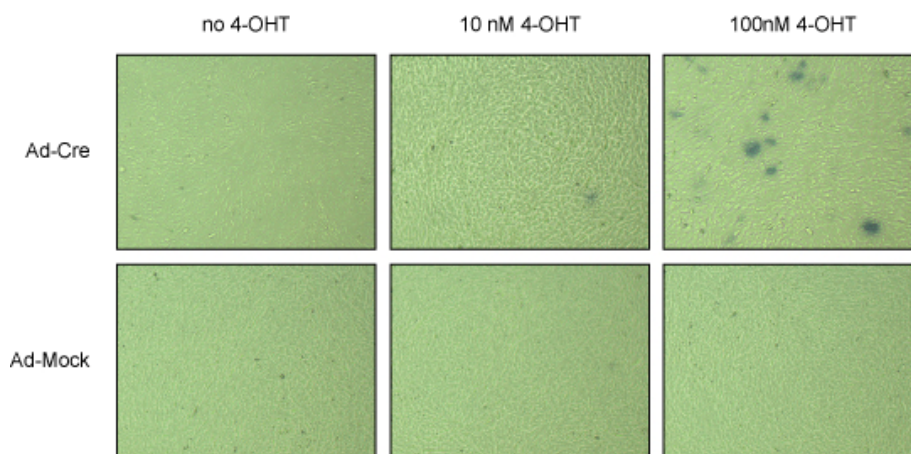


Figure 5.2.8: *FlpERT2* activity *in vitro*. Ad-Cre and Ad-Mock infected LSL-*FlpERT2*; PLAP MEFs were treated with 10 and 100nM 4-OHT and incubated with BM Purple solution containing NBT and BCIP to detect alkaline phosphatase activity. Ad-Cre infected cells that were treated with 100nM 4-OHT showed some alkaline phosphatase positivity.

In summary, I have created two genetically engineered mouse strains, which are currently being characterized in detail. LSL-B-Raf<sup>V619E</sup> mice displayed no overt phenotype indicating that oncogenic B-Raf is not expressed in the absence of Cre activity. When crossed to TyrCreERt2 mice and treated with Tamoxifen, LSL-B-Raf<sup>V619E</sup> mice showed increased pigmentation of skin, due to expansion of the pool of melanocytes. *In vitro*, MEFs were transformed by expression of B-Raf<sup>V619E</sup>, and reversibility of the allele was demonstrated by infecting with Ad-Flp. Thus, the LSL-B-Raf<sup>V619E</sup> allele was shown to be functional *in vivo* and *in vitro*. MEFs derived from R26-LSL-FlpERt2 mice harboring a Flp reporter were infected with Ad-Cre and treated with 4-OHT. This resulted in PLAP activity, indicating that this allele, too, is functional. These alleles will be useful tools to further investigate the role of oncogenic B-Raf in tumor biology.

## **5. Results and Discussion**

5.3 The role of B-Raf and C-Raf in K-Ras<sup>G12D</sup>-induced lung tumorigenesis (unpublished data)

### 5.3.1 Rationale

Ras is mutated in approximately 30% of human cancers (Bos, 1989). Of the three Ras family members, K-Ras is predominantly found mutated and mouse models have provided experimental evidence that K-Ras has oncogenic properties in the lung, pancreas, hematopoietic system, colon, endometrium, and soft tissue (Karreth and Tuveson, 2009). Therapeutic targeting of Ras itself has been unsuccessful so far. Targeting Ras effector pathways may therefore represent an alternative therapeutic option to treat Ras mutant tumors. Thus, the Ras effector pathway(s) required for transmitting the effects of oncogenic Ras need to be determined. In the lung, PI3K and Rac have been shown to be critical for K-Ras<sup>G12D</sup>-mediated tumorigenesis (Gupta et al., 2007; Kissil et al., 2007). In human cells, RalA but not RalB is critical for oncogenic Ras-induced cell transformation (Lim et al., 2005). Finally, C-Raf is essential for tumor formation and maintenance in a squamous cell carcinoma model (Ehrenreiter et al., 2009). However, the role of the Raf-MEK-ERK pathway downstream of endogenous K-Ras<sup>G12D</sup> in lung tumorigenesis remains to be investigated. To this end, B-Raf<sup>fl/fl</sup>; K-Ras<sup>G12D</sup> and C-Raf<sup>fl/fl</sup>; K-Ras<sup>G12D</sup> compound mutant mice were generated to analyze the importance of B-Raf and C-Raf in mediating the oncogenic K-Ras<sup>G12D</sup> effects in the lung.

### 5.3.2 Lung tumor development

B-Raf<sup>fl/fl</sup>; K-Ras<sup>G12D</sup> and C-Raf<sup>fl/fl</sup>; K-Ras<sup>G12D</sup> mutant mice and control mice (B-Raf<sup>fl/wt</sup>; K-Ras<sup>G12D</sup> and C-Raf<sup>fl/wt</sup>; K-Ras<sup>G12D</sup>, respectively as well as K-Ras<sup>G12D</sup> mice on the same genetic background as the compound mutant mice) were infected with Ad-Cre via intranasal instillation at 4-6 weeks of age. Mice were

aged for 6, 9, and 12 weeks, and tumor burden examined. Even though there was a trend towards reduced tumor burden in B-Raf<sup>fl/fl</sup>; K-Ras<sup>G12D</sup> mice compared to control mice at all investigated time points, it never reached statistical significance (Figure 5.3.1). Similarly, C-Raf<sup>fl/fl</sup>; K-Ras<sup>G12D</sup> mice showed slightly but not significantly reduced lung tumor burden at 6 and 9 weeks when compared to control mice. However, at 12 weeks following Ad-Cre infection, lung tumor burden of C-Raf<sup>fl/fl</sup>; K-Ras<sup>G12D</sup> was significantly reduced (Figure 5.3.1). These data suggest that C-Raf may play a more important role than B-Raf in K-Ras<sup>G12D</sup>-mediated lung tumorigenesis at these early stages.

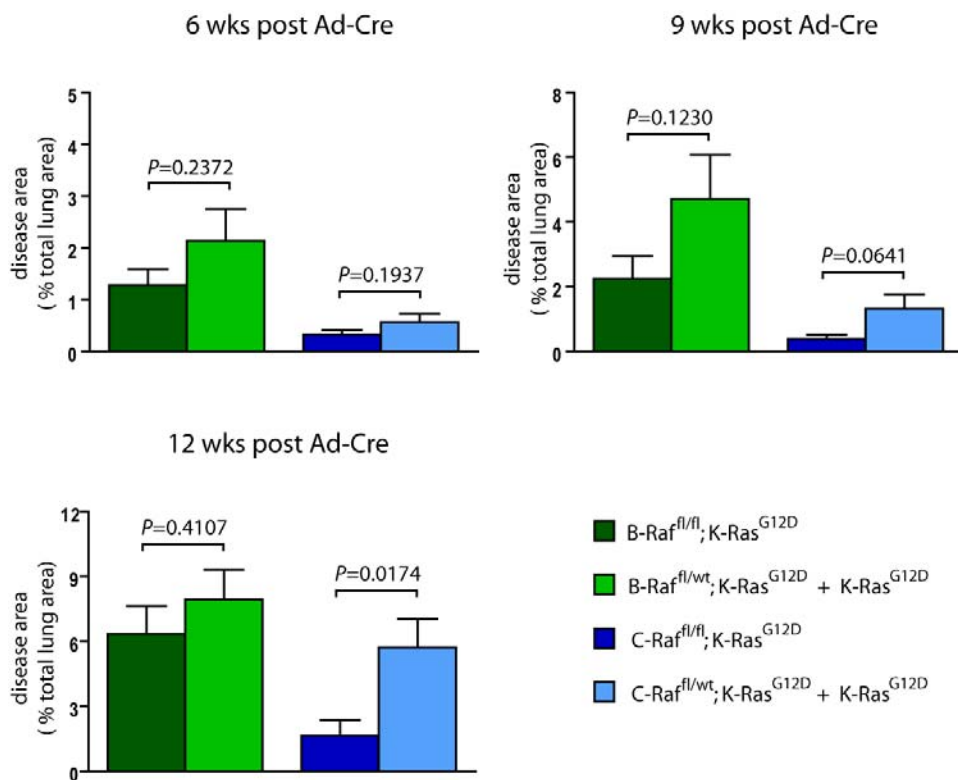
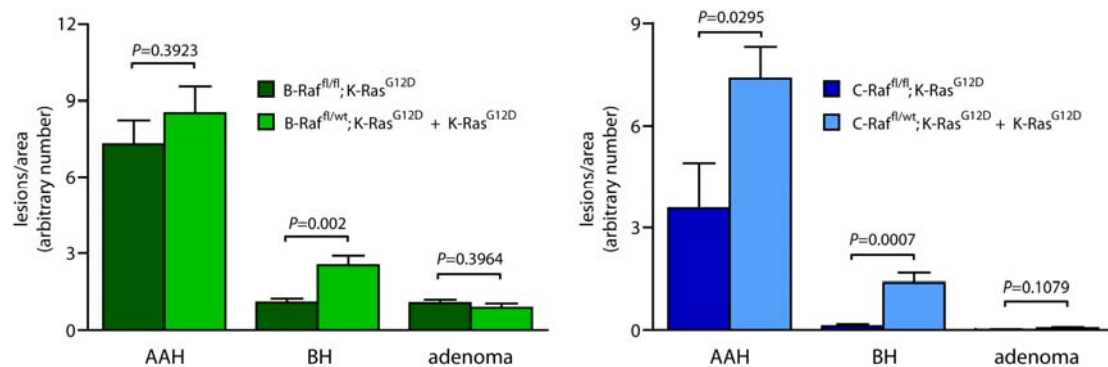


Figure 5.3.1: Lung tumor burden. Tumor burden at 6 weeks (top left), 9 weeks (top right), and 12 weeks (bottom left) post Ad-Cre infection. B-Raf<sup>fl/fl</sup>; K-Ras<sup>G12D</sup> mice display slightly decreased tumor burden compared to B-Raf<sup>fl/wt</sup>; K-Ras<sup>G12D</sup> mice.

*K-Ras<sup>G12D</sup>* and *K-Ras<sup>G12D</sup>* control mice at all three time-points; however, the decrease was not statistically significant. Tumor burden of *C-Raf<sup>fl/fl</sup>; K-Ras<sup>G12D</sup>* mice was significantly reduced 12 weeks post Ad-Cre infection when compared to control mice, and slightly but not significantly at earlier time-points.

Next, the number of neoplasms per lung area at 12 weeks was determined. *B-Raf<sup>fl/fl</sup>; K-Ras<sup>G12D</sup>* displayed a reduced number of the least abundant type of neoplasm, bronchiolar hyperplasias (BH), but no significant reduction of adenomatous alveolar hyperplasias (AAH) and adenomas (Figure 5.3.2). In contrast, *C-Raf<sup>fl/fl</sup>; K-Ras<sup>G12D</sup>* mice exhibited a significant reduction in BH, AAH, and adenomas (Figure 5.3.2), suggesting that the lower number of neoplasms results in reduced lung tumor burden of *C-Raf<sup>fl/fl</sup>; K-Ras<sup>G12D</sup>* mice. These findings suggest that C-Raf may play a role in tumor initiation by *K-Ras<sup>G12D</sup>*.



*Figure 5.3.2: Number of neoplasms. B-Raf<sup>fl/fl</sup>; K-Ras<sup>G12D</sup> mice develop fewer BH than control mice but the number of AAH and adenomas is not reduced (left panel). The number of AAH, BH, and adenomas is significantly decreased in C-Raf<sup>fl/fl</sup>; K-Ras<sup>G12D</sup> mice (right panel).*

### 5.3.3 Survival of B-Raf<sup>fl/fl</sup>; K-Ras<sup>G12D</sup> and C-Raf<sup>fl/fl</sup>; K-Ras<sup>G12D</sup> mice

B-Raf<sup>fl/fl</sup>; K-Ras<sup>G12D</sup> and C-Raf<sup>fl/fl</sup>; K-Ras<sup>G12D</sup> and appropriate control mice were aged to assess survival of these mice. Mice were sacrificed once they showed signs of rapid, labored breathing, piloerection, hunched posture, inactivity, loss of social behavior with cage mates and loss of a significant amount of their body weight (>20%). Interestingly, genetic ablation of both B-Raf and C-Raf in the context of oncogenic K-Ras<sup>G12D</sup> extended the median survival for approximately 50 days (Figure 5.3.3). Thus, while extended survival of C-Raf<sup>fl/fl</sup>; K-Ras<sup>G12D</sup> mice is likely due to reduced initiation of neoplasms, tumor development in B-Raf<sup>fl/fl</sup>; K-Ras<sup>G12D</sup> mice appears to be impaired at later stages, leading to increased survival.

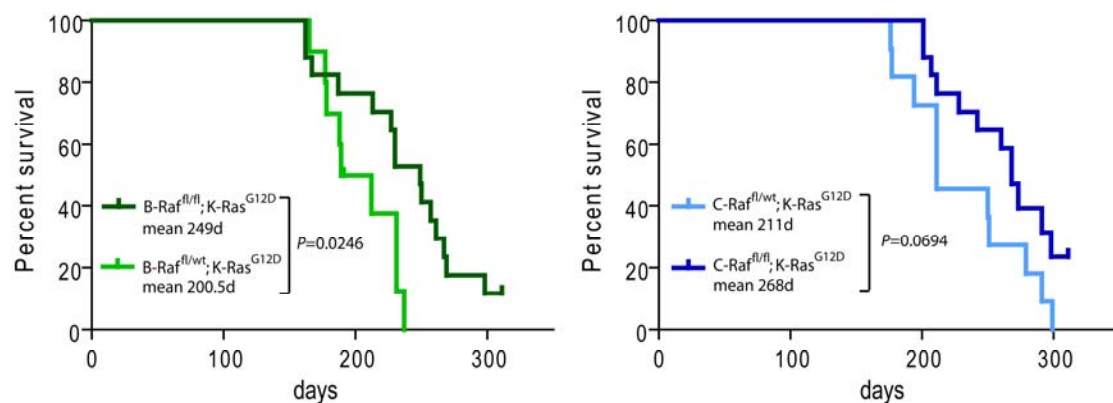
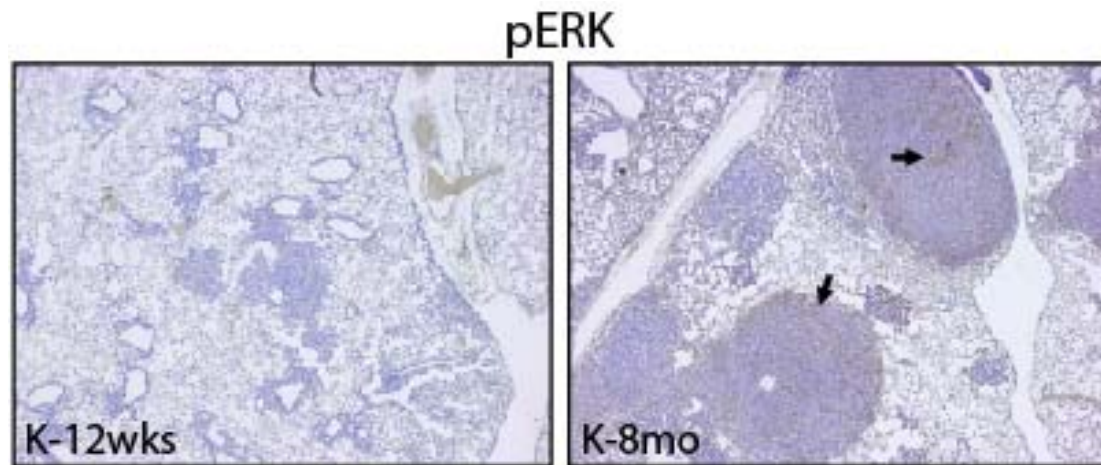


Figure 5.3.3: Survival curves. Homozygous deletion of B-Raf in K-Ras<sup>G12D</sup> lung cells significantly extends survival compared to B-Raf<sup>fl/wt</sup>; K-Ras<sup>G12D</sup> mice (median survival: B-Raf<sup>fl/fl</sup>; K-Ras<sup>G12D</sup>, 249 days vs. B-Raf<sup>fl/wt</sup>; K-Ras<sup>G12D</sup>, 200.5 days) (left panel). Similarly, C-Raf<sup>fl/fl</sup>; K-Ras<sup>G12D</sup> mice display an increase in median survival (268 days) compared to C-Raf<sup>fl/wt</sup>; K-Ras<sup>G12D</sup> mice (211 days) (right panel).

#### 5.3.4 MAPK activation and proliferation *in vivo*

To determine whether increased survival of B-Raf<sup>fl/fl</sup>; K-Ras<sup>G12D</sup> and C-Raf<sup>fl/fl</sup>; K-Ras<sup>G12D</sup> mice is due to impaired MAPK activation, lung sections were stained for pERK. Unfortunately, pERK levels are not increased in lung neoplasms compared to normal alveolar tissue at 6, 9, and 12 weeks post Ad-Cre infection independent of the genotype (Figure 5.3.4). This is likely due to K-Ras<sup>G12D</sup> mediated activation of negative regulators of the MAPK pathway, such as Sprouty proteins (Shaw et al., 2007).



*Figure 5.3.4: pERK staining in lung neoplasms of K-Ras<sup>G12D</sup> mice. No immunohistochemical staining was detected at early time-points (K-12wks, K-Ras<sup>G12D</sup> mouse 12 weeks post Ad-Cre infection), while some neoplasms showed pERK positivity at late time-points (K-8mo, K-Ras<sup>G12D</sup> mouse 8 months post Ad-Cre infection).*

Next, proliferation of neoplasms at 12 weeks post Ad-Cre infection was assessed by staining lung sections for Ki-67. Proliferation of neoplasms in C-Raf<sup>fl/fl</sup>; K-Ras<sup>G12D</sup> mice was not significantly different when compared to



control mice (Figure 5.3.5). Intriguingly, proliferation of AAH and early grade adenomas was reduced in B-Raf<sup>fl/fl</sup>; K-Ras<sup>G12D</sup> mice, demonstrating that increased survival of these mice correlates with a slower growth of neoplasms. Thus, both B-Raf and C-Raf are important for K-Ras<sup>G12D</sup>-driven lung tumorigenesis.

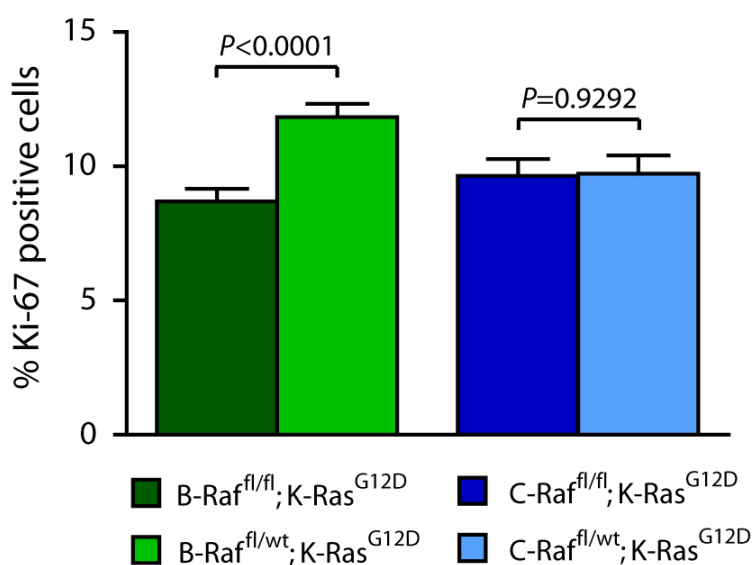


*Figure 5.3.5: Proliferation of early grade neoplasms. Percentage of Ki-67 positive cells in AAH and adenomas 12 weeks post Ad-Cre infection is shown. Homozygous deletion of B-Raf in K-Ras<sup>G12D</sup> expressing neoplastic cells impairs proliferation, whereas ablation of C-Raf expression has no effect on proliferation.*

### 5.3.5 B-Raf<sup>fl/fl</sup>; K-Ras<sup>G12D</sup> and C-Raf<sup>fl/fl</sup>; K-Ras<sup>G12D</sup> MEFs

Endogenous expression of oncogenic K-Ras<sup>G12D</sup> partially transforms mouse embryonic fibroblasts. K-Ras<sup>G12D</sup> MEFs show increased rates of proliferation, loss of contact inhibition and are immortal (Tuveson et al., 2004). Features of

oncogenic K-Ras activity were examined in B-Raf<sup>fl/fl</sup>; K-Ras<sup>G12D</sup> and C-Raf<sup>fl/fl</sup>; K-Ras<sup>G12D</sup> MEFs. First, proliferation was assessed in 10% and 2% fetal calf serum. Interestingly, Ad-Cre infected C-Raf<sup>fl/fl</sup>; K-Ras<sup>G12D</sup> MEFs displayed increased proliferation compared to Ad-Mock infected control cells similar to K-Ras<sup>G12D</sup> cells (Figure 5.3.6A, B). In contrast, K-Ras<sup>G12D</sup> cells lacking B-Raf proliferate similar to Ad-Mock infected control cells (Figure 5.3.6A, B), indicating that B-Raf but not C-Raf is required for K-Ras<sup>G12D</sup> to promote proliferation of MEFs. Next, signaling downstream of Raf was investigated. pERK levels are slightly decreased when K-Ras<sup>G12D</sup>-expressing cells are grown in 10% FCS (Tuveson et al., 2004). Similar decreases in pERK levels were observed in Ad-Cre infected B-Raf<sup>fl/fl</sup>; K-Ras<sup>G12D</sup> MEFs, while C-Raf<sup>fl/fl</sup>; K-Ras<sup>G12D</sup> MEFs displayed higher levels of pERK. Interestingly, when grown in 2% FCS, pERK levels in Ad-Cre infected K-Ras<sup>G12D</sup> and C-Raf<sup>fl/fl</sup>; K-Ras<sup>G12D</sup> cells were not significantly different from those of Ad-Mock infected cells. In contrast, pERK levels were markedly decreased in Ad-Cre infected B-Raf<sup>fl/fl</sup>; K-Ras<sup>G12D</sup> MEFs compared to Ad-Mock infected controls when grown in 2% FCS (Figure 5.3.7), indicating that K-Ras<sup>G12D</sup> activates the MAPK pathway primarily through B-Raf under these conditions. These *in vitro* data corroborate the *in vivo* finding of reduced proliferation of AAH and adenomas in B-Raf<sup>fl/fl</sup>; K-Ras<sup>G12D</sup> mice, which is likely due to impaired MAPK signaling.

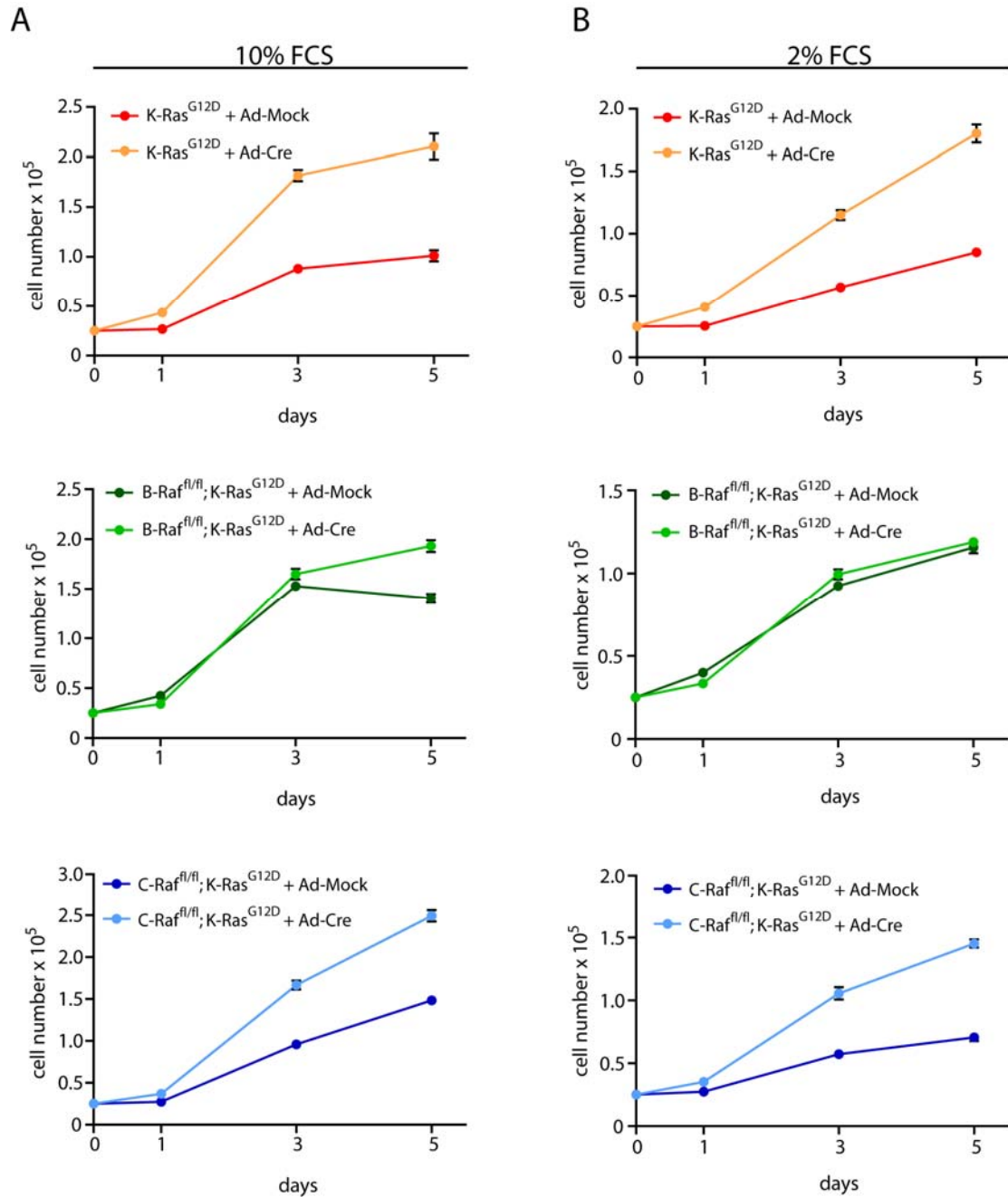


Figure 5.3.6: Proliferation of MEFs in 10% and 2% serum. (A) Proliferation curves of Ad-Mock or Ad-Cre infected K-Ras<sup>G12D</sup>, B-Raf<sup>fl/fl</sup>; K-Ras<sup>G12D</sup>, or C-Raf<sup>fl/fl</sup>; K-Ras<sup>G12D</sup> MEFs in 10% FCS. (B) Proliferation curves of Ad-Mock or Ad-Cre infected K-Ras<sup>G12D</sup>, B-Raf<sup>fl/fl</sup>; K-Ras<sup>G12D</sup>, or C-Raf<sup>fl/fl</sup>; K-Ras<sup>G12D</sup> MEFs in 2% FCS.

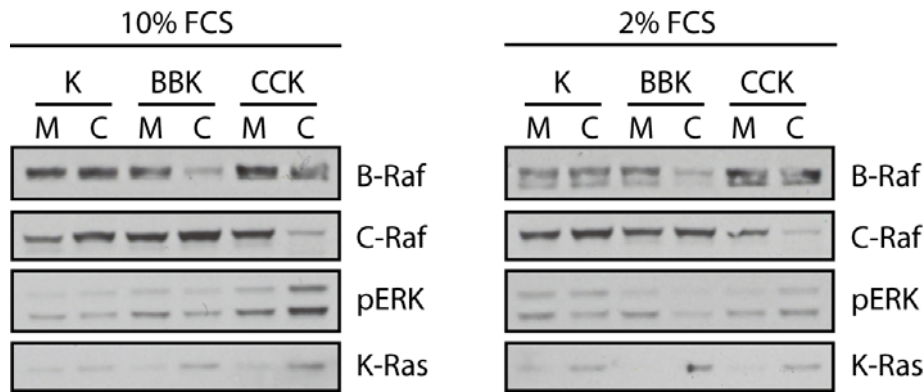


Figure 5.3.7: Western blot analysis in 10% and 2% serum. B-Raf, C-Raf and K-Ras blots show appropriate recombination of the respective alleles when infected with Ad-Cre. pERK levels are markedly reduced in B-Raf<sup>Δ/Δ</sup>; K-Ras<sup>G12D</sup> MEFs grown in 2% serum. K, K-Ras<sup>G12D</sup>; BBK, B-Raf<sup>fl/fl</sup>; K-Ras<sup>G12D</sup>; CCK, C-Raf<sup>fl/fl</sup>; K-Ras<sup>G12D</sup>; M, Ad-Mock; C, Ad-Cre.

C-Raf has been shown to have anti-apoptotic activity by antagonizing ASK1, MST2, ROK $\alpha$ , and BAD (Chen et al., 2001; O'Neill et al., 2004; Piazzolla et al., 2005; Wang et al., 1996). Therefore, a potential anti-apoptotic role of C-Raf in K-Ras<sup>G12D</sup> MEFs was investigated. K-Ras<sup>G12D</sup>, B-Raf<sup>fl/fl</sup>; K-Ras<sup>G12D</sup> and C-Raf<sup>fl/fl</sup>; K-Ras<sup>G12D</sup> MEFs infected with Ad-Cre showed no apoptotic phenotype; however, K-Ras<sup>G12D</sup> MEFs were less sensitive to induction of apoptosis by either TNF $\alpha$  or Staurosporine when compared to Ad-Mock infected control cells (Figure 5.3.8). Genetic ablation of B-Raf in K-Ras<sup>G12D</sup> cells did not prevent the K-Ras<sup>G12D</sup>-mediated protection from apoptosis. Intriguingly, deletion of C-Raf negated the anti-apoptotic effect of K-Ras<sup>G12D</sup> (Figure 5.3.8), indicating that K-Ras<sup>G12D</sup> signals through C-Raf to confer reduced sensitivity to apoptotic stimuli. Whether the lack of C-Raf in K-Ras<sup>G12D</sup> lung epithelial cells induces apoptosis remains to be determined. No

increased apoptosis was detected in C-Raf<sup>fl/fl</sup>; K-Ras<sup>G12D</sup> neoplasms at 6, 9, and 12 weeks post Ad-Cre infection (Figure 5.3.9), indicating that if the lack of C-Raf induces apoptosis in K-Ras<sup>G12D</sup>-expressing cells, it occurs immediately after induction of oncogenic K-Ras expression.

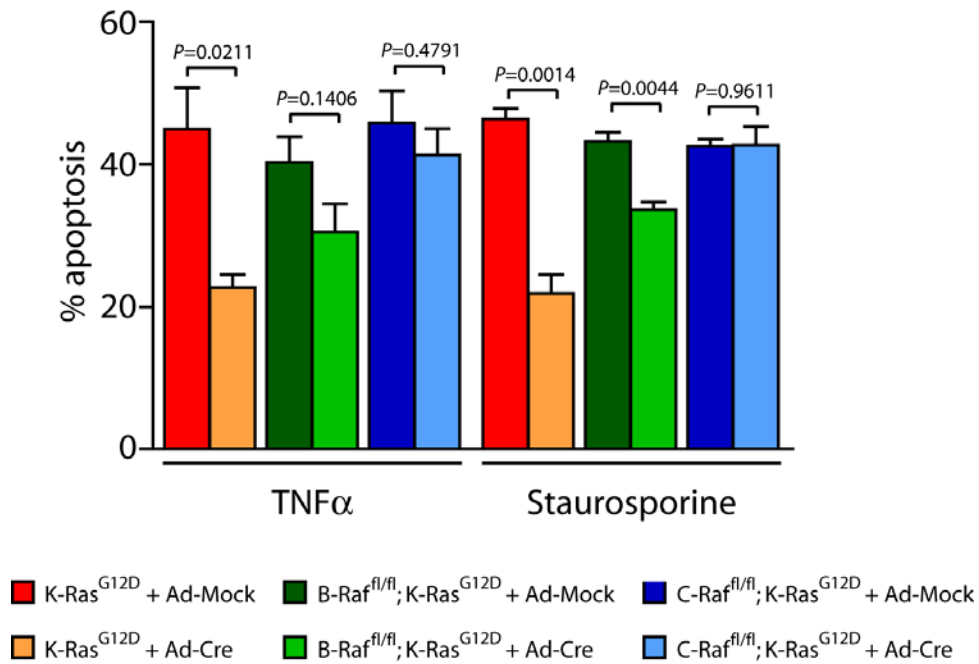


Figure 5.3.8: Anti-apoptotic effect of K-Ras<sup>G12D</sup> requires C-Raf. Apoptosis was induced by treatment with 10ng/ml TNFα or 5nM Staurosporine of Ad-Mock or Ad-Cre infected K-Ras<sup>G12D</sup>, B-Raf<sup>fl/fl</sup>; K-Ras<sup>G12D</sup>, or C-Raf<sup>fl/fl</sup>; K-Ras<sup>G12D</sup> MEFs.

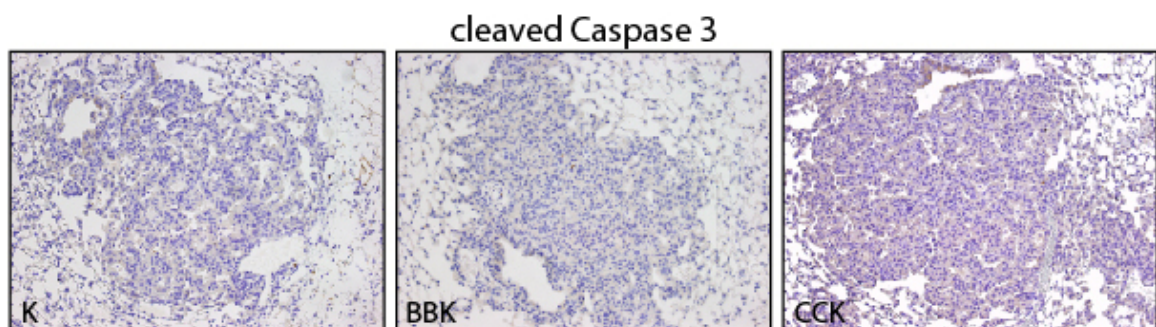


Figure 5.3.9: Apoptosis in vivo. No apoptosis of neoplastic cells in K-Ras<sup>G12D</sup>, B-Raf<sup>fl/fl</sup>; K-Ras<sup>G12D</sup>, or C-Raf<sup>fl/fl</sup>; K-Ras<sup>G12D</sup> mice 12 weeks post Ad-Cre

*infection. Lungs were immunohistochemically stained for cleaved Caspase 3. K, K-Ras<sup>G12D</sup>; BBK, B-Raf<sup>fl/fl</sup>; K-Ras<sup>G12D</sup>; CCK, C-Raf<sup>fl/fl</sup>; K-Ras<sup>G12D</sup>.*

### 5.3.6 Future directions

I have shown that both B-Raf and C-Raf are important for K-Ras<sup>G12D</sup>-mediated lung tumor development. Interestingly, B-Raf and C-Raf play distinct roles: while B-Raf regulates MAPK signaling and proliferation, C-Raf is dispensable for MEK/ERK activation but rather is critical for survival of K-Ras mutant cells *in vitro* and tumor initiation *in vivo*. Several experiments will be performed to further elucidate the role of B-Raf and C-Raf in K-Ras<sup>G12D</sup>-driven tumorigenesis. First, the recombination efficiency of the floxed B-Raf and C-Raf alleles in K-Ras<sup>G12D</sup> mutant lung tumor cells will be determined. As B-Raf and/or C-Raf could be absolutely required for K-Ras<sup>G12D</sup>-mediated lung tumorigenesis, the developing lesions could have undergone only heterozygous recombination of the floxed alleles. To further determine the role of B-Raf in MAPK signaling and cell cycle regulation in response to K-Ras<sup>G12D</sup>, expression of cell cycle regulators *in vitro* and *in vivo* will be examined. Furthermore, pERK levels will be analyzed in advanced tumors, where they have been shown to be elevated (Jackson et al., 2005). Moreover, the activation of anti-apoptotic effectors downstream of C-Raf as well as expression of pro-/anti-apoptotic proteins in K-Ras<sup>G12D</sup> mutant MEFs will be analyzed to better understand the pro-survival function of C-Raf in such cells. Finally, to further investigate the mechanism of reduced tumor initiation in C-Raf<sup>fl/fl</sup>; K-Ras<sup>G12D</sup> mice, compound mutant mice carrying a Cre reporter were generated. Apoptosis and proliferation will be assessed in Cre reporter

positive lung epithelial cells to determine the immediate biological response to K-Ras<sup>G12D</sup> activation. These additional data will hopefully provide some mechanistic insights and will allow publication of this project.

## **6. Conclusions**

The goal of this thesis was to genetically and biochemically dissect the functions of Raf proteins in tumorigenesis. Given the frequent occurrence of B-Raf mutations in melanoma as well as the lack of a tractable mouse model of melanoma at the time of commencement of this thesis, the primary objective was to create and characterize a conditional LSL-B-Raf<sup>V619E</sup> mutant mouse. My design of the transgenic allele included three features: (1) endogenous expression of oncogenic B-Raf<sup>V619E</sup>, (2) activation upon Cre expression to direct B-Raf<sup>V619E</sup> to the cell type of choice and (3) reversibility of B-Raf<sup>V619E</sup> expression by means of a Flp/FRT recombinase system. Endogenous expression of B-Raf<sup>V619E</sup> upon Cre expression is required to closely mimic the genetic context of the human cancer that is being modeled. Deactivation of oncogenic B-Raf<sup>V619E</sup> is the first attempt to genetically abolish expression of an endogenously expressed oncogene. Even though genetic and pharmacological means of inactivating oncogenic B-Raf are not equivalent, this approach will be informative as to whether oncogenic B-Raf itself is a suitable therapeutic target in established tumors. The design of the LSL-B-Raf<sup>V619E</sup> allele also has two main limitations: (1) ES cells had to be targeted three times, which was time and labor intensive and led to reduced pluripotency of some ES cell clones due to the stress inflicted by prolonged time in culture and multiple targeting. (2) Cells not expressing oncogenic B-Raf will be heterozygous for B-Raf. Even though B-Raf heterozygosity in mice results in no overt phenotype, B-Raf gene dosage could influence the response of the microenvironment to tumor formation.



Despite several setbacks (e.g. poor targeting efficiency due to short homology arms of the targeting vectors and no germline transmission with the first ES cell line used), the LSL-B-Raf<sup>V619E</sup> mouse as well as the R26-LSL-FlpERT2 mouse were created and are currently being characterized in detail. Initial analysis of the LSL-B-Raf<sup>V619E</sup> mouse model revealed that expression of oncogenic B-Raf induced hyper-pigmentation in a fashion similar to two previously published oncogenic B-Raf mouse models (Dankort et al., 2009; Dhomen et al., 2009). Therefore, this mouse model is a useful tool to study the biology of oncogenic B-Raf in melanoma development and genetically assess whether B-Raf is a suitable therapeutic target. Furthermore, when combined with loss of melanoma-associated tumor suppressor genes to accelerate tumor formation, this mouse model can be utilized to evaluate novel therapeutic agents in a preclinical setting. Moreover, this mouse model can be employed in a transposon-based forward genetic screen in an effort to identify tumor suppressor genes and oncogenes that co-operate with B-Raf<sup>V619E</sup> in melanoma development. Finally, this mouse model will be useful to further investigate the interplay between oncogenic B-Raf and C-Raf *in vivo*.

Oncogenic B-Raf mutants with impaired kinase activity towards MEK have been shown to activate C-Raf, thereby leading to aberrant MAPK signaling. It had been known that Raf proteins form heterodimers in a Ras-dependant manner (Farrar et al., 1996; Luo et al., 1996; Weber et al., 2001) and that different Raf dimers possess varying kinase activities (Rushworth et al., 2006); however, the notion that Raf proteins affect the activity of each other added a new layer of complexity to the regulation of the MAPK pathway.

During my PhD I discovered that while the interaction of C-Raf with impaired activity B-Raf mutants promoted hyperactivation of the MAPK pathway, C-Raf antagonizes B-Raf<sup>V600E</sup>-mediated MAPK signaling. Interestingly, C-Raf inhibits B-Raf<sup>V600E</sup> by lowering its kinase activity. These data together with the finding that impaired activity mutant B-Raf induces C-Raf kinase activity suggest that B-Raf activates C-Raf while C-Raf inhibits B-Raf. Thus, in a B-Raf–C-Raf heterodimer, C-Raf might be the MEK-activating component, while B-Raf has functions other than activating MEK. My findings contribute to the understanding of the regulation of MAPK activation by oncogenic B-Raf and could potentially be explored therapeutically by developing drugs that specifically stabilize B-Raf<sup>V600E</sup>–C-Raf heterodimers.

As part of the B-Raf<sup>V600E</sup>–C-Raf interaction study, I discovered a previously uncharacterized alternative murine B-Raf splice variant. Splicing occurs in the regulatory, N-terminal part of B-Raf by utilizing alternative splice donor and acceptor sites within exon 3 and leads to deletion of a Serine-rich peptide (SRP). Intra-exonic splicing is a rare alternative splicing event, which has also been observed for human thrombopoietin and fibronectin genes (Chang et al., 1995; Sasaki et al., 1999; Vibe-Pedersen et al., 1986). Alternative splicing of B-Raf cDNA did not occur, implying that the 99 nucleotides are recognized as an intron only in the presence of constitutive introns, similar to the thrombopoietin gene (Romano et al., 2001). It has been suggested by Romano et al that the assembly of the splicing machinery on constitutive introns is required for intra-exonic splicing to occur. Alternative splicing has been observed for B-Raf exons 10 and 8b, which alters the kinase activity of

the different isoforms (Barnier et al., 1995; Papin et al., 1998). These splice forms locate to the hinge region between conserved regions 2 and 3 (CR2 and CR3) of B-Raf and are therefore likely to modify the conformation of active B-Raf as proposed by Papin et al. Alternative splicing of the N-terminal regulatory region had no effect on kinase activity. Moreover, binding of B-Raf to Ras was not disrupted despite the proximity of the SRP to the Ras binding domain (chapter 5.1). Interestingly, the SRP is phosphorylated in response to H-Ras<sup>G12V</sup> overexpression. Phosphorylation does not affect MAPK signaling or B-Raf–C-Raf heterodimerization, indicating that SRP phosphorylation could be important for MAPK-independent functions. However, phosphorylation could be an artifact of concomitant B-Raf and H-Ras<sup>G12V</sup> overexpression and remains to be further evaluated.

I describe how oncogenic Ras activates C-Raf, thereby promoting association with oncogenic B-Raf. In the case of impaired activity mutant B-Raf this augments activation of MEK. However, Ras-induced association of C-Raf with B-Raf<sup>V600E</sup> antagonizes MAPK signaling. Indeed, oncogenic Ras mutations and B-Raf<sup>V600E</sup> mutations are mutually exclusive in human cancer while Ras and non-B-Raf<sup>V600E</sup> mutations have been reported to co-occur (Thomas et al., 2007). Previously, the exclusivity of Ras and B-Raf<sup>V600E</sup> was attributed to redundant activation of downstream pathways. However, it appears that hyperactivation of the MAPK pathway is antagonized rather than promoted by expression of both oncogenes. Co-operation of oncogenes has been well established and analyzed in numerous contexts; however, to my knowledge this is the first report of oncogene antagonism.

Identification of the pathways employed by oncogenic Ras to induce and maintain a transformed state of a cell is crucial to therapeutically target Ras cancers as targeting Ras itself has been unsuccessful so far. The PI3K and Rac pathways in lung cancer (Gupta et al., 2007; Kissil et al., 2007) and C-Raf–ROK $\alpha$ –myc axis in squamous cell carcinoma (Ehrenreiter et al., 2009) have been shown to be important for Ras-driven tumorigenesis. Lung tumors in PI3K and K-Ras mutant mice regressed upon combination treatment with AKT and MEK inhibitors (Engelman et al., 2008), implicating the MAPK pathway in maintenance of K-Ras mutant lung tumors. Which Raf protein is employed to activate MEK/ERK in K-Ras<sup>G12D</sup> mutant tumors is unknown. Genetic deletion of either B-Raf or C-Raf in K-Ras<sup>G12D</sup> expressing lung epithelial cells extended survival of these animals, indicating that both Raf proteins are important for tumorigenesis. Interestingly, B-Raf and C-Raf appear to serve distinct functions in the context of K-Ras<sup>G12D</sup>. Similar to wildtype cells, B-Raf is the major activator of the MAPK pathway in K-Ras<sup>G12D</sup> mutant cells and controls proliferation. In contrast, C-Raf is dispensable for MAPK activation and control of proliferation but is important for tumor initiation *in vivo* and survival *in vitro*. The mechanisms of these independent functions remain to be further elucidated. Importantly, using this approach B-Raf or C-Raf was deleted at the same time as expression of oncogenic K-Ras was initiated. It therefore needs to be established whether genetic or pharmacological inactivation of B-Raf and/or C-Raf (and A-Raf) in an established tumor inhibits tumorigenesis. In that case Raf inhibitors alone or in combination with drugs targeting other Ras effector pathways could be beneficial to cancer patients.

Hyperactivation of the MAPK pathway by oncogenic Ras or B-Raf and the consequent cell transformation has been firmly established. However, the regulation of these signals is complex and only incompletely understood. For example, MEFs expressing K-Ras<sup>G12D</sup> display increased levels of cyclins, known targets of the MAPK pathway, even though phosphorylation of ERK is attenuated (Tuveson et al., 2004). Recent studies have shed some light on how interactions of Raf proteins with each other or oncogenic Ras affect MAPK signaling and cell transformation. It is becoming increasingly clear that regulation of the MAPK pathway in wildtype and oncogenic contexts is more complex than anticipated. For instance, B-Raf has been determined to be the major activator of the MAPK pathway and is the only Raf protein mutated in cancer due to its mode of activation. C-Raf, on the other hand is very rarely mutated in cancer. The fact that C-Raf is essential for MAPK hyperactivation by impaired activity mutant B-Raf indicates that C-Raf, too, plays pivotal roles in cancer development in some contexts. Furthermore, C-Raf is critical in Ras-driven lung and skin cancer, suggesting that Ras-mediated activation of the MAPK pathway alone is not sufficient to induce and maintain neoplasms. The extensive complexity of the MAPK pathway represents ample opportunities for identifying suitable therapeutic targets. However, hitting these targets may be clinically relevant only in certain scenarios, for instance in cancers harboring an impaired activity B-Raf mutation. Therefore, determining the B-Raf mutation status in tumors to choose the most appropriate therapy will be imperative for personalized cancer treatment.

## **7. References**

- Awatramani, R., Soriano, P., Mai, J.J., and Dymecki, S. (2001). An Flp indicator mouse expressing alkaline phosphatase from the ROSA26 locus. *Nat Genet* *29*, 257-259.
- Barnier, J.V., Papin, C., Eychene, A., Lecoq, O., and Calothy, G. (1995). The mouse B-raf gene encodes multiple protein isoforms with tissue-specific expression. *J Biol Chem* *270*, 23381-23389.
- Beck, T.W., Huleihel, M., Gunnell, M., Bonner, T.I., and Rapp, U.R. (1987). The complete coding sequence of the human A-raf-1 oncogene and transforming activity of a human A-raf carrying retrovirus. *Nucleic Acids Res* *15*, 595-609.
- Bos, J.L. (1989). ras oncogenes in human cancer: a review. *Cancer Res* *49*, 4682-4689.
- Bosenberg, M., Muthusamy, V., Curley, D.P., Wang, Z., Hobbs, C., Nelson, B., Nogueira, C., Horner, J.W., 2nd, Depinho, R., and Chin, L. (2006). Characterization of melanocyte-specific inducible Cre recombinase transgenic mice. *Genesis* *44*, 262-267.
- Braun, R.E., Lo, D., Pinkert, C.A., Widera, G., Flavell, R.A., Palmiter, R.D., and Brinster, R.L. (1990). Infertility in male transgenic mice: disruption of sperm development by HSV-tk expression in postmeiotic germ cells. *Biol Reprod* *43*, 684-693.
- Brose, M.S., Volpe, P., Feldman, M., Kumar, M., Rishi, I., Gerrero, R., Einhorn, E., Herlyn, M., Minna, J., Nicholson, A., *et al.* (2002). BRAF and RAS mutations in human lung cancer and melanoma. *Cancer Res* *62*, 6997-7000.
- Chang, M.S., McNinch, J., Basu, R., Shutter, J., Hsu, R.Y., Perkins, C., Mar, V., Suggs, S., Welcher, A., Li, L., and *et al.* (1995). Cloning and characterization of the human megakaryocyte growth and development factor (MGDF) gene. *J Biol Chem* *270*, 511-514.
- Chen, A.P., Ohno, M., Giese, K.P., Kuhn, R., Chen, R.L., and Silva, A.J. (2006). Forebrain-specific knockout of B-raf kinase leads to deficits in hippocampal long-term potentiation, learning, and memory. *J Neurosci Res* *83*, 28-38.
- Chen, J., Fujii, K., Zhang, L., Roberts, T., and Fu, H. (2001). Raf-1 promotes cell survival by antagonizing apoptosis signal-regulating kinase 1 through a MEK-ERK independent mechanism. *Proc Natl Acad Sci U S A* *98*, 7783-7788.
- Chesa, P.G., Rettig, W.J., Melamed, M.R., Old, L.J., and Niman, H.L. (1987). Expression of p21ras in normal and malignant human tissues: lack of association with proliferation and malignancy. *Proc Natl Acad Sci U S A* *84*, 3234-3238.
- Chin, L., Tam, A., Pomerantz, J., Wong, M., Holash, J., Bardeesy, N., Shen, Q., O'Hagan, R., Pantginis, J., Zhou, H., *et al.* (1999). Essential role for oncogenic Ras in tumour maintenance. *Nature* *400*, 468-472.
- Chong, H., Lee, J., and Guan, K.L. (2001). Positive and negative regulation of Raf kinase activity and function by phosphorylation. *EMBO J* *20*, 3716-3727.
- Dankort, D., Curley, D.P., Cartledge, R.A., Nelson, B., Karnezis, A.N., Damsky, W.E., Jr., You, M.J., DePinho, R.A., McMahon, M., and Bosenberg, M. (2009). Braf(V600E) cooperates with Pten loss to induce metastatic melanoma. *Nat Genet* *41*, 544-552.
- Dankort, D., Filenova, E., Collado, M., Serrano, M., Jones, K., and McMahon, M. (2007). A new mouse model to explore the initiation, progression, and therapy of BRAFV600E-induced lung tumors. *Genes Dev* *21*, 379-384.

Davies, H., Bignell, G.R., Cox, C., Stephens, P., Edkins, S., Clegg, S., Teague, J., Woffendin, H., Garnett, M.J., Bottomley, W., *et al.* (2002). Mutations of the BRAF gene in human cancer. *Nature* *417*, 949-954.

Der, C.J., Krontiris, T.G., and Cooper, G.M. (1982). Transforming genes of human bladder and lung carcinoma cell lines are homologous to the ras genes of Harvey and Kirsten sarcoma viruses. *Proc Natl Acad Sci U S A* *79*, 3637-3640.

Dhillon, A.S., Meikle, S., Yazici, Z., Eulitz, M., and Kolch, W. (2002). Regulation of Raf-1 activation and signalling by dephosphorylation. *EMBO J* *21*, 64-71.

Dhillon, A.S., von Kriegsheim, A., Grindlay, J., and Kolch, W. (2007). Phosphatase and feedback regulation of Raf-1 signaling. *Cell Cycle* *6*, 3-7.

Dhomen, N., Reis-Filho, J.S., da Rocha Dias, S., Hayward, R., Savage, K., Delmas, V., Larue, L., Pritchard, C., and Marais, R. (2009). Oncogenic Braf induces melanocyte senescence and melanoma in mice. *Cancer Cell* *15*, 294-303.

Dong, C., Waters, S.B., Holt, K.H., and Pessin, J.E. (1996). SOS phosphorylation and disassociation of the Grb2-SOS complex by the ERK and JNK signaling pathways. *J Biol Chem* *271*, 6328-6332.

Dougherty, M.K., Muller, J., Ritt, D.A., Zhou, M., Zhou, X.Z., Copeland, T.D., Conrads, T.P., Veenstra, T.D., Lu, K.P., and Morrison, D.K. (2005). Regulation of Raf-1 by direct feedback phosphorylation. *Mol Cell* *17*, 215-224.

Douville, E., and Downward, J. (1997). EGF induced SOS phosphorylation in PC12 cells involves P90 RSK-2. *Oncogene* *15*, 373-383.

Downward, J. (2003). Targeting RAS signalling pathways in cancer therapy. *Nat Rev Cancer* *3*, 11-22.

Dumaz, N., Hayward, R., Martin, J., Ogilvie, L., Hedley, D., Curtin, J.A., Bastian, B.C., Springer, C., and Marais, R. (2006). In melanoma, RAS mutations are accompanied by switching signaling from BRAF to CRAF and disrupted cyclic AMP signaling. *Cancer Res* *66*, 9483-9491.

DuPage, M., Dooley, A.L., and Jacks, T. (2009). Conditional mouse lung cancer models using adenoviral or lentiviral delivery of Cre recombinase. *Nat Protoc* *4*, 1064-1072.

Ehrenreiter, K., Kern, F., Velamoor, V., Meissl, K., Galabova-Kovacs, G., Sibilias, M., and Baccarini, M. (2009). Raf-1 addiction in Ras-induced skin carcinogenesis. *Cancer Cell* *16*, 149-160.

Ehrenreiter, K., Piazzolla, D., Velamoor, V., Sobczak, I., Small, J.V., Takeda, J., Leung, T., and Baccarini, M. (2005). Raf-1 regulates Rho signaling and cell migration. *J Cell Biol* *168*, 955-964.

Eisen, T., Ahmad, T., Flaherty, K.T., Gore, M., Kaye, S., Marais, R., Gibbens, I., Hackett, S., James, M., Schuchter, L.M., *et al.* (2006). Sorafenib in advanced melanoma: a Phase II randomised discontinuation trial analysis. *Br J Cancer* *95*, 581-586.

Ellis, R.W., Defeo, D., Shih, T.Y., Gonda, M.A., Young, H.A., Tsuchida, N., Lowy, D.R., and Scolnick, E.M. (1981). The p21 src genes of Harvey and Kirsten sarcoma viruses originate from divergent members of a family of normal vertebrate genes. *Nature* *292*, 506-511.

Emuss, V., Garnett, M., Mason, C., and Marais, R. (2005). Mutations of C-RAF are rare in human cancer because C-RAF has a low basal kinase activity compared with B-RAF. *Cancer Res* *65*, 9719-9726.

Engelman, J.A., Chen, L., Tan, X., Crosby, K., Guimaraes, A.R., Upadhyay, R., Maira, M., McNamara, K., Perera, S.A., Song, Y., *et al.* (2008). Effective use of PI3K

and MEK inhibitors to treat mutant Kras G12D and PIK3CA H1047R murine lung cancers. *Nat Med* *14*, 1351-1356.

Esteban, L.M., Vicario-Abejon, C., Fernandez-Salguero, P., Fernandez-Medarde, A., Swaminathan, N., Yienger, K., Lopez, E., Malumbres, M., McKay, R., Ward, J.M., *et al.* (2001). Targeted genomic disruption of H-ras and N-ras, individually or in combination, reveals the dispensability of both loci for mouse growth and development. *Mol Cell Biol* *21*, 1444-1452.

Farrar, M.A., Alberol, I., and Perlmutter, R.M. (1996). Activation of the Raf-1 kinase cascade by coumermycin-induced dimerization. *Nature* *383*, 178-181.

Fisher, G.H., Wellen, S.L., Klimstra, D., Lenczowski, J.M., Tichelaar, J.W., Lizak, M.J., Whitsett, J.A., Koretsky, A., and Varmus, H.E. (2001). Induction and apoptotic regression of lung adenocarcinomas by regulation of a K-Ras transgene in the presence and absence of tumor suppressor genes. *Genes Dev* *15*, 3249-3262.

Furth, M.E., Aldrich, T.H., and Cordon-Cardo, C. (1987). Expression of ras proto-oncogene proteins in normal human tissues. *Oncogene* *1*, 47-58.

Galabova-Kovacs, G., Catalanotti, F., Matzen, D., Reyes, G.X., Zezula, J., Herbst, R., Silva, A., Walter, I., and Baccharini, M. (2008). Essential role of B-Raf in oligodendrocyte maturation and myelination during postnatal central nervous system development. *J Cell Biol* *180*, 947-955.

Galabova-Kovacs, G., Matzen, D., Piazzolla, D., Meissl, K., Plyushch, T., Chen, A.P., Silva, A., and Baccharini, M. (2006). Essential role of B-Raf in ERK activation during extraembryonic development. *Proc Natl Acad Sci U S A* *103*, 1325-1330.

Garnett, M.J., Rana, S., Paterson, H., Barford, D., and Marais, R. (2005). Wild-type and mutant B-RAF activate C-RAF through distinct mechanisms involving heterodimerization. *Mol Cell* *20*, 963-969.

Gupta, S., Ramjaun, A.R., Haiko, P., Wang, Y., Warne, P.H., Nicke, B., Nye, E., Stamp, G., Alitalo, K., and Downward, J. (2007). Binding of ras to phosphoinositide 3-kinase p110alpha is required for ras-driven tumorigenesis in mice. *Cell* *129*, 957-968.

Hall, A., Marshall, C.J., Spurr, N.K., and Weiss, R.A. (1983). Identification of transforming gene in two human sarcoma cell lines as a new member of the ras gene family located on chromosome 1. *Nature* *303*, 396-400.

Hancock, J.F. (2003). Ras proteins: different signals from different locations. *Nat Rev Mol Cell Biol* *4*, 373-384.

Harvey, J.J. (1964). An Unidentified Virus Which Causes the Rapid Production of Tumours in Mice. *Nature* *204*, 1104-1105.

Heidecker, G., Huleihel, M., Cleveland, J.L., Kolch, W., Beck, T.W., Lloyd, P., Pawson, T., and Rapp, U.R. (1990). Mutational activation of c-raf-1 and definition of the minimal transforming sequence. *Mol Cell Biol* *10*, 2503-2512.

Hingorani, S.R., Jacobetz, M.A., Robertson, G.P., Herlyn, M., and Tuveson, D.A. (2003). Suppression of BRAF(V599E) in human melanoma abrogates transformation. *Cancer Res* *63*, 5198-5202.

Huebner, K., ar-Rushdi, A., Griffin, C.A., Isobe, M., Kozak, C., Emanuel, B.S., Nagarajan, L., Cleveland, J.L., Bonner, T.I., Goldsborough, M.D., and *et al.* (1986). Actively transcribed genes in the raf oncogene group, located on the X chromosome in mouse and human. *Proc Natl Acad Sci U S A* *83*, 3934-3938.

Huleihel, M., Goldsborough, M., Cleveland, J., Gunnell, M., Bonner, T., and Rapp, U.R. (1986). Characterization of murine A-raf, a new oncogene related to the v-raf oncogene. *Mol Cell Biol* *6*, 2655-2662.



Hunter, N.L., Awatramani, R.B., Farley, F.W., and Dymecki, S.M. (2005). Ligand-activated Flpe for temporally regulated gene modifications. *Genesis* *41*, 99-109.

Huser, M., Luckett, J., Chiloeches, A., Mercer, K., Iwobi, M., Giblett, S., Sun, X.M., Brown, J., Marais, R., and Pritchard, C. (2001). MEK kinase activity is not necessary for Raf-1 function. *EMBO J* *20*, 1940-1951.

Ikawa, S., Fukui, M., Ueyama, Y., Tamaoki, N., Yamamoto, T., and Toyoshima, K. (1988). B-raf, a new member of the raf family, is activated by DNA rearrangement. *Mol Cell Biol* *8*, 2651-2654.

Ise, K., Nakamura, K., Nakao, K., Shimizu, S., Harada, H., Ichise, T., Miyoshi, J., Gondo, Y., Ishikawa, T., Aiba, A., and Katsuki, M. (2000). Targeted deletion of the H-ras gene decreases tumor formation in mouse skin carcinogenesis. *Oncogene* *19*, 2951-2956.

Jackson, E.L., Olive, K.P., Tuveson, D.A., Bronson, R., Crowley, D., Brown, M., and Jacks, T. (2005). The differential effects of mutant p53 alleles on advanced murine lung cancer. *Cancer Res* *65*, 10280-10288.

Jackson, E.L., Willis, N., Mercer, K., Bronson, R.T., Crowley, D., Montoya, R., Jacks, T., and Tuveson, D.A. (2001). Analysis of lung tumor initiation and progression using conditional expression of oncogenic K-ras. *Genes Dev* *15*, 3243-3248.

Jain, M., Arvanitis, C., Chu, K., Dewey, W., Leonhardt, E., Trinh, M., Sundberg, C.D., Bishop, J.M., and Felsher, D.W. (2002). Sustained loss of a neoplastic phenotype by brief inactivation of MYC. *Science* *297*, 102-104.

Jansen, H.W., Lurz, R., Bister, K., Bonner, T.I., Mark, G.E., and Rapp, U.R. (1984). Homologous cell-derived oncogenes in avian carcinoma virus MH2 and murine sarcoma virus 3611. *Nature* *307*, 281-284.

Jansen, H.W., Patschinsky, T., and Bister, K. (1983a). Avian oncovirus MH2: molecular cloning of proviral DNA and structural analysis of viral RNA and protein. *J Virol* *48*, 61-73.

Jansen, H.W., Ruckert, B., Lurz, R., and Bister, K. (1983b). Two unrelated cell-derived sequences in the genome of avian leukemia and carcinoma inducing retrovirus MH2. *EMBO J* *2*, 1969-1975.

Johnson, L., Greenbaum, D., Cichowski, K., Mercer, K., Murphy, E., Schmitt, E., Bronson, R.T., Umanoff, H., Edelman, W., Kucherlapati, R., and Jacks, T. (1997). K-ras is an essential gene in the mouse with partial functional overlap with N-ras. *Genes Dev* *11*, 2468-2481.

Karbowiczek, M., Cash, T., Cheung, M., Robertson, G.P., Astrinidis, A., and Henske, E.P. (2004). Regulation of B-Raf kinase activity by tuberin and Rheb is mammalian target of rapamycin (mTOR)-independent. *J Biol Chem* *279*, 29930-29937.

Karbowiczek, M., Robertson, G.P., and Henske, E.P. (2006). Rheb inhibits C-raf activity and B-raf/C-raf heterodimerization. *J Biol Chem* *281*, 25447-25456.

Karreth, F.A., and Tuveson, D.A. (2009). Modelling oncogenic Ras/Raf signalling in the mouse. *Curr Opin Genet Dev* *19*, 4-11.

Kerkhoff, E., Fedorov, L.M., Siefken, R., Walter, A.O., Papadopoulos, T., and Rapp, U.R. (2000). Lung-targeted expression of the c-Raf-1 kinase in transgenic mice exposes a novel oncogenic character of the wild-type protein. *Cell Growth Differ* *11*, 185-190.

Kim, H.J., and Bar-Sagi, D. (2004). Modulation of signalling by Sprouty: a developing story. *Nat Rev Mol Cell Biol* *5*, 441-450.

Kirsten, W.H., and Mayer, L.A. (1967). Morphologic responses to a murine erythroblastosis virus. *J Natl Cancer Inst* 39, 311-335.

Kissil, J.L., Walmsley, M.J., Hanlon, L., Haigis, K.M., Bender Kim, C.F., Sweet-Cordero, A., Eckman, M.S., Tuveson, D.A., Capobianco, A.J., Tybulewicz, V.L., and Jacks, T. (2007). Requirement for Rac1 in a K-ras induced lung cancer in the mouse. *Cancer Res* 67, 8089-8094.

Koera, K., Nakamura, K., Nakao, K., Miyoshi, J., Toyoshima, K., Hatta, T., Otani, H., Aiba, A., and Katsuki, M. (1997). K-ras is essential for the development of the mouse embryo. *Oncogene* 15, 1151-1159.

Kolbus, A., Pilat, S., Husak, Z., Deiner, E.M., Stengl, G., Beug, H., and Baccarini, M. (2002). Raf-1 antagonizes erythroid differentiation by restraining caspase activation. *J Exp Med* 196, 1347-1353.

Kolch, W. (2005). Coordinating ERK/MAPK signalling through scaffolds and inhibitors. *Nat Rev Mol Cell Biol* 6, 827-837.

Konstantinopoulos, P.A., Karamouzis, M.V., and Papavassiliou, A.G. (2007). Post-translational modifications and regulation of the RAS superfamily of GTPases as anticancer targets. *Nat Rev Drug Discov* 6, 541-555.

Kuilman, T., Michaloglou, C., Vredeveld, L.C., Douma, S., van Doorn, R., Desmet, C.J., Aarden, L.A., Mooi, W.J., and Peeper, D.S. (2008). Oncogene-induced senescence relayed by an interleukin-dependent inflammatory network. *Cell* 133, 1019-1031.

Lee, J.W., Soung, Y.H., Kim, S.Y., Park, W.S., Nam, S.W., Min, W.S., Kim, S.H., Lee, J.Y., Yoo, N.J., and Lee, S.H. (2005). Mutational analysis of the ARAF gene in human cancers. *APMIS* 113, 54-57.

Leon, J., Guerrero, I., and Pellicer, A. (1987). Differential expression of the ras gene family in mice. *Mol Cell Biol* 7, 1535-1540.

Lim, K.H., Baines, A.T., Fiordalisi, J.J., Shipitsin, M., Feig, L.A., Cox, A.D., Der, C.J., and Counter, C.M. (2005). Activation of RalA is critical for Ras-induced tumorigenesis of human cells. *Cancer Cell* 7, 533-545.

Luo, Z., Tzivion, G., Belshaw, P.J., Vavvas, D., Marshall, M., and Avruch, J. (1996). Oligomerization activates c-Raf-1 through a Ras-dependent mechanism. *Nature* 383, 181-185.

Mason, C.S., Springer, C.J., Cooper, R.G., Superti-Furga, G., Marshall, C.J., and Marais, R. (1999). Serine and tyrosine phosphorylations cooperate in Raf-1, but not B-Raf activation. *EMBO J* 18, 2137-2148.

Mercer, K., Chiloiches, A., Huser, M., Kiernan, M., Marais, R., and Pritchard, C. (2002). ERK signalling and oncogene transformation are not impaired in cells lacking A-Raf. *Oncogene* 21, 347-355.

Mercer, K., Giblett, S., Green, S., Lloyd, D., DaRocha Dias, S., Plumb, M., Marais, R., and Pritchard, C. (2005). Expression of endogenous oncogenic V600EB-raf induces proliferation and developmental defects in mice and transformation of primary fibroblasts. *Cancer Res* 65, 11493-11500.

Mercer, K.E., and Pritchard, C.A. (2003). Raf proteins and cancer: B-Raf is identified as a mutational target. *Biochim Biophys Acta* 1653, 25-40.

Mikula, M., Schreiber, M., Husak, Z., Kucerova, L., Ruth, J., Wieser, R., Zatloukal, K., Beug, H., Wagner, E.F., and Baccarini, M. (2001). Embryonic lethality and fetal liver apoptosis in mice lacking the c-raf-1 gene. *Embo J* 20, 1952-1962.

Murphy, D.J., Junttila, M.R., Pouyet, L., Karnezis, A., Shchors, K., Bui, D.A., Brown-Swigart, L., Johnson, L., and Evan, G.I. (2008). Distinct thresholds govern Myc's biological output in vivo. *Cancer Cell* 14, 447-457.

O'Neill, E., Rushworth, L., Baccharini, M., and Kolch, W. (2004). Role of the kinase MST2 in suppression of apoptosis by the proto-oncogene product Raf-1. *Science* 306, 2267-2270.

Okada, T., Hu, C.D., Jin, T.G., Kariya, K., Yamawaki-Kataoka, Y., and Kataoka, T. (1999). The strength of interaction at the Raf cysteine-rich domain is a critical determinant of response of Raf to Ras family small GTPases. *Mol Cell Biol* 19, 6057-6064.

Papin, C., Denouel-Galy, A., Laugier, D., Calothy, G., and Eychene, A. (1998). Modulation of kinase activity and oncogenic properties by alternative splicing reveals a novel regulatory mechanism for B-Raf. *J Biol Chem* 273, 24939-24947.

Parada, L.F., Tabin, C.J., Shih, C., and Weinberg, R.A. (1982). Human EJ bladder carcinoma oncogene is homologue of Harvey sarcoma virus ras gene. *Nature* 297, 474-478.

Pavey, S., Johansson, P., Packer, L., Taylor, J., Stark, M., Pollock, P.M., Walker, G.J., Boyle, G.M., Harper, U., Cozzi, S.J., *et al.* (2004). Microarray expression profiling in melanoma reveals a BRAF mutation signature. *Oncogene* 23, 4060-4067.

Pelengaris, S., Khan, M., and Evan, G.I. (2002). Suppression of Myc-induced apoptosis in beta cells exposes multiple oncogenic properties of Myc and triggers carcinogenic progression. *Cell* 109, 321-334.

Perez de Castro, I., Diaz, R., Malumbres, M., Hernandez, M.I., Jagirdar, J., Jimenez, M., Ahn, D., and Pellicer, A. (2003). Mice deficient for N-ras: impaired antiviral immune response and T-cell function. *Cancer Res* 63, 1615-1622.

Peters, R.L., Rabstein, L.S., VanVleck, R., Kelloff, G.J., and Huebner, R.J. (1974). Naturally occurring sarcoma virus of the BALB/cCr mouse. *J Natl Cancer Inst* 53, 1725-1729.

Piazzolla, D., Meissl, K., Kucerova, L., Rubiolo, C., and Baccharini, M. (2005). Raf-1 sets the threshold of Fas sensitivity by modulating Rok-alpha signaling. *J Cell Biol* 171, 1013-1022.

Plowman, S.J., Williamson, D.J., O'Sullivan, M.J., Doig, J., Ritchie, A.M., Harrison, D.J., Melton, D.W., Arends, M.J., Hooper, M.L., and Patek, C.E. (2003). While K-ras is essential for mouse development, expression of the K-ras 4A splice variant is dispensable. *Mol Cell Biol* 23, 9245-9250.

Pollock, P.M., Harper, U.L., Hansen, K.S., Yudt, L.M., Stark, M., Robbins, C.M., Moses, T.Y., Hostetter, G., Wagner, U., Kakareka, J., *et al.* (2003). High frequency of BRAF mutations in nevi. *Nat Genet* 33, 19-20.

Pollock, P.M., and Meltzer, P.S. (2002). A genome-based strategy uncovers frequent BRAF mutations in melanoma. *Cancer Cell* 2, 5-7.

Pritchard, C.A., Bolin, L., Slattery, R., Murray, R., and McMahon, M. (1996). Post-natal lethality and neurological and gastrointestinal defects in mice with targeted disruption of the A-Raf protein kinase gene. *Curr Biol* 6, 614-617.

Rapp, U.R., Goldsborough, M.D., Mark, G.E., Bonner, T.I., Groffen, J., Reynolds, F.H., Jr., and Stephenson, J.R. (1983). Structure and biological activity of v-raf, a unique oncogene transduced by a retrovirus. *Proc Natl Acad Sci U S A* 80, 4218-4222.

Rasband, W.S. (1997-2008). ImageJ. (U. S. National Institutes of Health, Bethesda, Maryland, USA).

Rasheed, S., Gardner, M.B., and Huebner, R.J. (1978). In vitro isolation of stable rat sarcoma viruses. *Proc Natl Acad Sci U S A* 75, 2972-2976.

Reddy, E.P., Reynolds, R.K., Santos, E., and Barbacid, M. (1982). A point mutation is responsible for the acquisition of transforming properties by the T24 human bladder carcinoma oncogene. *Nature* 300, 149-152.

Robinson, M.J., and Cobb, M.H. (1997). Mitogen-activated protein kinase pathways. *Curr Opin Cell Biol* 9, 180-186.

Romano, M., Marcucci, R., and Baralle, F.E. (2001). Splicing of constitutive upstream introns is essential for the recognition of intra-exonic suboptimal splice sites in the thrombopoietin gene. *Nucleic Acids Res* 29, 886-894.

Rubiolo, C., Piazzolla, D., Meissl, K., Beug, H., Huber, J.C., Kolbus, A., and Baccarini, M. (2006). A balance between Raf-1 and Fas expression sets the pace of erythroid differentiation. *Blood* 108, 152-159.

Rushworth, L.K., Hindley, A.D., O'Neill, E., and Kolch, W. (2006). Regulation and role of Raf-1/B-Raf heterodimerization. *Mol Cell Biol* 26, 2262-2272.

Santos, E., Tronick, S.R., Aaronson, S.A., Pulciani, S., and Barbacid, M. (1982). T24 human bladder carcinoma oncogene is an activated form of the normal human homologue of BALB- and Harvey-MSV transforming genes. *Nature* 298, 343-347.

Sarkisian, C.J., Keister, B.A., Stairs, D.B., Boxer, R.B., Moody, S.E., and Chodosh, L.A. (2007). Dose-dependent oncogene-induced senescence in vivo and its evasion during mammary tumorigenesis. *Nat Cell Biol* 9, 493-505.

Sasaki, Y., Takahashi, T., Miyazaki, H., Matsumoto, A., Kato, T., Nakamura, K., Iho, S., Okuno, Y., and Nakao, K. (1999). Production of thrombopoietin by human carcinomas and its novel isoforms. *Blood* 94, 1952-1960.

Scholl, C., Frohling, S., Dunn, I.F., Schinzel, A.C., Barbie, D.A., Kim, S.Y., Silver, S.J., Tamayo, P., Wadlow, R.C., Ramaswamy, S., *et al.* (2009). Synthetic lethal interaction between oncogenic KRAS dependency and STK33 suppression in human cancer cells. *Cell* 137, 821-834.

Serrano, M., Lin, A.W., McCurrach, M.E., Beach, D., and Lowe, S.W. (1997). Oncogenic ras provokes premature cell senescence associated with accumulation of p53 and p16INK4a. *Cell* 88, 593-602.

Shaw, A.T., Meissner, A., Dowdle, J.A., Crowley, D., Magendantz, M., Ouyang, C., Parisi, T., Rajagopal, J., Blank, L.J., Bronson, R.T., *et al.* (2007). Sprouty-2 regulates oncogenic K-ras in lung development and tumorigenesis. *Genes Dev* 21, 694-707.

Shih, C., and Weinberg, R.A. (1982). Isolation of a transforming sequence from a human bladder carcinoma cell line. *Cell* 29, 161-169.

Shinkai, M., Masuda, T., Kariya, K., Tamada, M., Shirouzu, M., Yokoyama, S., and Kataoka, T. (1996). Difference in the mechanism of interaction of Raf-1 and B-Raf with H-Ras. *Biochem Biophys Res Commun* 223, 729-734.

Sithanandam, G., Kolch, W., Duh, F.M., and Rapp, U.R. (1990). Complete coding sequence of a human B-raf cDNA and detection of B-raf protein kinase with isozyme specific antibodies. *Oncogene* 5, 1775-1780.

Sobczak, I., Galabova-Kovacs, G., Sadzak, I., Kren, A., Christofori, G., and Baccarini, M. (2008). B-Raf is required for ERK activation and tumor progression in a mouse model of pancreatic beta-cell carcinogenesis. *Oncogene* 27, 4779-4787.

Stanton, V.P., Jr., Nichols, D.W., Laudano, A.P., and Cooper, G.M. (1989). Definition of the human raf amino-terminal regulatory region by deletion mutagenesis. *Mol Cell Biol* 9, 639-647.

Sutrave, P., Bonner, T.I., Rapp, U.R., Jansen, H.W., Patschinsky, T., and Bister, K. (1984). Nucleotide sequence of avian retroviral oncogene v-mil: homologue of murine retroviral oncogene v-raf. *Nature* 309, 85-88.

Thomas, R.K., Baker, A.C., Debiasi, R.M., Winckler, W., Laframboise, T., Lin, W.M., Wang, M., Feng, W., Zander, T., MacConaill, L., *et al.* (2007). High-throughput oncogene mutation profiling in human cancer. *Nat Genet* 39, 347-351.

To, M.D., Wong, C.E., Karnezis, A.N., Del Rosario, R., Di Lauro, R., and Balmain, A. (2008). Kras regulatory elements and exon 4A determine mutation specificity in lung cancer. *Nat Genet* 40, 1240-1244.

Tucker, K.L., Wang, Y., Dausman, J., and Jaenisch, R. (1997). A transgenic mouse strain expressing four drug-selectable marker genes. *Nucleic Acids Res* 25, 3745-3746.

Tuveson, D.A., Shaw, A.T., Willis, N.A., Silver, D.P., Jackson, E.L., Chang, S., Mercer, K.L., Grochow, R., Hock, H., Crowley, D., *et al.* (2004). Endogenous oncogenic K-ras(G12D) stimulates proliferation and widespread neoplastic and developmental defects. *Cancer Cell* 5, 375-387.

Umanoff, H., Edelmann, W., Pellicer, A., and Kucherlapati, R. (1995). The murine N-ras gene is not essential for growth and development. *Proc Natl Acad Sci U S A* 92, 1709-1713.

Vibe-Pedersen, K., Magnusson, S., and Baralle, F.E. (1986). Donor and acceptor splice signals within an exon of the human fibronectin gene: a new type of differential splicing. *FEBS Lett* 207, 287-291.

Voice, J.K., Klemke, R.L., Le, A., and Jackson, J.H. (1999). Four human ras homologs differ in their abilities to activate Raf-1, induce transformation, and stimulate cell motility. *J Biol Chem* 274, 17164-17170.

Wan, P.T., Garnett, M.J., Roe, S.M., Lee, S., Niculescu-Duvaz, D., Good, V.M., Jones, C.M., Marshall, C.J., Springer, C.J., Barford, D., and Marais, R. (2004). Mechanism of activation of the RAF-ERK signaling pathway by oncogenic mutations of B-RAF. *Cell* 116, 855-867.

Wang, H.G., Rapp, U.R., and Reed, J.C. (1996). Bcl-2 targets the protein kinase Raf-1 to mitochondria. *Cell* 87, 629-638.

Waters, S.B., Holt, K.H., Ross, S.E., Syu, L.J., Guan, K.L., Saltiel, A.R., Koretzky, G.A., and Pessin, J.E. (1995). Desensitization of Ras activation by a feedback disassociation of the SOS-Grb2 complex. *J Biol Chem* 270, 20883-20886.

Weber, C.K., Slupsky, J.R., Herrmann, C., Schuler, M., Rapp, U.R., and Block, C. (2000). Mitogenic signaling of Ras is regulated by differential interaction with Raf isozymes. *Oncogene* 19, 169-176.

Weber, C.K., Slupsky, J.R., Kalmes, H.A., and Rapp, U.R. (2001). Active Ras induces heterodimerization of cRaf and BRaf. *Cancer Res* 61, 3595-3598.

Wellbrock, C., Karasarides, M., and Marais, R. (2004a). The RAF proteins take centre stage. *Nat Rev Mol Cell Biol* 5, 875-885.

Wellbrock, C., Ogilvie, L., Hedley, D., Karasarides, M., Martin, J., Niculescu-Duvaz, D., Springer, C.J., and Marais, R. (2004b). V599EB-RAF is an oncogene in melanocytes. *Cancer Res* 64, 2338-2342.

Wilhelm, S.M., Carter, C., Tang, L., Wilkie, D., McNabola, A., Rong, H., Chen, C., Zhang, X., Vincent, P., McHugh, M., *et al.* (2004). BAY 43-9006 exhibits broad spectrum oral antitumor activity and targets the RAF/MEK/ERK pathway and receptor tyrosine kinases involved in tumor progression and angiogenesis. *Cancer Res* 64, 7099-7109.

Wojnowski, L., Zimmer, A.M., Beck, T.W., Hahn, H., Bernal, R., Rapp, U.R., and Zimmer, A. (1997). Endothelial apoptosis in Braf-deficient mice. *Nat Genet* 16, 293-297.

- Yamaguchi, O., Watanabe, T., Nishida, K., Kashiwase, K., Higuchi, Y., Takeda, T., Hikoso, S., Hirotsu, S., Asahi, M., Taniike, M., *et al.* (2004). Cardiac-specific disruption of the c-raf-1 gene induces cardiac dysfunction and apoptosis. *J Clin Invest* *114*, 937-943.
- Zebisch, A., Staber, P.B., Delavar, A., Bodner, C., Hiden, K., Fischereder, K., Janakiraman, M., Linkesch, W., Auner, H.W., Emberger, W., *et al.* (2006). Two transforming C-RAF germ-line mutations identified in patients with therapy-related acute myeloid leukemia. *Cancer Res* *66*, 3401-3408.
- Zhang, B.H., and Guan, K.L. (2000). Activation of B-Raf kinase requires phosphorylation of the conserved residues Thr598 and Ser601. *EMBO J* *19*, 5429-5439.
- Zhang, Z., Wang, Y., Vikis, H.G., Johnson, L., Liu, G., Li, J., Anderson, M.W., Sills, R.C., Hong, H.L., Devereux, T.R., *et al.* (2001). Wildtype Kras2 can inhibit lung carcinogenesis in mice. *Nat Genet* *29*, 25-33.
- Zhong, J., Li, X., McNamee, C., Chen, A.P., Baccharini, M., and Snider, W.D. (2007). Raf kinase signaling functions in sensory neuron differentiation and axon growth in vivo. *Nat Neurosci* *10*, 598-607.

## **8. List of Figures**

### Introduction

3.1 The Ras/Raf/MEK/ERK signaling pathway.....	9
3.2 Post-translational modification of Ras.....	11
3.3 Schematic outline of Raf proteins.....	16

### 5.1 C-Raf inhibits MAPK activation and transformation by B-Raf<sup>V600E</sup>

Karreth et al., Figure 1.....	85
Karreth et al., Figure 2.....	86
Karreth et al., Figure 3.....	87
Karreth et al., Figure 4.....	88
Karreth et al., Figure 5.....	89
Karreth et al., Figure 6.....	90
Karreth et al., Suppl. Figure 1.....	91
Karreth et al., Suppl. Figure 2.....	92
Karreth et al., Suppl. Figure 3.....	93
Karreth et al., Suppl. Figure 4.....	94
Karreth et al., Suppl. Figure 5.....	95
Karreth et al., Suppl. Figure 6.....	96
Karreth et al., Suppl. Figure 7.....	97
5.1.1 Phosphorylation of SRP.....	99

### 5.2 Generation of an inducible and reversible oncogenic B-Raf mutant mouse model

5.2.1 Conditional and reversible activation of oncogenic B-Raf.....	105
---	-----

5.2.2 Schematic outline of the B-Raf <sup>V619E</sup> allele.....	107
5.2.3 The LoxP-STOP-LoxP cassette.....	107
5.2.4 Targeting of the LSL cassette.....	109
5.2.5 Targeting of the V619E mutation.....	112
5.2.6 Characterization of LSL-B-Raf <sup>V619E</sup> MEFs and mice.....	115
5.2.7 Targeting of the LSL-FlpERT2 allele.....	118
5.2.8 FlpERT2 activity <i>in vitro</i> .....	119
<u>5.3 The role of B-Raf and C-Raf in K-Ras<sup>G12D</sup>-induced lung tumorigenesis</u>	
5.3.1 Lung tumor burden.....	123
5.3.2 Number of neoplasms.....	124
5.3.3 Survival curves.....	125
5.3.4 pERK staining in lung neoplasms of K-Ras <sup>G12D</sup> mice.....	126
5.3.5 Proliferation of early grade neoplasms.....	127
5.3.6 Proliferation of MEFs in 10% and 2% serum.....	129
5.3.7 Western blot analysis in 10% and 2% serum.....	130
5.3.8 Anti-apoptotic effect of K-Ras <sup>G12D</sup> requires C-Raf.....	131
5.3.9 Apoptosis <i>in vivo</i> .....	131



## **9. Curriculum vitae**

### **Personal Data**

Name: Florian Alexander Karreth  
Degree: Master of Science (Magister rerum naturalium)  
Nationality: German  
Date of Birth: June 15<sup>th</sup> 1979  
Place of Birth: Gross-Gerau, Germany

Work Address: Cambridge Research Institute  
Cancer Research UK  
Robinson Way  
Cambridge CB2 0RE, UK

Home Address: 28 Ventress Farm Court  
Cambridge CB1 8HD  
United Kingdom

### **Education**

1986-1998 Schools in Germany and Austria  
1998-2001 Studies of Biology, University of Vienna, Vienna, Austria  
2001-2004 Studies of Genetics, University of Vienna, Vienna, Austria  
Graduation (M.S.) Jan. 2004  
2004-2006 PhD Thesis in Cancer Biology, University of Vienna, Vienna, Austria. Conducted at AFCRI, University of Pennsylvania, PA, USA  
Since 2006 PhD Thesis in Cancer Biology, University of Vienna, Vienna, Austria. Conducted at CRI, Cancer Research UK, Cambridge, UK

### **Training and Work Experience**

2001-2002 Scientific Assistant, School of Dentistry, Department of Oral Surgery, University of Vienna, Vienna, Austria, "The effect of platelets on bone cells"  
2002-2004 Diploma Thesis, Group of Erwin F. Wagner, Research Institute of Molecular Pathology (IMP), Vienna, Austria, "The role of the Fos protein Fra-2 in skeletal development"

since 2004 PhD Thesis, Group of David A. Tuveson, Abramson Family Cancer Research Institute, University of Pennsylvania, Philadelphia, USA and Cancer Research Institute, Cancer Research UK, Cambridge, UK, “Modulation of oncogenic transformation by Raf proteins”

### **Honors and Awards**

Nov. 2004 – Mar. 2007 Boehringer Ingelheim Fonds BIF PhD scholar

### **Teaching Responsibilities**

Jun. – Aug. 2004 Supervision of Undergraduate Student SueAnn Kim (Wellesley College)

Jun. – Aug. 2005 Supervision of Undergraduate Student Stephen Winter (University of Michigan)

May – Aug. 2006 Supervision of Undergraduate Student Stephen Winter (University of Michigan)

### **Poster and Oral Presentations**

1. **Karreth F**, Hoebertz A, Eferl R, Wagner EF. *Skeletal development: FRAMing an answer*. 2<sup>nd</sup> Wittgenstein conference: “Bone and Cartilage in Health and Disease”, Vienna, Austria, 2003. (poster)
2. **Karreth F**, Jacobetz M, Tuveson DA. *Modeling melanoma in mice by expression of endogenous oncogenic B-Raf alleles*. 70<sup>th</sup> Cold Spring Harbor Symposium: “Molecular Approaches to Controlling Cancer”, Cold Spring Harbor, NY, USA, 2005. (poster)
3. **Karreth F**, Tuveson DA. *Identification and characterization of a novel B-Raf splice variant*. International PhD student conference, CRI, Cambridge, UK, 2007. (poster)
4. **Karreth F**. *Regulation of MAPK signaling by Raf dimerization*. International PhD student conference, NKI, Amsterdam, the Netherlands, 2008. (oral presentation)
5. **Karreth F**, Tuveson DA. *Regulation of MAP kinase signaling by alternative splicing of B-Raf uncovers a suppressive role for C-Raf in tumorigenesis*. Cold Spring Harbor Conference: “Mechanisms & Models of Cancer”, Cold Spring Harbor, NY, USA, 2008. (poster)

6. **Karreth FA**, Perez-Mancera PA, Tuveson DA. *Sleeping Beauty screens in melanoma*. Wellcome Trust Sanger Institute "Genetic Screens in Mouse Cancer Models", Hinxton, UK, 2009. (poster)
7. **Karreth FA**, Tuveson DA. *Differential roles of C-Raf in transformation depend on the oncogenic context*. Wellcome Trust Sanger Institute "Models and Mechanisms of Cancer", Hinxton, UK, 2009. (poster)
8. **Karreth FA**. *C-Raf Differentially Modulates Transformation by B-RafV600E and K-RasG12D*. Salk Institute Conference: "Mechanisms & Models of Cancer", La Jolla, CA, USA, 2009. (oral presentation)

### **Publications**

1. Gruber R, **Karreth F**, Fischer MB, Watzek G. *Platelet-released supernatants stimulate formation of osteoclast-like cells through a prostaglandin/RANKL-dependent mechanism*. Bone. 2002 May;30(5):726-32.
2. Gruber R, Schofnagl M, **Karreth F**, Fischer MB, Watzek G. *The stable analog carbocyclic TXA2 but not platelet-released TXA2 induces osteoclast-like cell formation*. Prostaglandins Leukot Essent Fatty Acids. 2003 Apr;68(4):267-72.
3. Gruber R, **Karreth F**, Frommlet F, Fischer MB, Watzek G. *Platelets are mitogenic for periosteum-derived cells*. J Orthop Res. 2003 Sep;21(5):941-8.
4. Kenner L, Hoebertz A, Beil T, Keon N, **Karreth F**, Eferl R, Scheuch H, Szremska A, Amling M, Schorpp-Kistner M, Angel P, Wagner EF. *Mice lacking JunB are osteopenic due to cell-autonomous osteoblast and osteoclast defects*. J Cell Biol. 2004 Feb 16;164(4):613-23.
5. Gruber R, **Karreth F**, Kandler B, Fuerst G, Rot A, Fischer MB, Watzek G. *Platelet-released supernatants increase migration and proliferation, and decrease osteogenic differentiation of bone marrow-derived mesenchymal progenitor cells under in vitro conditions*. Platelets. 2004 Feb;15(1):29-35.
6. Meixner A, **Karreth F**, Kenner L, Wagner EF. *JunD regulates lymphocyte proliferation and T helper cell cytokine expression*. EMBO J. 2004 Mar 24;23(6):1325-35.
7. Eferl R, Hoebertz A, Schilling AF, Rath M, **Karreth F**, Kenner L, Amling M, Wagner EF. *The Fos-related antigen Fra-1 is an activator of bone matrix formation*. EMBO J, 2004 Jul 21;23(14):2789-99
8. **Karreth F**, Hoebertz A, Eferl R, Wagner EF. *The AP-1 transcription factor Fra-2 is required for efficient cartilage development*. Development, 2004 131: 5717-5725.

9. **Karreth F** and Tuveson DA. *Twist induces an epithelial-mesenchymal transition to facilitate tumor metastasis*. *Cancer Biol Ther*, 2004 Nov;3(11):1058-9.
10. King AJ, Patrick DR, Batorsky RS, Ho ML, Do HT, Zhang SY, Kumar R, Rusnak DW, Takle AK, Wilson DM, Hugger E, Wang L, **Karreth F**, Loughheed JC, Lee J, Chau D, Stout TJ, May EW, Rominger CM, Schaber MD, Luo L, Lakdawala AS, Adams JL, Contractor RG, Smalley KS, Herlyn M, Morrissey MM, Tuveson DA, Huang PS. *Demonstration of a genetic therapeutic index for tumors expressing oncogenic BRAF by the kinase inhibitor SB-590885*. *Cancer Res*. 2006 Dec 1;66(23):11100-5.
11. **Karreth FA**, Tuveson DA. *Modelling oncogenic Ras/Raf signaling in the mouse*. *Curr Opin Genet Dev*. 2009;19(1):4-11.
12. **Karreth FA**, DeNicola GM, Winter SP, Tuveson DA. *C-Raf inhibits MAPK activation and transformation by B-RafV600E*. *Mol Cell*, in press